Investigation and Comparison of DC and AC NanoGrids

By

Farrukh ibne Mahmood

00000117513

Session 2015-17

Supervised by

Asst. Prof. Dr. Hassan Abdullah Khalid

A Thesis submitted to the U.S.-Pakistan Center for Advanced Studies in Energy in partial fulfillment of the requirements for the degree of

MASTERS of SCIENCE in

ENERGY SYSTEMS ENGINEERING

U.S.-Pakistan Center for Advanced Studies in Energy (USPCAS-E)

National University of Sciences and Technology (NUST)

H-12, Islamabad 44000, Pakistan

November 2017

Investigation and Comparison of DC and AC NanoGrids

By

Farrukh ibne Mahmood

00000117513

Session 2015-17

Supervised by

Asst. Prof. Dr. Hassan Abdullah Khalid

A Thesis submitted to the U.S.-Pakistan Center for Advanced Studies in Energy in partial fulfillment of the requirements for the degree of

MASTERS of SCIENCE in

ENERGY SYSTEMS ENGINEERING

U.S.-Pakistan Center for Advanced Studies in Energy (USPCAS-E)

National University of Sciences and Technology (NUST)

H-12, Islamabad 44000, Pakistan

November 2017

THESIS ACCEPTANCE CERTIFICATE

Certified that final copy of MS/MPhil thesis written by Mr. Farrukh ibne Mahmood, (Registration No. 00000117513), of U.S.-Pakistan Center for Advanced Studies in Energy has been vetted by undersigned, found complete in all respects as per NUST Statues/Regulations, is free of plagiarism, errors, and mistakes and is accepted as partial fulfillment for award of MS/MPhil degree. It is further certified that necessary amendments as pointed out by GEC members of the scholar have also been incorporated in the said thesis.

Signature: ______________________________

Name of Supervisor ________________________

Date: ________________________

Signature (HoD): ________________________

Date: ____________________________________

Signature (Dean/Principal): __________________

Date: ____________________________________

Certificate

This is to certify that work in this thesis has been carried out by **Mr. Farrukh ibne Mahmood** and completed under my supervision in, U.S.-Pakistan Center for Advanced Studies in Energy, National University of Sciences and Technology, H-12, Islamabad, Pakistan.

Supervisor: _________________

Dr. Hassan Abdullah Khalid
U.S.-Pakistan Centre for Advanced Studies in Energy
NUST, Islamabad

GEC member # 1: _________________

Dr. Kashif Imran
U.S.-Pakistan Center for Advanced Studies in Energy
NUST, Islamabad

GEC member # 2: _________________

Dr. Nadia Shahzad
U.S.-Pakistan Center for Advanced Studies in Energy
NUST, Islamabad

GEC member # 3: _________________

Engr. Rashid Wazir
U.S.-Pakistan Center for Advanced Studies in Energy
NUST, Islamabad

HoD-USPCAS-E _________________

Dr. Zuhair S. Khan
U.S.-Pakistan Center for Advanced Studies in Energy
NUST, Islamabad

Dean/Principal _________________

Dr. M. Bilal Khan
U.S.-Pakistan Center for Advanced Studies in Energy
NUST, Islamabad

Dedication

This work is dedicated to my parents and teachers

Acknowledgement

I would like to thank Allah Almighty without whose help I would not have been able to complete my Thesis. All the help and support from my parents and teachers were only because of Allah's will.

I would like to thank my supervisor Dr. Hassan Abdullah Khalid who provided me with the necessary tools to carry out my research work.

I would like to thank Dr. Govindasamy Tamizhmani for his support throughout my stay at the Photovoltaic Reliability Lab.

I would like to thank Dr. Muhammad Bilal Khan (Principal), Dr. Zuhair S Khan (HoD), my GEC committee, lab engineers, lab technicians, USPCAS-E and USAID for their support throughout the program.

I would also like to thank my parents who supported me throughout my Master's program.

Table of Contents

Abstract x
List of Figures xi
List of Tables xiv
List of Conference Papers 1
List of Abbreviations 2
CHAPTER 1 3
Introduction 3
1.1 Purpose of Study 3
1.2 Objectives 4
1.3 Limitations 4
1.4 Methodology 5
1.5 Thesis Structure 7
CHAPTER 2 9
Literature Review 9
2.1 Global Energy Trends 9
2.2 Distributed Generation 11
2.3 MicroGrid 12
2.4 NanoGrid 13
2.4.1 Components of a NanoGrid 14
2.4.2 Local Power Source 14
2.4.3 Electrical Appliances 14
2.4.4 Energy Storage 15
2.4.5 Power Converters 15
2.4.6 Gateway 15
2.4.7 Controller 15
2.5 Types of NanoGrid 15
2.5.1 AC NanoGrid 15
2.5.2 DC NanoGrid 16
2.5.3 Hybrid NanoGrid 17
2.6 Converter Topologies used in NanoGrids 18

2.7 Comparison between AC and DC NanoGrid ... 19
CHAPTER 3 ... 25
System Modeling ... 25
3.1 AC NanoGrid ... 25
3.2 DC NanoGrid ... 26
3.3 PV System ... 28
3.4 Grid-Tied Inverter ... 32
3.5 Electric Vehicle ... 32
3.6 House Model ... 36
3.7 DC Load Modeling ... 36
3.7.1 LED Light ... 36
3.7.2 Laptop ... 37
3.7.3 LED TV ... 38
3.7.4 DC Fan ... 38
3.7.5 DC Refrigerator ... 38
3.7.6 DC Air conditioner ... 39
3.7.7 DC to DC converter control and overcurrent protection ... 39
3.7.8 Miscellaneous Load ... 40
3.8 AC Load Modeling ... 40
3.8.1 Air conditioner ... 40
3.8.2 Fan ... 41
3.8.3 Refrigerator ... 41
3.8.4 Miscellaneous Load ... 41
CHAPTER 4 ... 45
Simulation Results and Discussion ... 45
4.1 Case Studies ... 45
4.1.1 Case 1 ... 45
4.1.2 Case 2 ... 46
4.1.3 Case 3 ... 47
4.2 Steady State Loss Analysis ... 48
4.2.1 Breakdown of Energy Losses in the DC NG ... 48
4.2.2 Distribution Line Losses at the 380V DC Bus vs 48V DC Bus ... 48

4.2.3 Breakdown of Energy Losses in the AC NG 49
4.2.4 Comparison of Line Losses between the DC and AC NG 50
4.2.5 Comparison of Device Losses between the DC and AC NG 50
4.2.6 Comparison of Converter and Conversion Losses between the DC and AC NG ... 51
4.2.7 Comparison of Total Losses between the DC and AC NG 52
4.2.8 Comparison of Power Drawn from the Grid between the DC and AC NG 53
4.3 Economic Analysis 54
CHAPTER 5 59
Conclusion and Recommendations 59
5.1 Conclusion 59
5.2 Recommendations 59
CHAPTER 6 60
Photovoltaic Reliability 60
6.1 Introduction 60
6.2 Objectives 61
6.3 Limitations 61
6.4 Methodology 62
CHAPTER 7 64
Experimentation and Results 64
7.1 Methodology 64
7.1.1 Module Selection 64
7.1.2 Baseline light IV 66
7.1.3 Dark IV 67
7.1.4 EL imaging 67
7.1.5 IR Imaging 67
7.1.6 UV Imaging 68
7.2 Results and Discussion 68
7.3 Conclusion 81

Abstract

The depletion of fossil fuels and their damaging effects on the environment has shifted the focus towards renewable energy sources to meet the increasing global energy demand. To effectively use renewable sources of energy they should be used in combination with other sources. Therefore, their use is preferred in distributed generation. For efficient utilization of distributed generation, NanoGrid (NG) are formed. NG are typically small electrical networks consisting of a small building or a house. These NG can be AC or DC. Since presently the use of DC devices (Laptops, LED's, cell phones etc.) and DC generation sources like Photovoltaics (PV) and the wind have increased, the emphasis is shifting towards DC NG. There is a lot of debate among researchers as to which NG network is more energy efficient but a detailed analysis has not been carried out to determine which system is better. Therefore, in this study, a detailed simulation analysis is carried out on both DC and AC NG using various case studies to determine which is better in terms of energy efficiency. An architecture for both DC and AC NG is modeled in MATLAB Simulink consisting of a grid-tied inverter, PV system, an EV and several domestic loads (LED light, LED TV, Laptop, Air Conditioner, Fan, Refrigerator). Three case studies are made to carry out a detailed loss analysis on both networks. The simulation results show that the DC NG is better than an AC NG in terms of energy efficiency. An economic analysis is also done on DC and AC devices to check which system is better in terms of cost. The results of this study can also be used for modeling of future NG systems.

Keywords: *NanoGrids, DC, AC, Photovoltaic, Renewables, Domestic Loads, Energy Efficiency*

List of Figures

Figure 1: Methodology 6
Figure 2: World Energy Mix [2] 10
Figure 3: Difference between central and distribution generation [9] 11
Figure 4: Conceptual diagram of a MG [14] 13
Figure 5: Difference between the central grid, microgrid, and nanogrid [19] 14
Figure 6: Basic architecture of an AC NG 16
Figure 7: Basic architecture of a DC nanogrid 17
Figure 8: Basic architecture of a hybrid NG. 18
Figure 9: AC nanogrid design 25
Figure 10: DC nanogrid design 27
Figure 11: Nanogrid PV Array 29
Figure 12: Solar Irradiance (24-hour) for May and June 30
Figure 13: Solar Irradiance from 9 AM to 3 PM for some days of May and June 30
Figure 14: PV system in DC NG 31
Figure 15: PV system in AC NG 31
Figure 16: Incremental conductance method for MPPT [5] 31
Figure 17: Grid tie Inverter Control block diagram 32
Figure 18: Nominal Current Discharge Characteristic at 0.43478C (98.6957A) 33
Figure 19: E0 = 406.6346, R = 0.01652, K = 0.012376, A = 31.491, B = 0.269 33
Figure 20: EV in DC NG 33
Figure 21: EV in AC NG 34
Figure 22: Buck/Boost converter for EV 34
Figure 23: EV charging and over charging protection circuit 35
Figure 24: EV discharging and over discharging protection circuit 36
Figure 25: LED Light in DC NG 37
Figure 26: LED Light in AC NG 37
Figure 27: Laptop in DC NG 37
Figure 28: Laptop in AC NG 37
Figure 29: LED TV in DC NG 38

Figure 30: LED TV in AC NG 38
Figure 32: DC Fan/Refrigerator in DC NG 39
Figure 33: DC Air conditioner in DC NG 39
Figure 31: DC to DC converter control and overcurrent protection 40
Figure 34: Air conditioner/Fan/Refrigerator in AC NG 41
Figure 35: Breakdown of losses in the DC NG for all three cases 48
Figure 36: Distribution line losses using 380V DC Bus vs 48V DC Bus for all three cases 49
Figure 37: Breakdown of losses in the AC NG for all three cases 49
Figure 38: Total line losses in the DC NG vs AC NG for all three cases 50
Figure 39: Total Device losses in the DC NG vs AC NG for all three cases 51
Figure 40: Total Converter and Conversion losses in the DC NG vs AC NG for all three cases 52
Figure 41: Total system losses in the DC NG vs AC NG for all three cases 52
Figure 42: Total power from the grid in the DC NG vs AC NG for all three cases 53
Figure 43: Net power= (Total power from grid-Power from PV) from the grid in the DC NG vs AC NG for all three cases 54
Figure 44: Cost of DC vs AC Devices 55
Figure 45: Monthly Bill of DC vs AC Devices 56
Figure 46: Nameplate data of modules from manufacturer A 65
Figure 47: Nameplate data of modules from manufacturer B 65
Figure 48: Nameplate data of modules from manufacturer C 65
Figure 49: Nameplate data of modules from manufacturer D 66
Figure 50: Temperature coefficient for Pmax and open circuit voltage for modules from manufacturer A 69
Figure 51: Temperature coefficient for Pmax and open circuit voltage for modules from manufacturer B 69
Figure 52: Temperature coefficient for Pmax and open circuit voltage for modules from manufacturer C 70
Figure 53: Temperature coefficient for Pmax and open circuit voltage for modules from manufacturer D 70
Figure 54: Temperature coefficient for short circuit current for modules from manufacturer A . 71
Figure 55: Temperature coefficient for short circuit current for modules from manufacturer B . 71

Figure 56: Temperature coefficient for short circuit current for modules from manufacturer C . 72
Figure 57: Temperature coefficient for short circuit current for modules from manufacturer D . 72
Figure 58: Series resistance from baseline light and dark IV for all modules 73
Figure 59: Shunt resistance from baseline light and dark IV for all modules 74
Figure 60: Module from manufacturer A.. 75
Figure 61: Module from manufacturer B.. 76
Figure 62: Module from manufacturer C.. 77
Figure 63: Module from manufacturer A.. 78
Figure 64: Module from manufacturer B.. 78
Figure 65: Module from manufacturer C.. 79
Figure 66: Module from manufacturer D.. 79
Figure 67: Module from manufacturer A.. 80
Figure 68: Module from manufacturer C.. 80
Figure 69: Module from manufacturer D.. 81

List of Tables

Table 1: Wire Parameters [1] 26
Table 2: Wire Parameters [1] 28
Table 3: Load Distribution within the house 36
Table 4: Case 1 Monday to Friday (Load usage) 45
Table 5: Case 2 Saturday (Load usage, 5 pm to 12 pm house is empty) 46
Table 6: Case 3 Sunday (Load usage) 47
Table 7: Cost of DC and AC Devices [11], [12], [13], [14], [15], [16] 54
Table 8: Details of the PV modules used 64

List of Conference Papers

- Farrukh ibne Mahmood, Hassan Abdullah Khalid **“A Comparative Analysis of DC and AC Nanogrid”** 2nd International Conference on Impact of Nano-Science on Energy Technologies (Nano-Set 2017)
- Farrukh Mahmood, Hatif Majeed, Haider Agha, Saddam Ali, Sai Tatapudi, Telia Curtis, GovindaSamy TamizhMani **“Temperature Coefficient of Power (Pmax) of Field Aged PV Modules: Impact on Performance Ratio and Degradation Rate Determinations”** Proceedings of SPIE 10370, Reliability of Photovoltaic Cells, Modules, Components, and Systems.

List of Abbreviations

NG	NanoGrid
MG	MicroGrid
PV	Photovoltaic
MPPT	Maximum power point tracking
EV	Electric Vehicle
Mtoe	Million tons of oil equivalent
DG	Distributed generation
PI	Proportional Integral
PLL	Phase lock loop
PWM	Pulse width modulation
MOSFET	Metal oxide semiconductor field effect transistor
IGBT	Insulated gate bipolar transistor
BTU	British thermal unit
EL	Electroluminescence
IR	Infra-red
UV	Ultraviolet
I-V	Current-Voltage
Pmax	Maximum power
FF	Fill Factor
AM	Air Mass
EVA	Ethylene vinyl acetate

CHAPTER 1

Introduction

This chapter gives a brief overview of the purpose of the study, its main objectives, limitations and the methodology used to carry out the research work.

1.1 Purpose of Study

With the advent of urbanization and a continuous increase in the world population, the global energy demand is increasing every year. It is expected that between 2005 and 2030 the energy requirement is expected to increase by 55% [1]. Moreover, fossil fuels are depleting at a very fast rate and it is estimated that the remaining coal, oil and gas reserves will approximately last for 107, 35 and 37 years respectively [2]. Furthermore, the long-term use of fossil fuels has caused drastic effects on the environment such as air pollution, global warming, and climate change [3]. These factors have provided impetus to the use of renewable energy which is considered a green energy source and does not have problems such as source depletion. But there are also some issues related to renewable energy such as intermittency and unreliability, for example, solar power is dependent on solar irradiation and on a cloudy day, the output of a solar plant can radically reduce [4]. Therefore, renewable energy sources have to be used in conjunction with other sources and their use is preferred in distributed generation.

Distributed generation offers the advantage of producing electricity close to the consumer, this makes it easily manageable and also reduces the electricity cost to the user [5]. It is also ideal for far and rural areas where connecting the grid in uneconomical. To effectively manage distributed generation NG systems can be formed. A NG is a system with a bus in which various generators and loads are connected [6]. A NG network mainly covers a small building or a house. These NG can be either AC or DC.

When comparing DC and AC systems a number of facets need to be considered. Presently the use of DC devices in residential building has increased and more than half of the loads being used are DC. Moreover, use of PV in buildings has also increased exponentially. Also, there are no reactive losses in a DC system. Therefore, using a DC NG would reduce redundant converter stages increasing the system efficiency [7]. However present households are constructed to operate on AC as the National Grid supplies AC. Thus, to shift an existing house to DC is very costly, though making a new house to operate on DC is very much feasible [8]. Throughout the research literature proponents for AC and DC NG give various reasons as to which network is superior and should be preferred. But a detailed analysis to determine which system is more energy efficient has not been done. Therefore, in this study, a comprehensive analysis is performed in MATLAB Simulink on a DC and AC NG to determine which is better in terms of energy efficiency. The DC and AC NG architecture modeled includes a grid-tied inverter, a PV system, an electric vehicle and a house consisting of various domestic loads. The house is modeled on the concept of a modern home and comprises of six residential loads [9]. All loads are modeled on commercially available products. To determine which network is more energy efficient a detailed loss analysis is performed on both AC and DC NG using three case studies. An economic analysis is also done on DC and AC devices to check which is better in terms of cost.

1.2 Objectives

The main objective of this study is to model a DC and AC NG architecture in MATLAB Simulink and then evaluate which network is more energy efficient using various case studies. The main objectives include modeling of DC and AC NG architecture, modeling of DC and AC loads, integrating sources of generation (PV) and storage (EV), addition of grid-tied inverter and DC to DC converters, selection of proper voltages and wire gauges, designing the model for a house, making case studies for loss analysis, performing a comparison between both networks based on loss analysis and carrying out an economic analysis on DC and AC devices.

1.3 Limitations

Some limitations of this study include, inverter, and DC to DC converters work as ideal models and therefore do not cater for losses, for inverter and converters an actual efficiency curve is used for loss calculations, models for DC and AC appliances are only based on electrical parts, the PV panel model used works at a specific temperature and the model for EV is based on a lithium-ion battery.

1.4 Methodology

For this study first, a comprehensive literature review was done on nanogrids then MATLAB Simulink was learned. After that, an architecture was designed for the DC and AC NG in MATLAB Simulink. For the PV system, MPPT was implemented using incremental conductance method. Solar irradiance for the PV system was calculated using data from the MHP unit at NUST. DC to DC converters was added to the system as needed. DC and AC appliances based on product datasheets (LED light, LED TV, Laptop, DC Air conditioner, DC Fan, DC Refrigerator, AC Air conditioner, AC Fan, AC Refrigerator) were also modeled in the NG. Then a model for a house was designed consisting of a living room, 2 bedrooms, and kitchen. After this modeling and integration of grid-tied inverter and EV was done in the NG network. For power distribution, appropriate wire gauges were selected and integrated into the DC and AC NG. After system modeling was complete three case studies were developed for loss analysis and a comparison was done between the DC and AC NG based on that. Afterwards, an economic analysis was also done between the DC and AC devices.

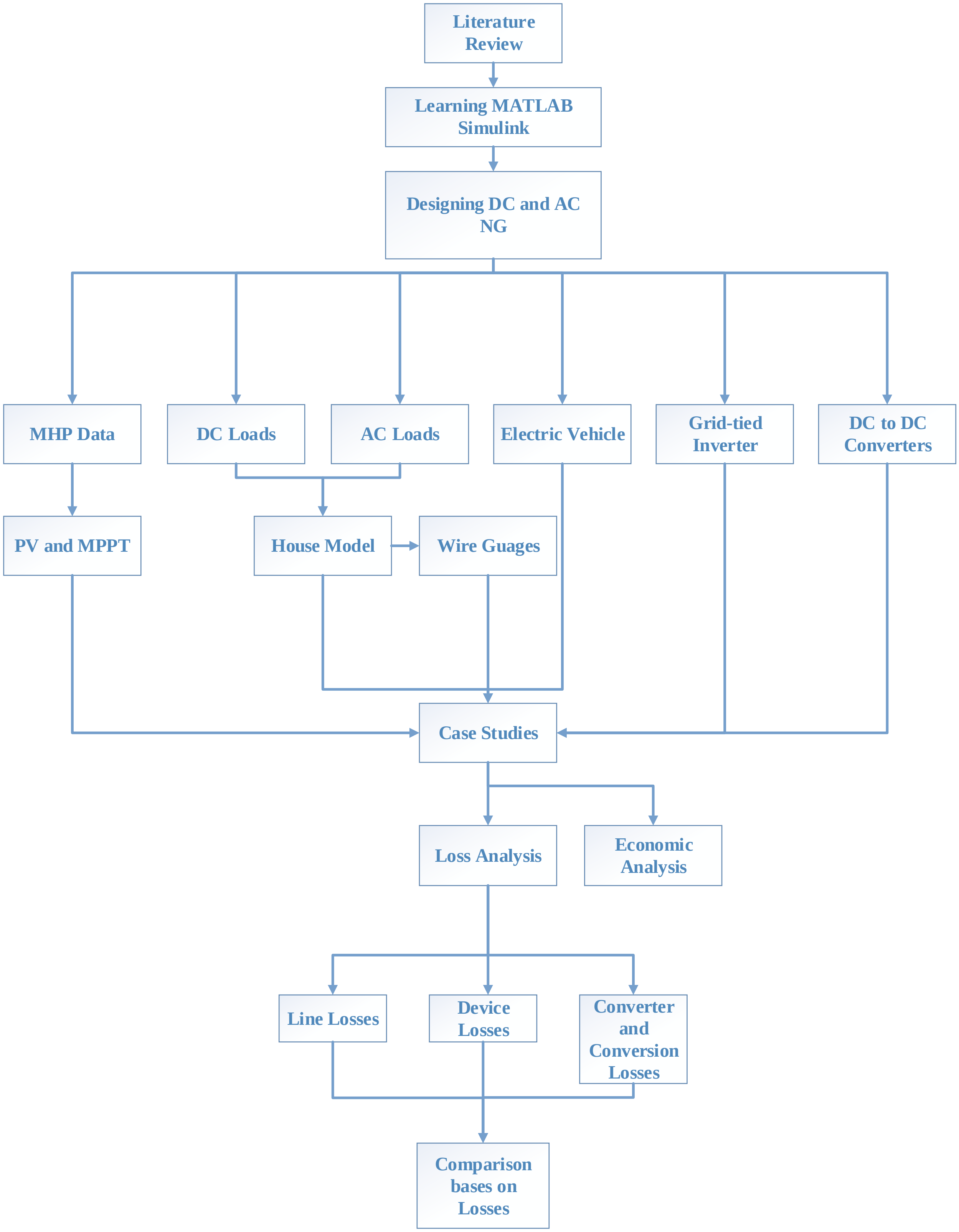

Figure 1: Methodology

1.5 Thesis Structure

The thesis is composed of seven chapters arranged in the following manner

Chapter 1 discusses the main purpose of the study, its objectives, limitations and the methodology used for the work.

Chapter 2 covers a detailed literature review on the NG technologies including types, design and recent work being done in the area.

Chapter 3 includes details about system modeling of both DC and AC NG comprising of a grid-tied inverter, PV system, EV and a house with domestic loads.

Chapter 4 covers the simulation results and discussions. The chapter gives detail about the case studies, how the loss and economic analysis is performed on both networks.

Chapter 5 gives the conclusion of the study. The chapter explains which system is better in terms of energy efficiency based on the results.

Chapter 6 and Chapter 7 discuss the work that was carried out at Arizona State University on PV reliability.

Summary

This chapter gives details about the purpose and motivation of this study. The chapter also talks about the main objectives, limitations and the methodology used for carrying out the research work.

References

[1] "BBC Bitesize - Higher Geography - Reasons for increase in demand for energy - Revision 1." [Online]. Available: https://www.bbc.co.uk/education/guides/zpmmmp3/revision. [Accessed: 10-Nov-2017].

[2] S. Shafiee and E. Topal, "When will fossil fuel reserves be diminished?," *Energy Policy*, vol. 37, no. 1, pp. 181–189, 2009.

[3] "The Hidden Costs of Fossil Fuels," *Union of Concerned Scientists Science for a healthy plant and safer world*. [Online]. Available: http://www.ucsusa.org/clean-energy/coal-and-other-fossil-fuels/hidden-cost-of-fossils#bf-toc-2. [Accessed: 10-Nov-2017].

[4] "Renewable Energy Intermittency Explained: Challenges, Solutions, and Opportunities - Scientific American Blog Network." [Online]. Available: https://blogs.scientificamerican.com/plugged-in/renewable-energy-intermittency-explained-challenges-solutions-and-opportunities/. [Accessed: 10-Nov-2017].

[5] "Introduction to Distributed Generation." [Online]. Available: http://www.dg.history.vt.edu/ch1/introduction.html. [Accessed: 10-Nov-2017].

[6] A. Goikoetxea, J. María, C. Roberto, P. Zumeta, P. Epele, and H. Gipuzkoa, "DC versus AC in residential buildings : efficiency comparison," pp. 3–7, 2006.

[7] E. Rodr, "Intelligent DC Microgrid Living Laboratories - A Chinese-Danish Cooperation Project," pp. 365–370, 2015.

[8] D. Burmester, R. Rayudu, W. Seah, and D. Akinyele, "A review of nanogrid topologies and technologies," *Renew. Sustain. Energy Rev.*, vol. 67, pp. 760–775, 2017.

[9] J. Crowfoot and J. Crowfoot, "Design and Modeling of the Cal Poly DC House Power Distribution System," 2011.

CHAPTER 2

Literature Review

This chapter gives a brief outline of the global energy trends and covers a detailed literature review on the NG literature covering NG components, types of NG, converter topologies being used in the NG and a comparison between DC and AC NG.

2.1 Global Energy Trends

Energy is the mainstay of economic growth of any nation. Without proper access to energy, the economic stability of any country can become stagnant. Thus, as the world population keeps increasing and more people tend to settle in the urban areas the demand for energy throughout the world is increasing. According to World Bank, the world population by 22^{nd} century is expected to increase from 6 billion to 12 billion resulting in an increase in the energy usage globally from 9000 million Mtoe to 15000-21000 Mtoe [1]. Consequently, to cater for this increase in energy usage more power plants and infrastructure will be needed. Currently, globally the main source of energy production is through the burning of coal, oil, and gas. Almost 85% of the world's energy comes from these fossil fuels. The pie chart below shows the world energy mix [2].

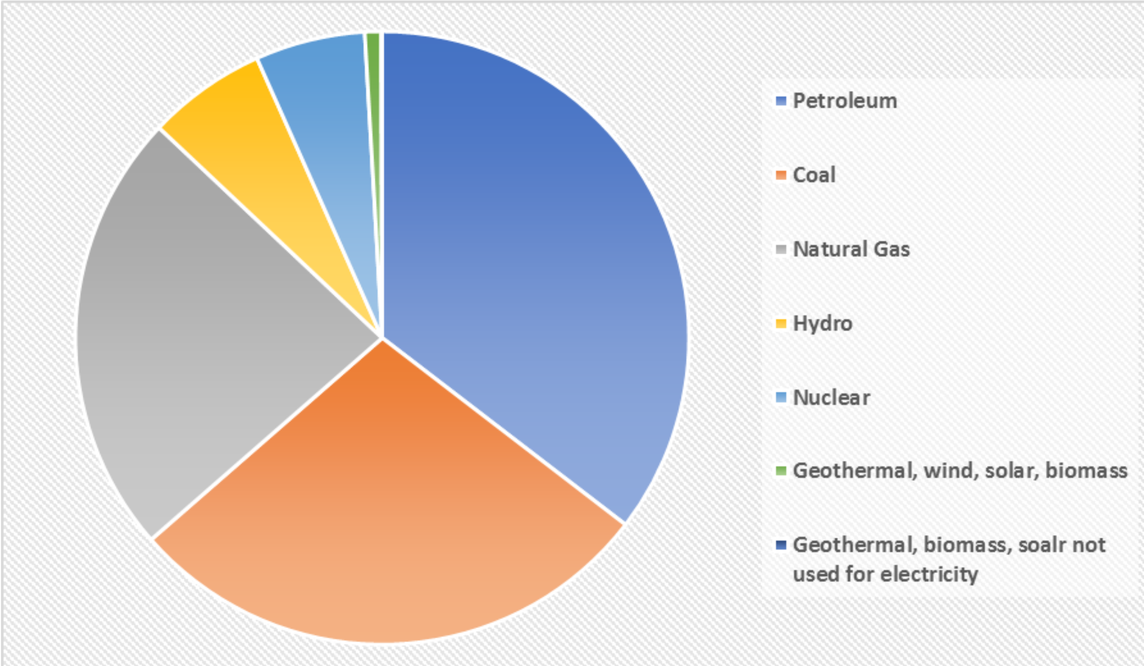

Figure 2: World Energy Mix [2]

Fossil fuels are non-renewable sources and therefore will not last forever. Furthermore, fossil fuels are depleting at a very fast rate and can only last for the next 50 to 100 years [3]. Apart from depletion fossil fuels pose a great threat to the environment. Continued use of fossil fuels has increased the amount of carbon dioxide leading to a greenhouse effect which causes more heat to be trapped in the earth's atmosphere [4]. This phenomenon has led to global warming and if the earth's average temperature increase is not kept below 2°C there could be drastic effects on the earth's environment [3]. Due to these reasons emphasis towards the use of renewable energy has increased globally. 19.3% of the total worldwide energy consumption in 2015 was due to renewable energy sources and this percentage has increased in subsequent years [5].

Main Renewable energy sources include solar, wind, geothermal, bioenergy, hydropower and ocean energy. These sources are green and therefore do not have harmful effects on the environment like fossil fuels. Moreover, these sources are abundantly available globally and do not have issues such as depletion [6]. Although renewable energy sources provide an attractive means to generate power without polluting the environment, there are still some issues associated with these sources. These problems include intermittency and unpredictability. Renewable energy sources are dependent on the weather conditions for production of power. Such as if there is insufficient solar radiation solar energy cannot be produced similarly if there is a lack of wind,

wind turbines cannot produce a reasonable amount of power [7]. Due to this these sources are preferred to be used in concurrence with other energy sources and are mostly superlative for distributed generation.

2.2 Distributed Generation

Distributed generation is the method of producing power close to the end user instead of traditional central power plants which are located very far from the consumer [8]. The figure below shows how distributed generation is different from central generation.

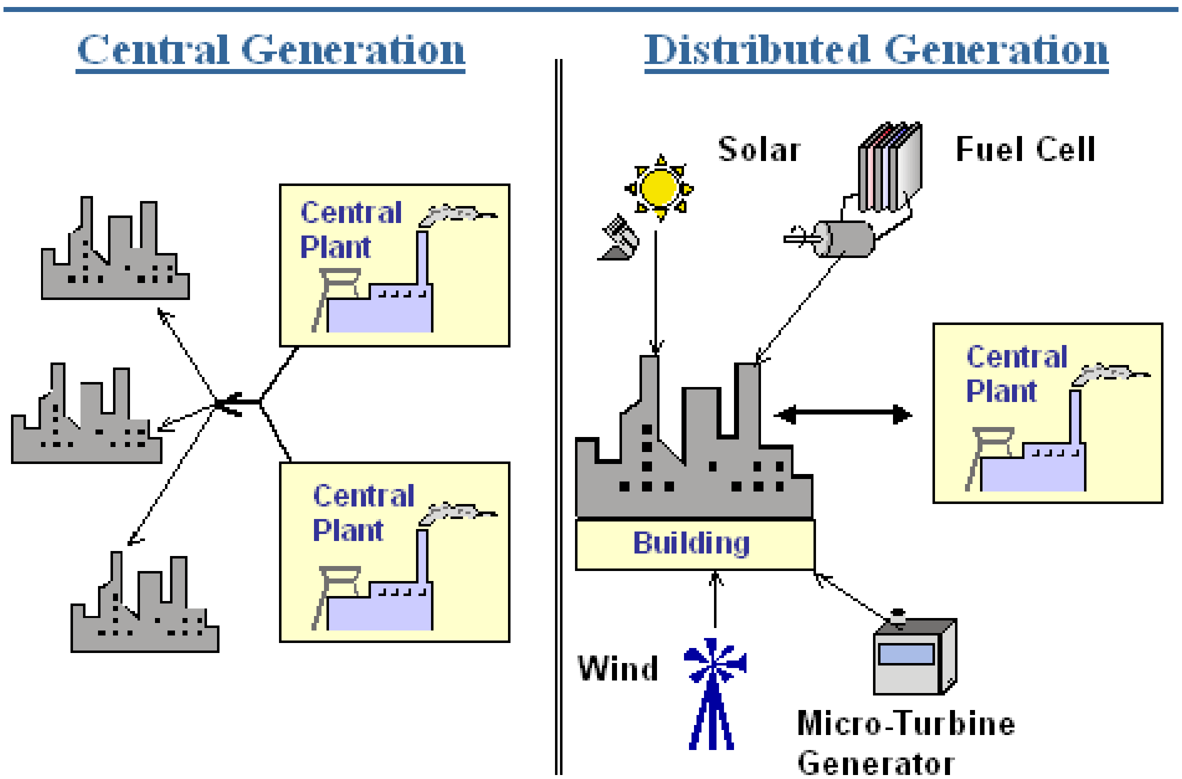

Figure 3: Difference between central and distribution generation [9]

Mostly DG includes small energy generators which are typically renewable energy sources. For domestic setup, mainly DG includes solar PV, small wind turbines, and diesel generators. These systems have the capability of working in islanding mode i.e. in isolation from the national grid or in grid-connected mode. DG is also more efficient than the traditional electrical setup in which power is produced at a central location and then carried to the point of consumption through long-distance transmission lines. Since DG is located very close to the consumer there are very few line losses as compared to the conventional power transfer through lengthy transmission lines [10]. Furthermore, as DG is close to the point of electricity production the cost to the consumer is also reduced and DG is ideal for remote and rural areas where connecting the national grid is very expensive. Thus, DG networks offer a number of advantages such as more system reliability, low electricity cost, increased efficiency, provision of power to the grid during peak times, better power quality and a safe electrical network less susceptible to safety threats [11]. But there are also some disadvantages of DG such as fluctuations in the system voltage when DG is connected to the grid, system protection becomes complicated and grid stability can be affected due to synchronization issues of frequency and voltage [12]. Therefore, to effectively manage distributed generation small electrical networks known as MG and NG are preferred.

2.3 MicroGrid

A MG is an electrical network operating in a small locality with a local energy source. These are small systems and in most cases, are less than 100KW [13]. MG has the capability of operating in both islanded and grid-connected mode. The figure below shows a simplified diagram of a MG.

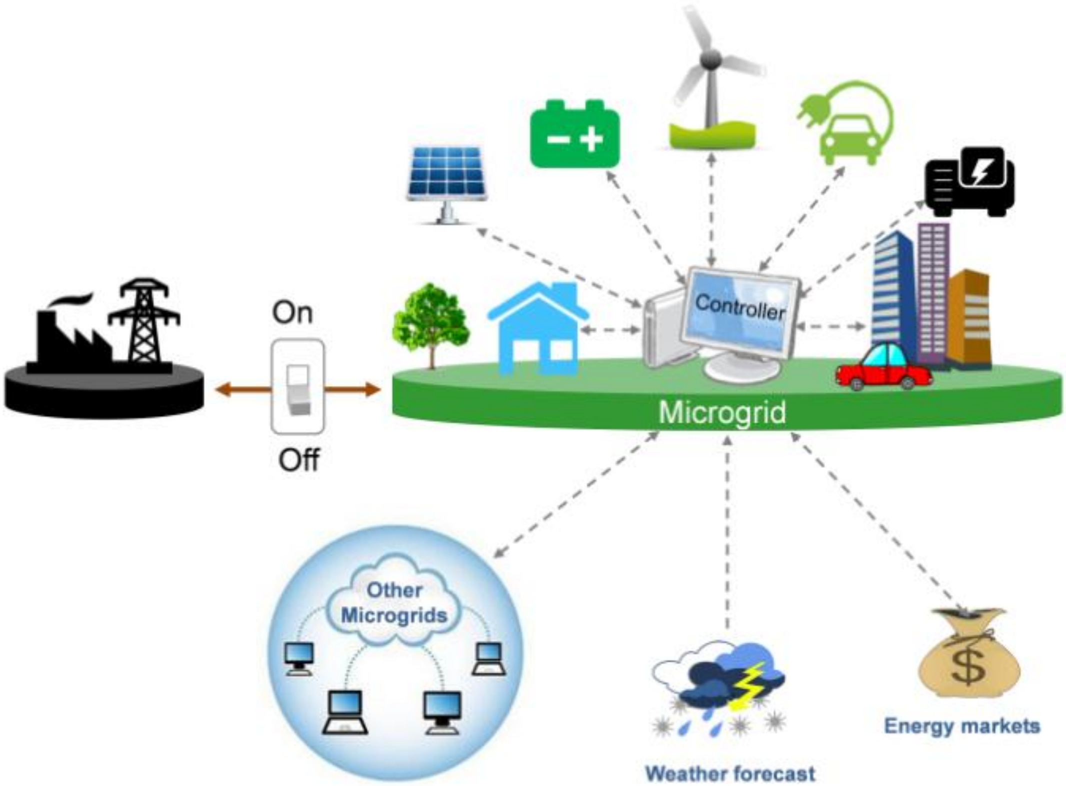

Figure 4: Conceptual diagram of a MG [14]

The MG have their own power source mostly comprising of solar PV, diesel generators, wind turbines and can comprise of a combination of these sources or a sole source for power production. MG can also act as backup systems for the grid in case of peak demand and since it can work in islanded mode if any fault occurs at the grid side a MG can still keep operating [15]. There are two main types of MG: customer MG and utility MG. Customer MG do not involve a utility company and are administered by the locality while utility MG consists of a part of the regulated grid [16]. Some of the well-known working examples of MG include the Fort Carson MG, Mesa del Sol MG, Sendai MG and MG at Illinois Institute of Technology [17].

2.4 NanoGrid

A NG is a small electrical network for a single house or a building and can work in both islanded and grid-connected modes. Power is produced locally with the possibility of energy storage to power local loads. The power capacity of a NG is small about 5KW but there are variations in the literature about this value [18]. MG and NG are different from each other as both cover a different area and have different capacities. According to the above definition, NG is small as compared to a MG and when a number of NG connect together a MG can be formed. The figure below clarifies the difference between a MG and NG.

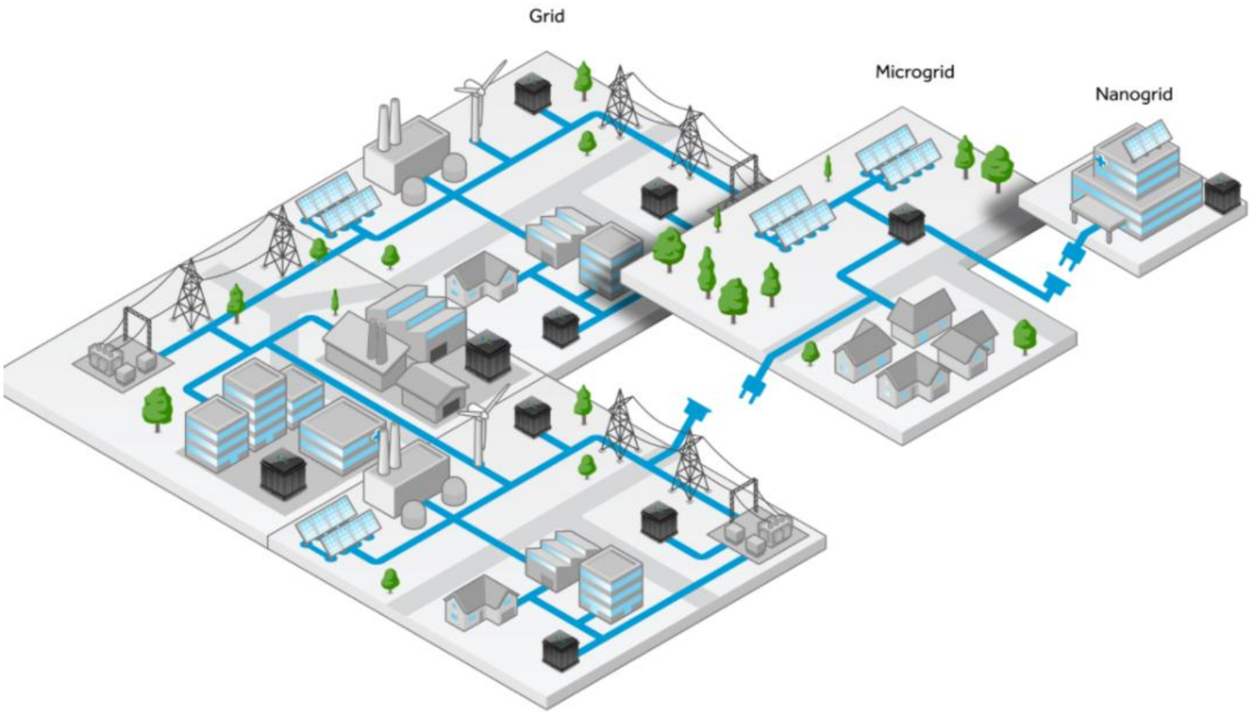

Figure 5: Difference between the central grid, microgrid, and nanogrid [19]

2.4.1 Components of a NanoGrid

A NG typically comprises the following six components.

2.4.2 Local Power Source

In a NG, the power is produced locally to power the loads. The network is very modular and therefore the system's power-producing capacity can be easily increased when the need arises. Both renewable and non-renewable sources can be used for generating energy in a NG. The non-renewable sources include diesel generators and renewable sources include solar PV and wind turbines [20], [21].

2.4.3 Electrical Appliances

The presence of at least one domestic appliance in a NG is essential. Electrical appliances include common residential loads such as TV, laptop, air-conditioner, refrigerator, fan etc. [22].

2.4.4 Energy Storage

Main energy storage devices used in a NG are batteries and EV. Energy storage provides backup during times when power from the sources is not available and it also makes the network more balanced. For a system to be considered a NG presence of energy storage components is not necessary but most NG is equipped with an energy storage device [23].

2.4.5 Power Converters

Power converters are an essential part of a NG. Many electronic converters (AC/DC DC/DC DC/AC) are employed in a NG to stabilize the voltage and provide the required output to the loads. Due to these power converters, bi-directional power flow is also possible which allows for electricity sharing and selling [24].

2.4.6 Gateway

Gateway is a two-way link that connects the NG to another NG, MG or the central grid. It also allows communication between the networks except for the national grid. When connected to other networks electricity sharing and selling is also possible through the gateway. The gateway also allows the NG to operate in islanded mode by separating it from the national grid [25], [26].

2.4.7 Controller

A controller is not necessary for a network to be considered a NG but is often present. The main purpose of the controller is to communicate with all power electronic converters within the NG to balance power production with demand. In doing so the controller can cut off specific loads, connect or disconnect from the grid or use auxiliary power sources to balance demand. The controller also stores the power flow data from power converters and loads [24], [18].

2.5 Types of NanoGrid

There are three main types of NG: AC NG, DC NG and Hybrid NG.

2.5.1 AC NanoGrid

The figure below shows the typical architecture of an AC NG.

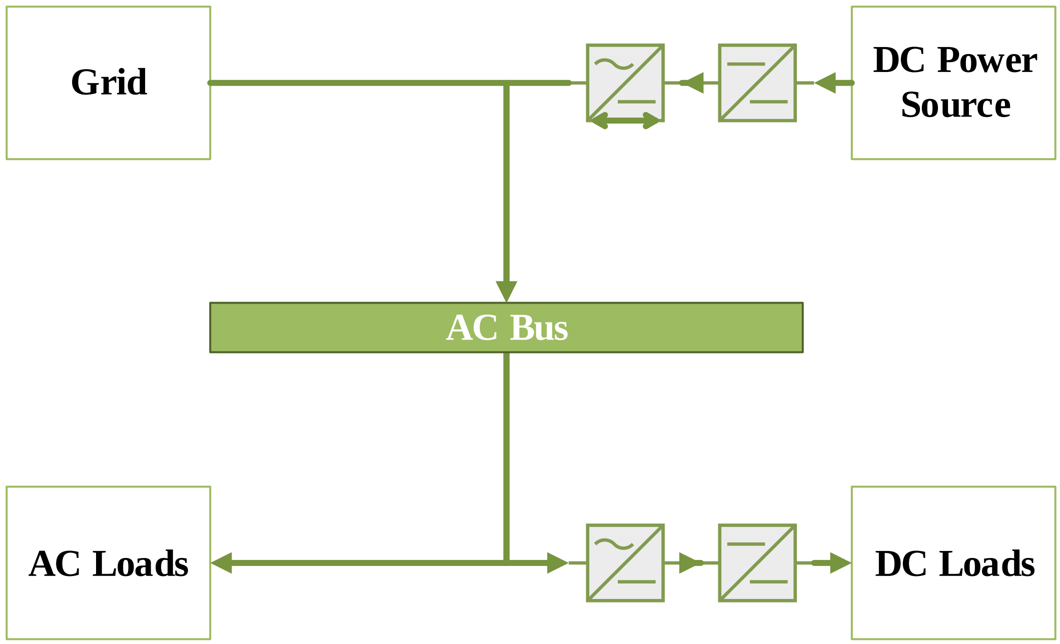

Figure 6: Basic architecture of an AC NG

Power from the national grid is directly fed to the AC bus at 230V. The power from the DC source goes through a DC to DC converter, in the case for PV this is the MPPT controller. After that, it goes through a grid-tied inverter which converts the DC to 230V AC. The inverter is also responsible for synchronization with the grid's frequency. Loads are connected to the bus and can utilize power from it. The AC loads can directly use power from the AC bus but in case of DC loads the AC power is converted to DC and then a DC to DC converter supplies the required voltage for the proper functioning of the DC load. In case an energy storage element is present it is also connected to the AC bus through an inverter and a DC to DC converter. The inverter topology for the energy storage device is similar to the one used with the DC source. Power from the bus is converted to DC and then regulated to the required value by the DC to DC converter for use by the storage device [27], [28].

2.5.2 DC NanoGrid

The figure below shows the typical architecture of a DC NG.

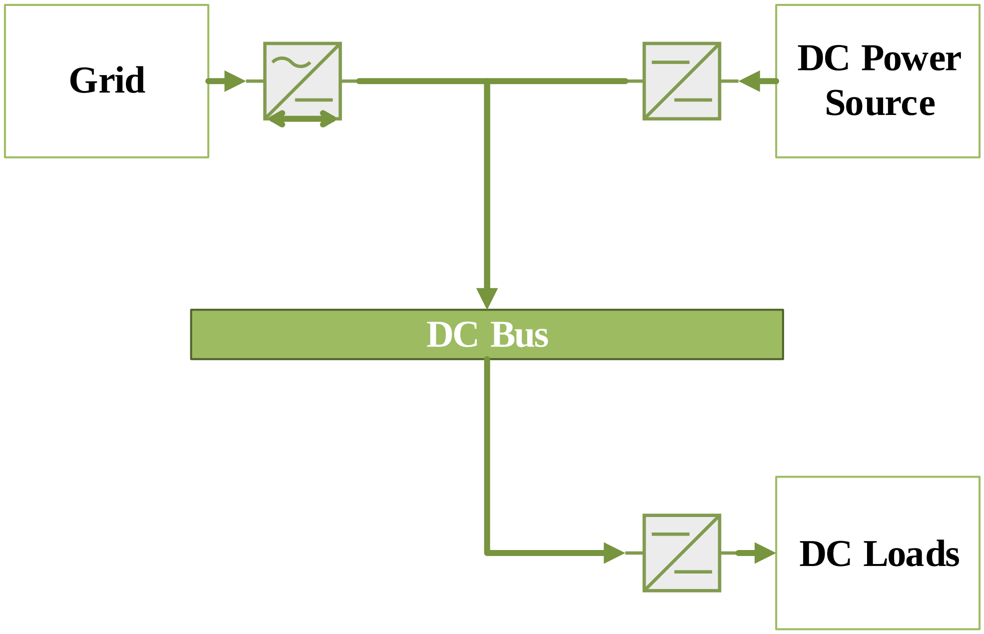

Figure 7: Basic architecture of a DC nanogrid

In a DC NG the power from the national grid is converted to DC through a grid-tied inverter. The inverter also synchronizes with the grid's frequency. The inverter outputs and regulates the voltage at 380V which is fed to the DC bus. In a DC NG, there can be multiple DC buses such as a 380V DC bus for high voltage sources and a 48,12 or 24V Bus for low voltage loads. The DC source is connected to the bus through a DC to DC converter which in case of solar PV is an MPPT controller. To take advantage of the DC NG mostly DC loads are used. The loads are connected to a low voltage DC bus and a DC to DC converter steps down the voltage from the 380V bus to the low voltage bus. Depending on the voltage requirement some loads are connected directly to the low voltage bus while some are connected through DC to DC converters for the required voltage supply needed for proper functioning of the load. If an energy storage element is present in the DC NG it is connected to the 380V DC bus. A DC to DC converter connected to the 380V bus supplies the needed voltage to the energy storage device. It is obvious from the description of both AC and DC NG that in a DC NG there are fewer energy conversions because most of the sources, loads and energy storage devices now are DC [29], [30].

2.5.3 Hybrid NanoGrid

There are slight variations throughout the literature on the basic architecture of a hybrid NG. The figure below shows the hybrid NG design as proposed by [31].

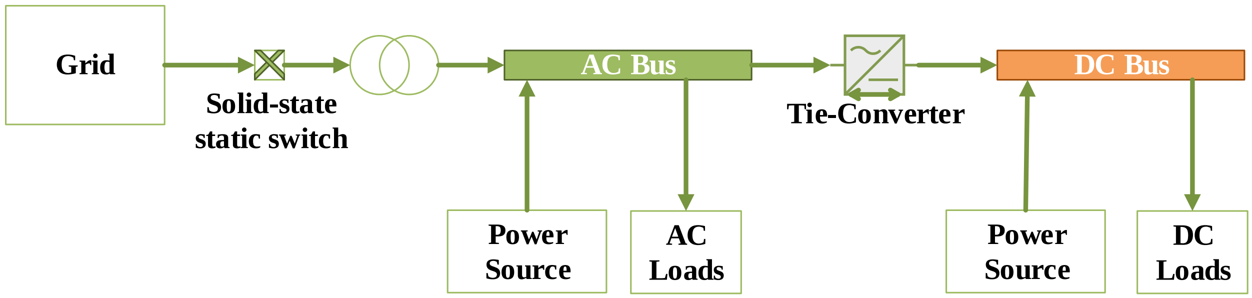

Figure 8: Basic architecture of a hybrid NG.

In this design both AC and DC buses are present. The tie converter is responsible for connecting both the buses together. The national grid is connected to the AC bus through a switch and a three-phase transformer. The AC bus is a three-phase system maintained at 400V and the DC bus is at 350V. The power sources and loads are connected to both buses through appropriate converters [31]. Although hybrid NG provides more flexibility in the system these systems are more complex and expensive than AC and DC NG [32].

2.6 Converter Topologies used in NanoGrids

A lot of literature on NG is focused on converter topologies. Main converter types include DC to DC, AC to DC and DC to AC. DC to DC converters have DC at their input and output and their function is to step up or step down the voltage as needed. In many cases, a control technique such as a PI controller is used for generating the required PWM which triggers the switching element such as a MOSFET or an IGBT to achieve the required voltage. The controller also ensures that the voltage is maintained at its required value. Main converters of this type include boost converter and the buck converter. Boost converter can be present with a source to step up the voltage to the bus voltage and buck converter is normally used at the load side to step down the voltage. These converters are also found in MPPT. AC to DC converters takes AC at their input and output DC. These converters can be present at both the source and load side. At the source side, they can be used for interfacing an AC source to the DC NG and mostly these converters are bi-directional if present at the source side. At the load side, they convert AC to DC for use by DC loads in an AC NG. DC to AC converters intakes DC and output AC. At the source side, they are used for interfacing sources and are normally bidirectional. At the load side, they can be used to convert DC to AC for use by AC loads in a DC NG [18].

Many converter topologies are discussed in the literature such as multi-port converter [33], boost-derived hybrid converter [34], two-stage bidirectional AC/DC converter [35], multi-input single inductor converter [36], grid interface bidirectional inverter [37], switched-inductor Cuk-derived hybrid converter [38], switched boost inverter [39]. For most of the topologies discussed in the research articles, the focus is towards increasing the converter efficiency, delivering higher power quality, making control easy in the NG and decreasing the size of the NG.

2.7 Comparison between AC and DC NanoGrid

Throughout the literature advocates for the DC or AC NG have given several reasons to support their claims. Therefore, when comparing both these networks many factors must be taken into consideration. Supporters for the DC NG suggest that DC distribution is ideal in a NG because most present-day loads and household appliances are now DC such as laptops, cell phones, LED TV etc. Even devices such as air-conditioners, refrigerators, and fans have DC counterparts commercially available and are also more efficient. Furthermore, the use of solar PV in residential settings is increasing exponentially and therefore it makes sense to use a DC NG to fully utilize the DC source [40], [41]. Also, energy storage devices such as batteries and EV are also DC and if they are integrated into a NG it is better to use DC distribution. Moreover, there are also no reactive power losses in a DC NG. Since, DC loads, sources and storage devices are readily available and their use in households is also increasing using a DC NG would remove many converter stages that would be necessary for an AC NG. As suggested by [42] the converter cost in the DC NG also reduces due to fewer converter stages. Due to this, the DC NG becomes much more efficient than an AC NG [43]. Power reliability is also more due to smooth transient DC power supply and very less voltage fluctuation. Moreover, control in a DC NG also becomes easy as only voltage regulation is needed unlike in an AC system where both voltage and frequency must be controlled [42].

However, proponents of the AC NG suggest that an AC NG is better because the national grid supplies AC and our current houses are built to support AC infrastructure. Furthermore, the AC loads are cheaper as compared to DC loads and have a high availability [44]. Therefore, to refit an existing household to operate on DC would be very expensive however constructing a new house to work on DC is viable. The literature also points out that protection in a DC NG is more complex and short circuit and ground faults can occur at load side which can impair the network [45], [46].

Summary

In this chapter, a detailed literature review is done. The chapter talks about the global energy trends, how distributed generation is increasing and how NG is important. Furthermore, detail is provided about working of NG, their components, types, converter topologies that are being researched on and literature on the comparison between DC and AC NG.

References

[1] J. Sheffield, "World population growth and the role of annual energy use per capita.," *Technological forecasting and social change*, Sep-1998. [Online]. Available: http://www.ncbi.nlm.nih.gov/pubmed/12294507. [Accessed: 11-Nov-2017].

[2] "CASE STUDY: World Energy Use | Boundless Physics." [Online]. Available: https://courses.lumenlearning.com/boundless-physics/chapter/case-study-world-energy-use/. [Accessed: 11-Nov-2017].

[3] "How long before we run out of fossil fuels? - Our World in Data." [Online]. Available: https://ourworldindata.org/how-long-before-we-run-out-of-fossil-fuels/. [Accessed: 11-Nov-2017].

[4] N. Oreskes, "E SSAY on Climate Change," *Science (80-.).*, vol. 306, no. January, pp. 2004–2005, 2005.

[5] REN21, "Renewables 2017: global status report," 2017.

[6] "Why is renewable energy important?" [Online]. Available: http://www.renewableenergyworld.com/index/tech/why-renewable-energy.html. [Accessed: 11-Nov-2017].

[7] "Renewable Energy: The Advantages and Disadvantages of Renewable Energy." [Online]. Available: http://www.solarschools.net/resources/stuff/advantages_and_disadvantages.aspx. [Accessed: 11-Nov-2017].

[8] T. Ackermann, G. Ran Andersson, and L. Sö Der, "Distributed generation: a definition," *Electr. Power Syst. Res.*, vol. 57, pp. 195–204, 2001.

[9] "Teach Engineering." [Online]. Available: https://www.teachengineering.org/activities/view/cub_energy2_lesson07_activity3. [Accessed: 12-Nov-2017].

[10] "Introduction to Distributed Generation." [Online]. Available: http://www.dg.history.vt.edu/ch1/introduction.html. [Accessed: 12-Nov-2017].

[11] US DOE, "The Potential Benefits of Distributed Generation and the Rate- Related Issues That May Impede Its Expansion Report Pursuant to Section 1817 of the Energy Policy Act of 2005 Background," 2005.

[12] H. Kuang, S. Li, and Z. Wu, "Discussion on advantages and disadvantages of distributed

generation connected to the grid," in *2011 International Conference on Electrical and Control Engineering, ICECE 2011 - Proceedings*, 2011, pp. 170–173.

[13] R. H. Lasseter, "MicroGrids," in *2002 IEEE Power Engineering Society Winter Meeting. Conference Proceedings (Cat. No.02CH37309)*, 2002, vol. 1, pp. 305–308.

[14] "About Microgrids | Building Microgrid." [Online]. Available: https://building-microgrid.lbl.gov/about-microgrids. [Accessed: 12-Nov-2017].

[15] "What is microgrid?" [Online]. Available: http://whatis.techtarget.com/definition/microgrid. [Accessed: 12-Nov-2017].

[16] "Types of Microgrids | Building Microgrid." [Online]. Available: https://building-microgrid.lbl.gov/types-microgrids. [Accessed: 12-Nov-2017].

[17] "Examples of Microgrids | Building Microgrid." [Online]. Available: https://building-microgrid.lbl.gov/examples-microgrids. [Accessed: 12-Nov-2017].

[18] D. Burmester, R. Rayudu, W. Seah, and D. Akinyele, "A review of nanogrid topologies and technologies," *Renew. Sustain. Energy Rev.*, vol. 67, pp. 760–775, 2017.

[19] "Microgrids 101." [Online]. Available: http://blog.aquionenergy.com/microgrids-101. [Accessed: 12-Nov-2017].

[20] S. S. Nag, R. Adda, O. Ray, and S. K. Mishra, "Current-Fed Switched Inverter based hybrid topology for DC Nanogrid application," in *IECON Proceedings (Industrial Electronics Conference)*, 2013, pp. 7146–7151.

[21] J. Bryan, R. Duke, and S. Round, "Decentralized generator scheduling in a nanogrid using DC bus signaling," in *IEEE Power Engineering Society General Meeting*, 2004, vol. 1, pp. 977–982.

[22] B. Nordman and L. Berkeley, "Distribute Power Locally : The Promise of Nanogrids," 2012.

[23] "Solar PV plus Energy Storage Nanogrids." [Online]. Available: https://www.navigantresearch.com/research/solar-pv-plus-energy-storage-nanogrids. [Accessed: 12-Nov-2017].

[24] S. Teleke, L. Oehlerking, and M. Hong, "Nanogrids with Energy Storage for Future Electricity Grids," 2014, pp. 1–5.

[25] B. Nordman and K. Christensen, "Local power distribution with nanogrids," in *2013 International Green Computing Conference Proceedings*, 2013, pp. 1–8.

[26] B. Nordman and K. Christensen, “Nanogrids.” [Online]. Available: https://tools.ietf.org/html/draft-nordman-nanogrids-00. [Accessed: 12-Nov-2017].

[27] Shahab Poshtkouhi, “Modular AC Nano-Grid with Four-Quadrant Micro-Inverters and High-Efficiency DC-DC Conversion,” 2016.

[28] I. Cvetkovic, “Modeling , Analysis and Design of Renewable Energy Nanogrid Systems,” 2010.

[29] E. Rodr, “Intelligent DC Microgrid Living Laboratories - A Chinese-Danish Cooperation Project,” pp. 365–370, 2015.

[30] S. K. Mishra, “Nanogrid: DC Based Energy Distribution and Control,” 2013.

[31] R. P. S. Chandrasena, F. Shahnia, A. Ghosh, and S. Rajakaruna, “Operation and control of a hybrid AC-DC nanogrid for future community houses,” in *2014 Australasian Universities Power Engineering Conference, AUPEC 2014 - Proceedings*, 2014, no. October, pp. 1–6.

[32] V. Pal, S. Maheshwari, and A. Faisal, “Design and Analysis of Hybrid Nanogrid,” *Int. J. Adv. Res. , Ideas Innov. Technol.*, vol. 3, no. 3, pp. 1365–1373, 2017.

[33] O. Ray and S. Mishra, “A multi-port converter topology with simultaneous isolated and non-isolated outputs,” in *IECON Proceedings (Industrial Electronics Conference)*, 2013, pp. 7118–7123.

[34] O. Ray and S. Mishra, “Boost-derived hybrid converter with simultaneous DC and AC outputs,” *IEEE Trans. Ind. Appl.*, vol. 50, no. 2, pp. 1082–1093, 2014.

[35] F. Chen, R. Burgos, D. Boroyevich, and D. Dong, “Control Loop Design of a Two-stage Bidirectional AC / DC Converter for Renewable Energy Systems,” in *2014 IEEE Applied Power Electronics Conference and Exposition - APEC 2014*, 2014, pp. 2177–2183.

[36] S. Poshtkouhi and O. Trescases, “Multi-input single-inductor DC-DC converter for MPPT in parallel-connected photovoltaic applications,” in *Conference Proceedings - IEEE Applied Power Electronics Conference and Exposition - APEC*, 2011, vol. 4, pp. 41–47.

[37] D. Dong, F. Luo, X. Zhang, D. Boroyevich, and P. Mattavelli, “Grid-interface bidirectional converter for residential DC distribution systems - Part 2: AC and DC interface design with passive components minimization,” *IEEE Trans. Power Electron.*, vol. 28, no. 4, pp. 1667–1679, 2013.

[38] R. Sarath and P. Kanakasabapathy, “Switched-capacitor/switched-inductor Ćuk-derived

hybrid converter for nanogrid applications," in *4th IEEE Sponsored International Conference on Computation of Power, Energy, Information and Communication, ICCPEIC 2015*, 2015, pp. 430–435.

[39] R. Adda, O. Ray, S. Mishra, and A. Joshi, "Implementation and control of Switched Boost Inverer for DC nanogrid applications," in *2012 IEEE Energy Conversion Congress and Exposition, ECCE 2012*, 2012, pp. 3811–3818.

[40] K. Garbesi, V. Vossos, and H. Shen, "Catalog of DC Appliances and Power Systems," 2012.

[41] I. Cvetkovic *et al.*, "A testbed for experimental validation of a low-voltage DC nanogrid for buildings," in *15th International Power Electronics and Motion Control Conference and Exposition, EPE-PEMC 2012 ECCE Europe*, 2012, pp. 1–8.

[42] D. Chen and L. Xu, "Technologies and Applications for Smart Charging of Electric and Plug-in Hybrid Vehicles," pp. 39–65, 2017.

[43] A. Goikoetxea, J. M. Canales, R. Sanchez, and P. Zumeta, "DC versus AC in residential buildings: Efficiency comparison," *IEEE EuroCon 2013*, no. July, 2013.

[44] Amir, "Exploring the Efficiency of DC Nanogrids Versus the Traditional AC Grid System." [Online]. Available: https://www.authorea.com/users/166037/articles/193087-exploring-the-efficiency-of-dc-nanogrids-versus-the-traditional-ac-grid-system. [Accessed: 14-Nov-2017].

[45] M. M. H. Sajeeb, A. Rahman, and S. Arif, "Feasibility analysis of solar DC Nano grid for off grid rural Bangladesh," in *2015 International Conference on Green Energy and Technology, ICGET 2015*, 2015.

[46] P. Cairoli, I. Kondratiev, and R. A. Dougal, "Controlled power sequencing for fault protection in DC nanogrids," in *3rd International Conference on Clean Electrical Power: Renewable Energy Resources Impact, ICCEP 2011*, 2011, pp. 730–737.

CHAPTER 3

System Modeling

The chapter provides details about how the system model was designed in MATLAB. The chapter covers the designing of AC NG, DC NG, PV system, grid-tied inverter, electric vehicle, house, DC to DC converters, DC and AC loads.

3.1 AC NanoGrid

The main components in the AC NG are a grid-tied inverter, solar photovoltaic system with MPPT, an electric vehicle, 230V AC bus one for each phase, AWG 7 and 8 wiring between the AC bus and house, house consisting of four blocks (Living room, bedroom 1, bedroom 2, kitchen), various domestic loads within each house block and appliances which are both DC and AC. The AC NG architecture modeled in Simulink is shown in the figure below.

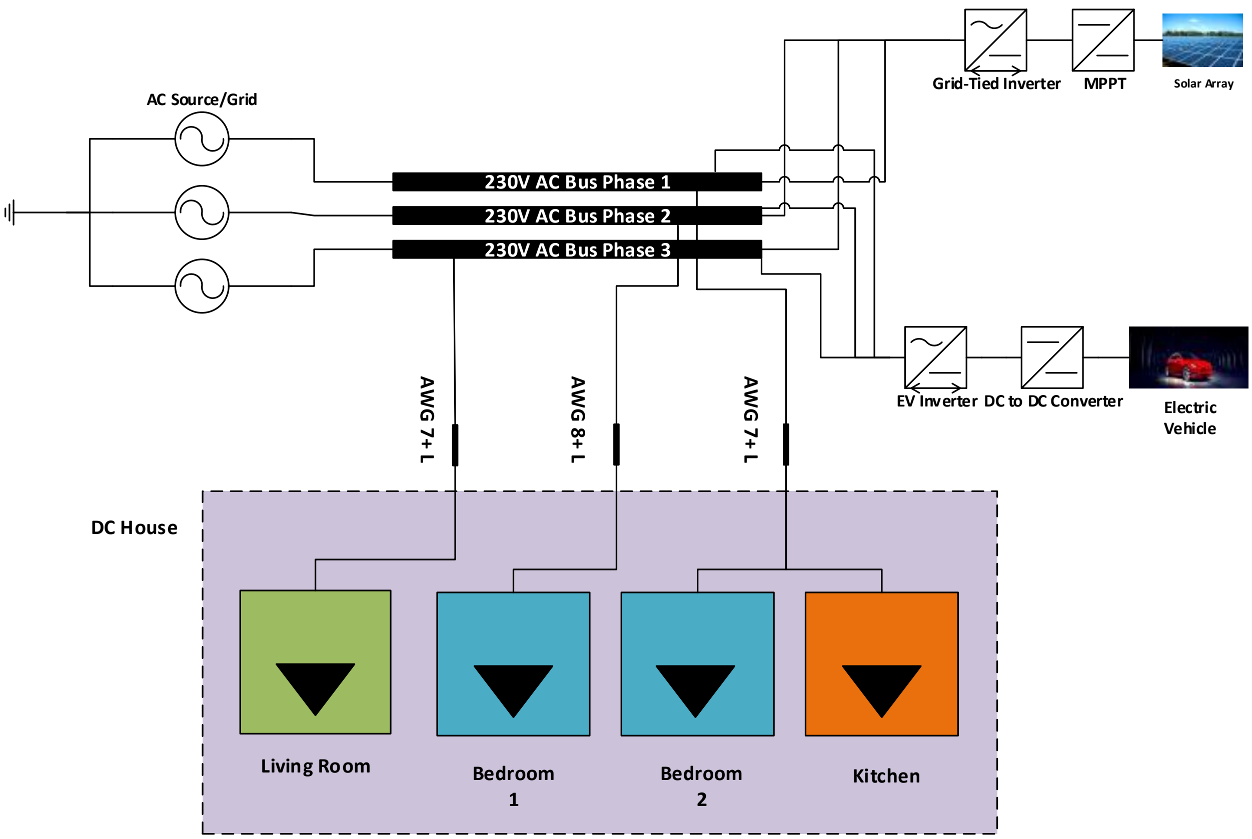

Figure 9: AC nanogrid design

Both the national grid and solar photovoltaic system feed the 230V AC bus. The MPPT extracts the maximum power available from the PV. The grid-tied inverter converts the DC output from solar PV to AC. EV is also connected to the 230V AC bus and an inverter/rectifier converts the incoming AC to DC or vice versa. The EV is then charged or discharged through a buck/boost converter. There are three 230V AC buses, one for each phase. From phase 1 AWG 7 wire is used to connect the house and from phase 2 and 3, AWG 8 wire is used for connecting the house. The house contains both DC and AC loads. Those DC loads are used which have no AC counterparts available commercially, these include a laptop, LED light and LED TV. The AC loads present in the house are a fan, refrigerator, air conditioner and a miscellaneous load. The loads in the AC NG are selected this way so that a fair comparison can be done between the DC and AC network. For DC loads AC output is converted to DC using a rectifier and then the voltage is regulated using a DC-DC converter. AWG 7 and AWG 8 wire of length 15.2 m were selected after measuring the peak current in all three phases.

Table 1: Wire Parameters [1]

AWG	Diameter (mm)	Area (mm^2)	Resistance (Ohms/km)
7	3.66522	10.5	1.634096
8	3.2639	8.37	2.060496

Since this is an AC network the wire was modeled using a resistor and an inductor. The resistance was calculated by the following relationship:

$$Resistance = Resistance\,(Ohms/km) * Wire\ length\ (km)$$

Line inductance was calculated using wire diameter and wire length [2].

3.2 DC NanoGrid

The main components in the DC NG are a grid-tied inverter, solar photovoltaic system with MPPT, an electric vehicle, 380V DC bus, 380V to 48V buck converter, AWG 4 wiring between the 380V DC bus and buck converter, 48V DC bus, house consisting of four blocks (Living room, bedroom 1, bedroom 2, kitchen), DC loads in the DC NG house and four AWG 4 wires connecting the 48V DC bus to the four blocks in the house. The DC NG architecture modeled in Simulink is shown in the figure below.

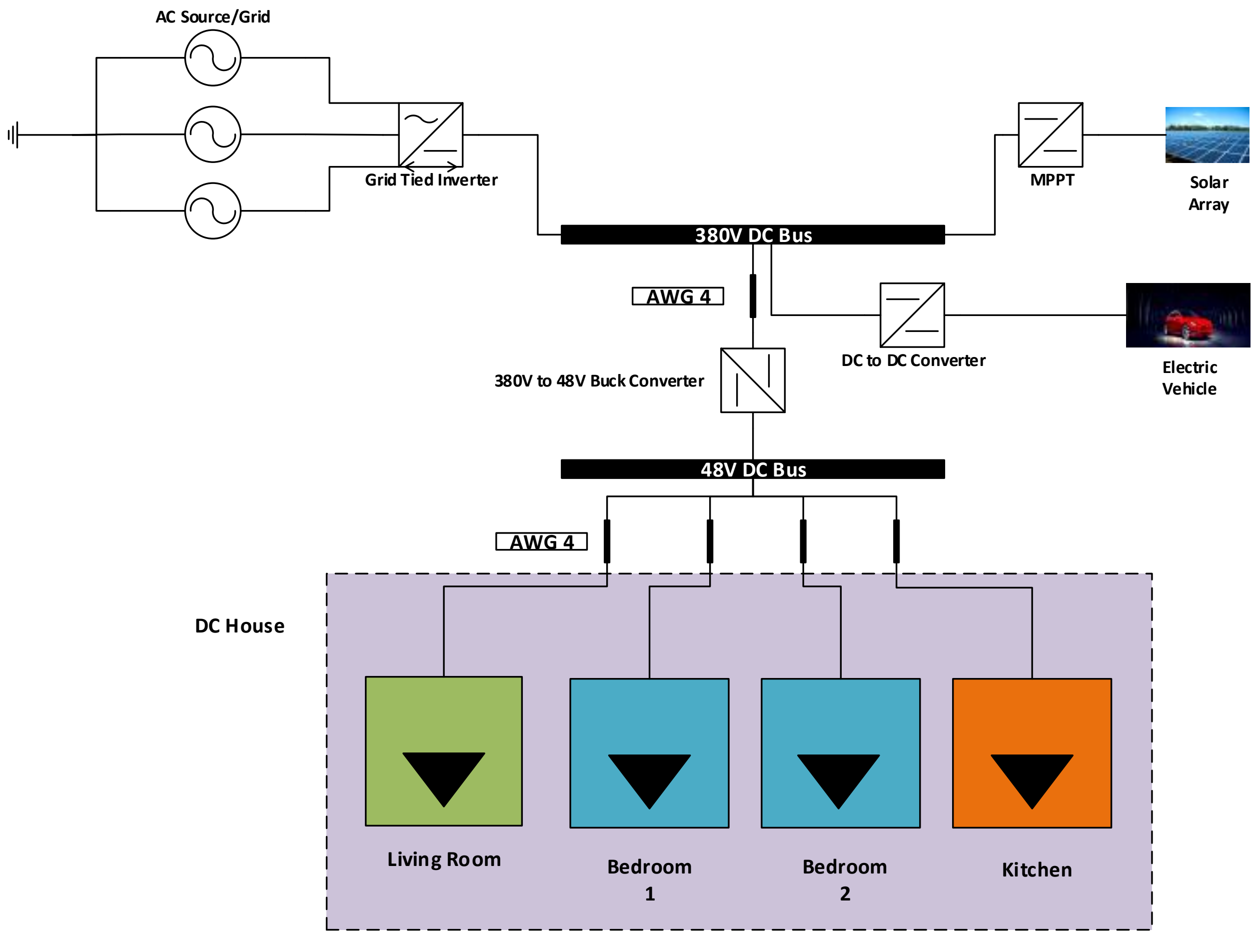

Figure 10: DC nanogrid design

Both the national grid and solar photovoltaic system feed the 380V DC bus. The grid-tied inverter converts the incoming AC from the National grid to DC. The EV is also connected to the 380V DC Bus and is charged and discharged through a buck/boost converter. A buck converter at the output of the 380V bus steps down and regulates the voltage to 48V at the 48V DC bus. All the house loads are connected to the 48V DC bus, with separate wiring for each block. Each house block consists of various domestic DC appliances which are connected to the 48V DC bus. Two cases were defined for power distribution in the NG as follows:

1. Using the 380V DC bus for distribution (single wire between 380V bus and buck converter)

2. Using the 48V DC bus for distribution (four wires connecting each house block with the 48V bus)

For both cases, peak current was determined and AWG 4 wire of length 15.2 meters was selected [3].

Table 2: Wire Parameters [1]

AWG	Diameter (mm)	Area (mm^2)	Resistance (Ohms/km)
4	5.18922	21.2	0.81508

The wire was modeled using a resistor and the resistance was calculated by the following relationship:

$$Resistance = Resistance(Ohms/km) * Wire\ length\ (km)$$

3.3 PV System

Both the DC and AC NG have a PV system comprising of seven modules connected in series. The modules used are 1Soltech 1STH-35-WH with the following performance parameters. Voc=51.5V, Isc=9.4A, Vmp=43V, Imp=8.13A and Maximum Power=349.59W. The total system rating is 2.45KW. The characteristics of the modules used is shown in the figure below.

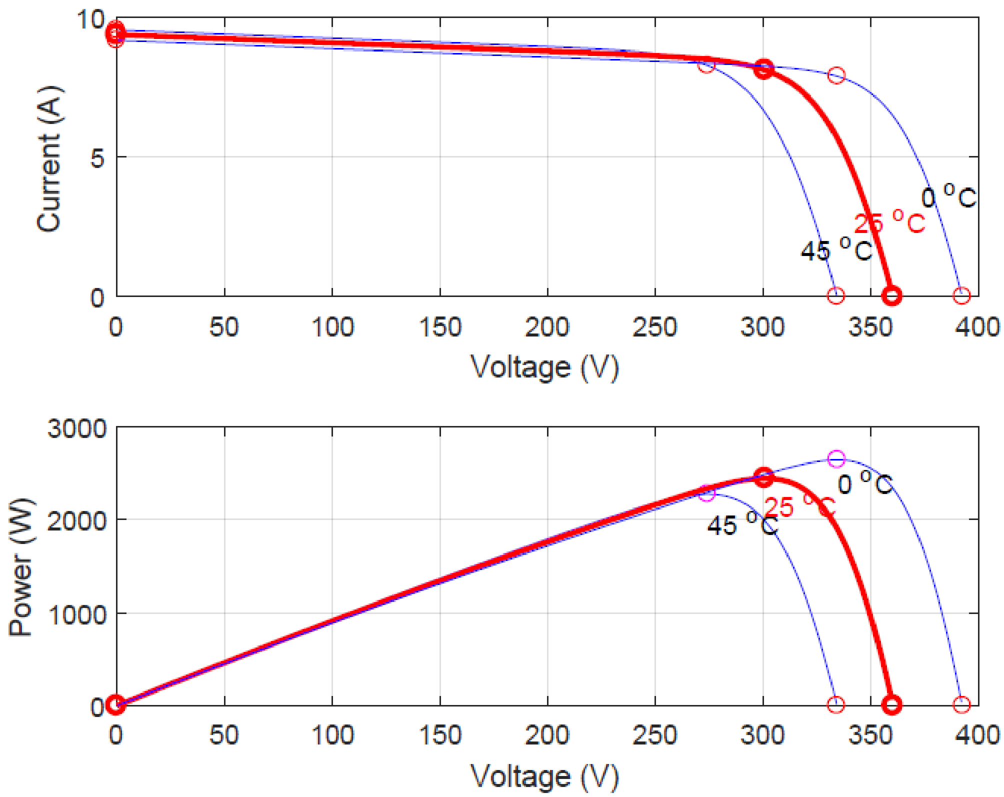

Figure 11: Nanogrid PV Array

The temperature for the PV array is set at 25°C. The data for Irradiance was obtained from Metrological High Precision Station mounted in NUST Islamabad. From the solar data, an average irradiance was calculated for some days of summer months of May and June for peak hours i.e. from 9 AM to 3 PM. The calculated average value of 816W/m^2 was used as the irradiance for the solar array in Matlab. Figure 12 shows the 24-hour irradiance data for the month of May and June, each peak in the graph represents a day. Figure 13 shows the solar irradiance data that was used.

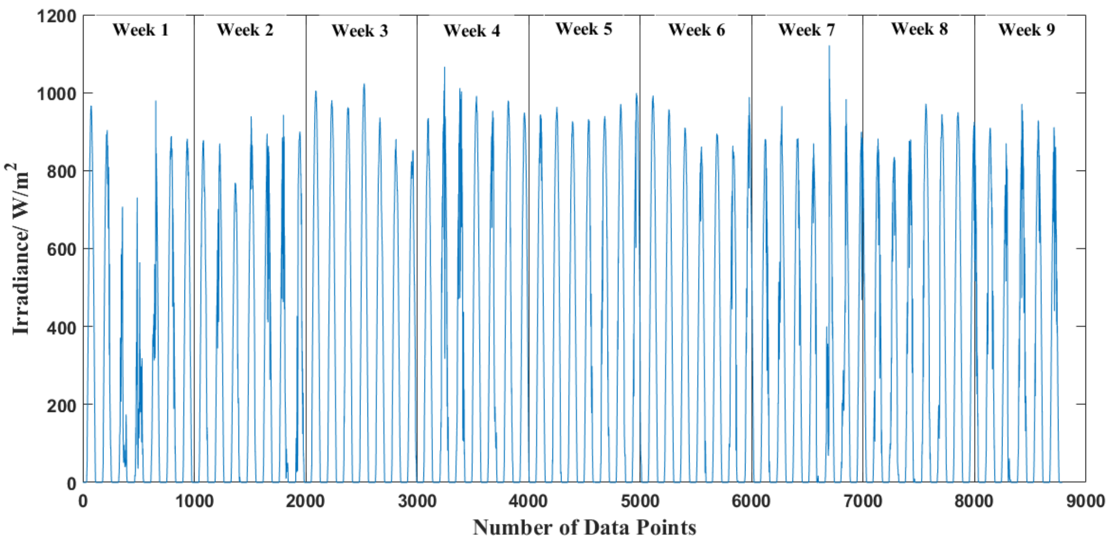

Figure 12: Solar Irradiance (24-hour) for May and June

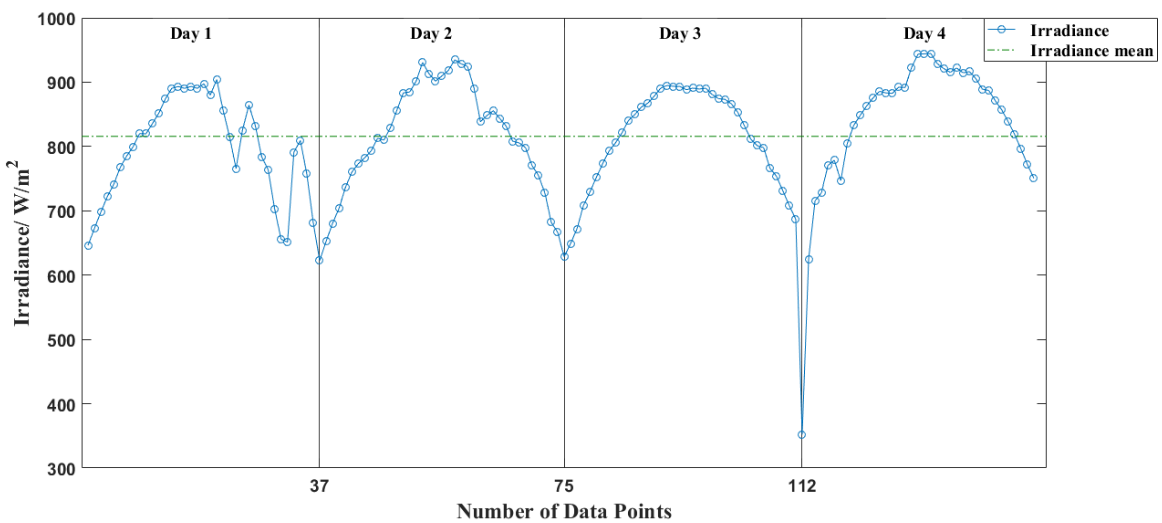

Figure 13: Solar Irradiance from 9 AM to 3 PM for some days of May and June

The PV array is connected to a boost converter which extracts maximum power from the modules using the incremental conductance MPPT technique [4]. Figure 16 shows the algorithm used in the incremental conductance method. For the DC NG the power from the PV system is fed to a 380V DC bus and for the AC NG the power is converted to AC and fed to a 230V AC bus. The figures below show the model for the PV system in both DC and AC NG.

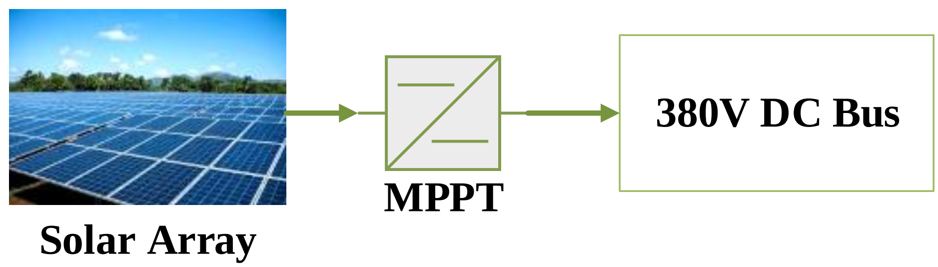

Figure 14: PV system in DC NG

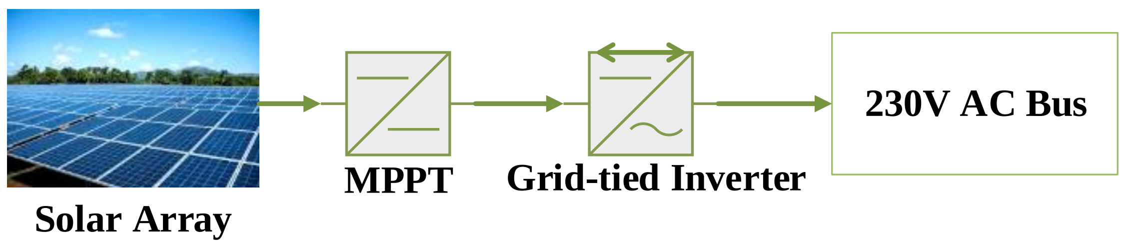

Figure 15: PV system in AC NG

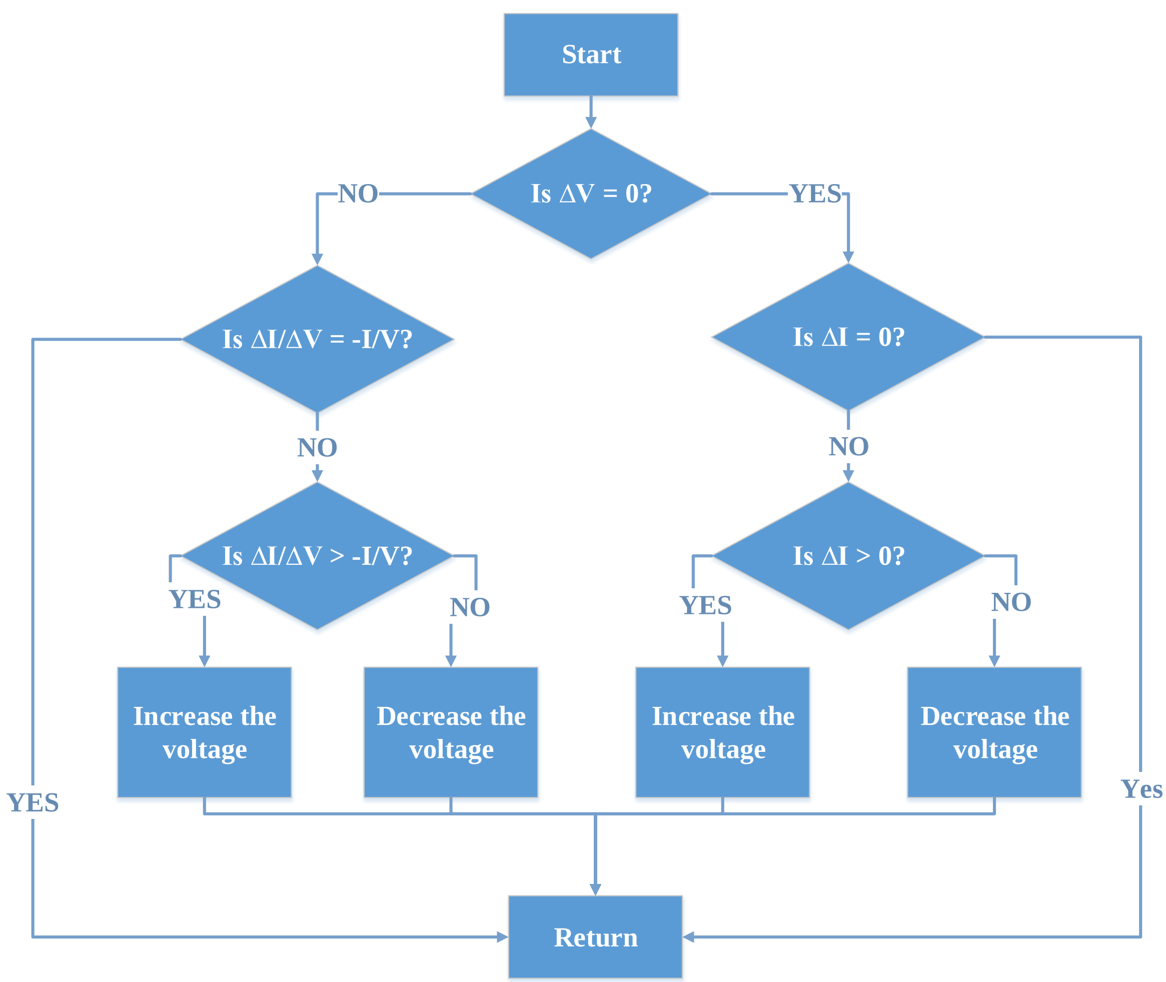

Figure 16: Incremental conductance method for MPPT [5]

3.4 Grid-Tied Inverter

The grid-tied inverter is modeled using a three-level IGBT inverter with an isolation transformer. The inverter maintains the DC bus voltage at 380V using a carrier frequency of 5 kHz for 50Hz grid frequency. The inverter controller consists of four basic components the voltage regulator, current regulator, Phase Lock Loop (PLL) and a Pulse Width Modulation (PWM) modulator which uses carrier based three-level PWM method. The voltage regulator maintains the 380V DC Bus voltage by regulating the active current reference for the current regulator. The reactive current reference is set to zero for nil reactive power injection. The current regulator then determines the required reference voltage using active and reactive current references. The PLL synchronizes with the grid voltage and provides the phase angle that is used for park transformation of voltages and currents. The PWM then generates gate pulses according to the required reference voltages to IGBT switches. The figure below shows the inverter control implemented in Matlab [6].

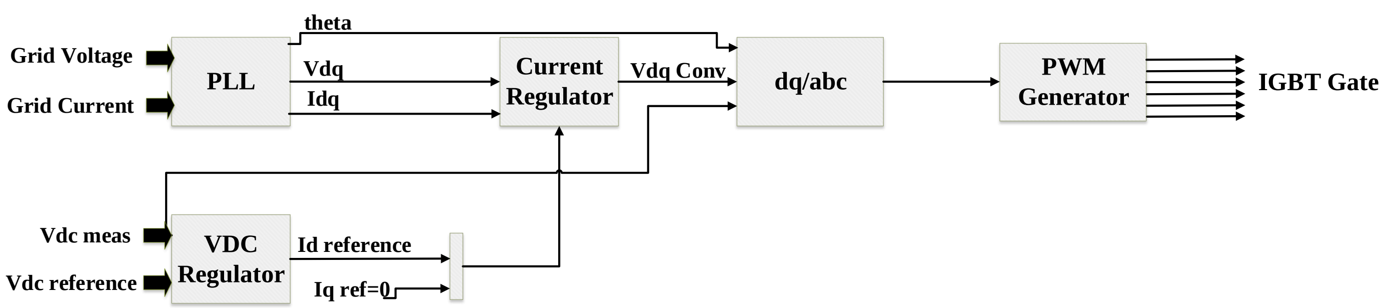

Figure 17: Grid tie Inverter Control block diagram

3.5 Electric Vehicle

The EV was modeled as a battery in Matlab. The battery model was based on Tesla’s Model S. The battery has an energy rating of 85KWh and a voltage of 375V. When charged at a voltage of 240V the battery takes 4 hours (90A) to charge completely as indicated by the datasheet [7]. The battery is connected to a Buck/Boost Converter. To charge the battery from the DC link the converter operates in buck mode and to discharge the battery the converter operates in boost mode. A state of charge (SOC) upper limit of 85% is set to prevent overcharging and a lower limit of 30% to prevent over-discharging. To prevent the converter and battery from high currents overcurrent protection is also modeled. The overcurrent protection works by limiting the duty cycle of the converter based on maximum charging or discharging current [8]. Figure 18 and 19 show the battery's characteristics as specified by the battery model in Matlab [9].

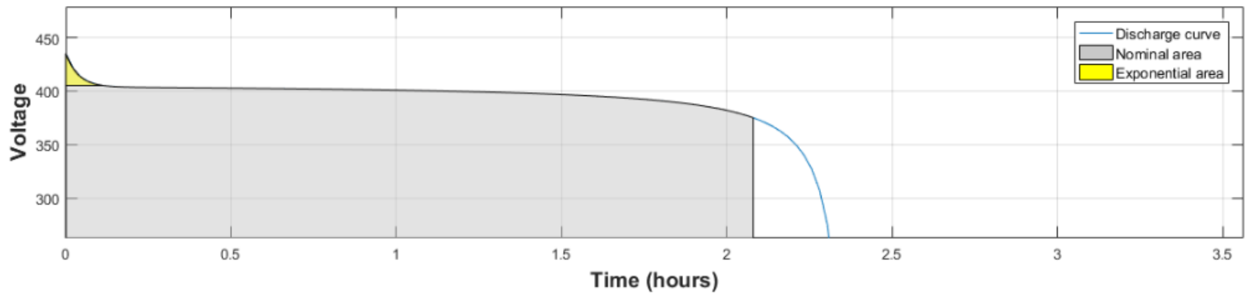

Figure 18: Nominal Current Discharge Characteristic at 0.43478C (98.6957A)

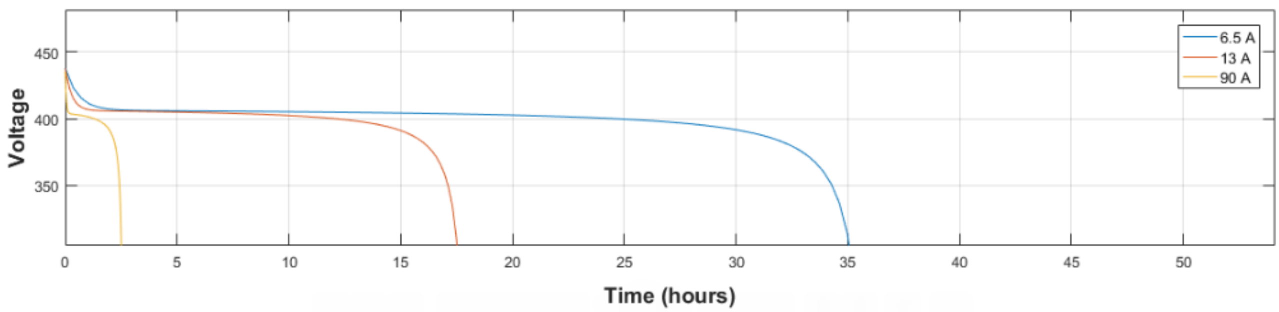

Figure 19: E0 = 406.6346, R = 0.01652, K = 0.012376, A = 31.491, B = 0.269

The figures below show the EV model implemented in Matlab.

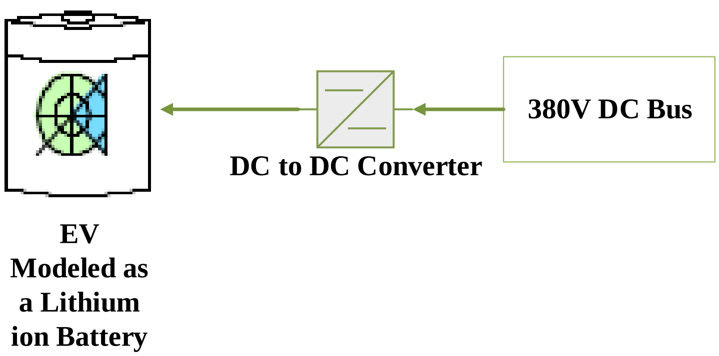

Figure 20: EV in DC NG

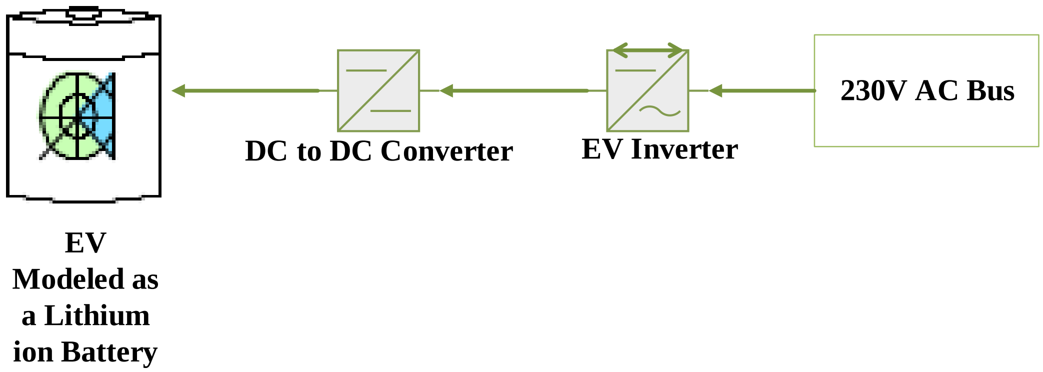

Figure 21: EV in AC NG

Figure 22 shows the buck/boost converter modeled in MATLAB for charging and discharging the battery. When charging signal is on the converter operates in buck mode and when the discharging signal is on the converter operates in boost mode.

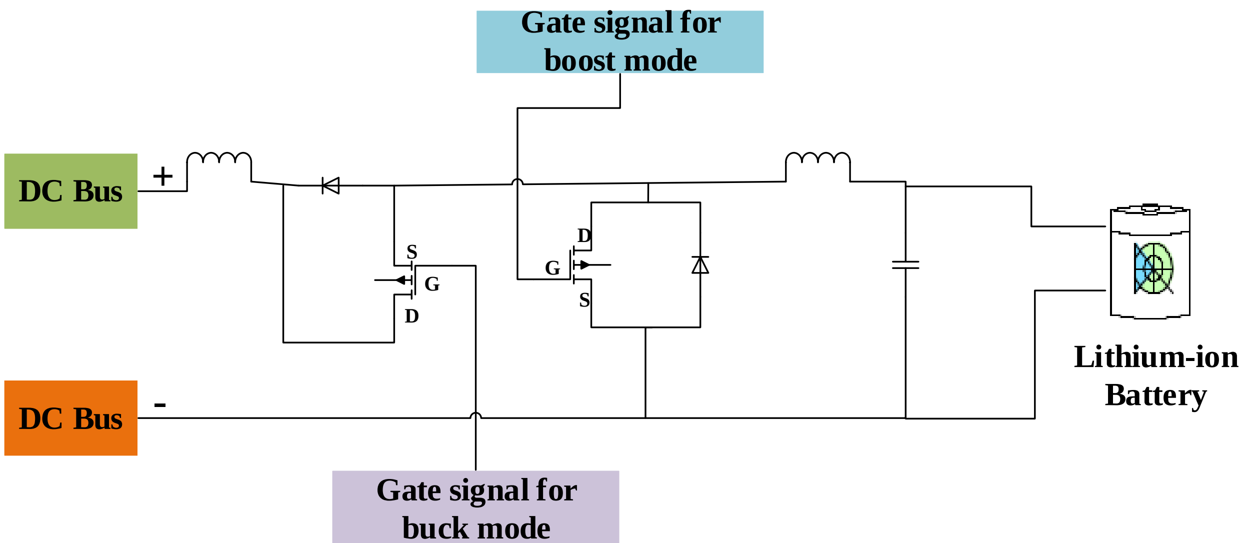

Figure 22: Buck/Boost converter for EV

Figure 23 shows the EV charging and over charging protection circuit. Maximum charging current is compared with the load current and the desired value for maximum charging current is controlled using a PI controller. This generates an upper limit for the duty cycle.

For regulating charging voltage, the reference voltage is compared with the load current and the error generated is then compared with the load voltage. The reference voltage is maintained using a PI controller. Then using a saturation dynamic block, the output from the PI controller is compared with the duty cycle limit, generated by comparison of the maximum charging current and load current. This protects the circuit from over charging. The output from the saturation dynamic block acts as an input to the PWM generator which generates pulses according to the required reference voltage to the MOSFET gate.

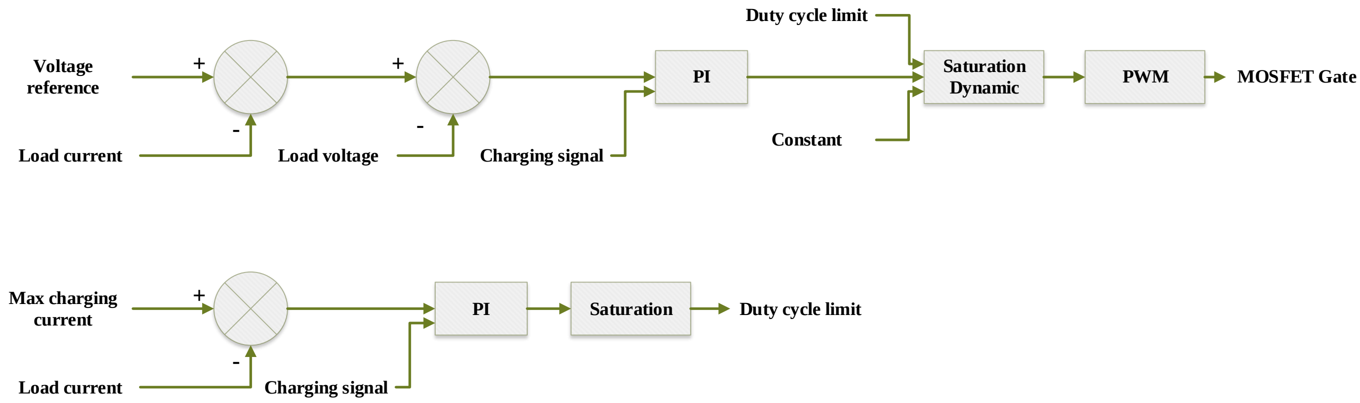

Figure 23: EV charging and over charging protection circuit

Figure 24 shows the EV discharging and over discharging protection circuit. Maximum discharging current is compared with the load current and the desired value for maximum discharging current is controlled using a PI controller. This generates an upper limit for the duty cycle.

For regulating discharging voltage, the reference voltage is compared with the load current and the error generated is then compared with the bus voltage. The reference voltage is maintained using a PI controller. Then using a saturation dynamic block, the output from the PI controller is compared with the duty cycle limit, generated by comparison of maximum discharging current and load current. This protects the circuit from over discharging. The output from the saturation dynamic block acts as an input to the PWM generator which generates pulses according to the required reference voltage to the MOSFET gate.

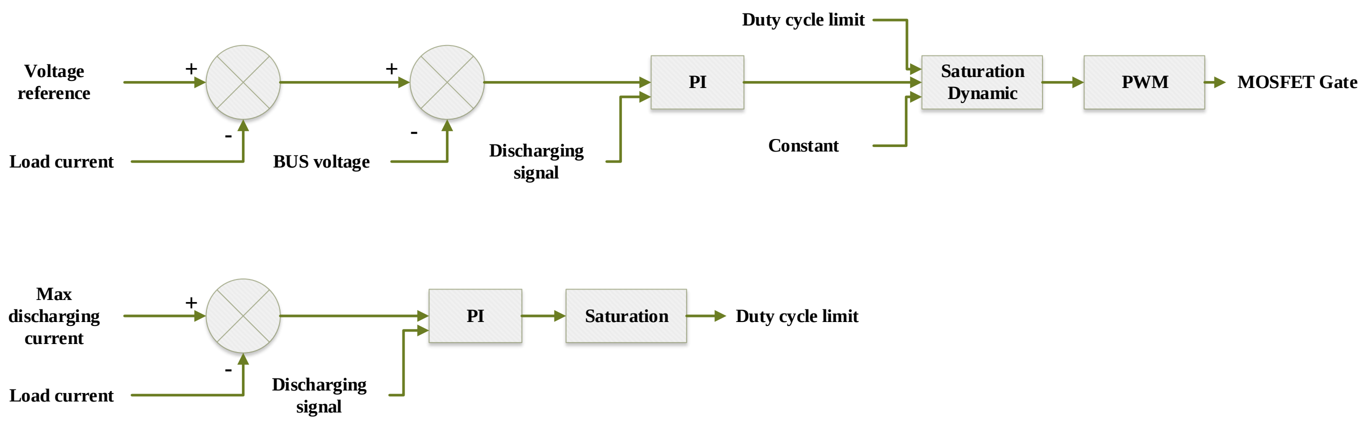

Figure 24: EV discharging and over discharging protection circuit

3.6 House Model

The house consists of four main blocks the living room, two bedrooms, and a kitchen. The loads are distributed within the four rooms as shown in the table.

Table 3: Load Distribution within the house

Block	LED Light	LED TV	Laptop	Fan	Air conditioner	Refrigerator	Miscellaneous Load
Living Room	✓	✓	×	✓	✓	×	×
Bedroom 1	✓	×	✓	✓	✓	×	×
Bedroom 2	✓	×	✓	✓	✓	×	×
Kitchen	✓	×	×	✓	×	✓	✓

3.7 DC Load Modeling

A total of seven DC loads are modeled in the DC NG. These include LED light, LED TV, DC fan, laptop, DC air conditioner, DC refrigerator and miscellaneous load.

3.7.1 LED Light

The LED light is modeled based on LED E26 model [10]. The lamp has a working voltage of 45 to 60 volts DC with recommended use at 48V. It consumes 0.21A and has a power consumption of 10W. The LED light has a lumen capacity of 950. The light is modeled using 10 diodes connected in series each having a forward voltage drop of 3.2V. A current limiting resistor is also added in series with the diodes. In the network, the bulb works at 48V with a power consumption of 10W as described in the datasheet. Figure 25 and 26 show the implementation of LED light in DC and AC NG respectively.

Figure 25: LED Light in DC NG

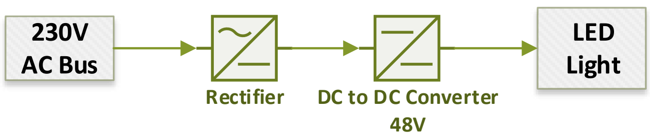

Figure 26: LED Light in AC NG

3.7.2 Laptop

The laptop is modeled based on Dell Inspiron N5110 model [11]. The laptop works on 19.5V and has a maximum power consumption of 90W and a normal power consumption of 46W which was checked through Intel Power Gadget 3.0. For modeling the laptop two cases were considered, a worst case in which the laptop consumes 90W and a normal case in which the laptop uses 46W. Both cases were modeled using resistors, for the 90W scenario a 4.221-ohm resistor was used and for the 46W scenario an 8.266-ohm resistor was used. Since the laptop is connected to a 48V bus and the working voltage is 19.5 a buck converter is used to step down and regulate the voltage at 19.5V. Figure 27 and 28 show the implementation of Laptop in DC and AC NG respectively.

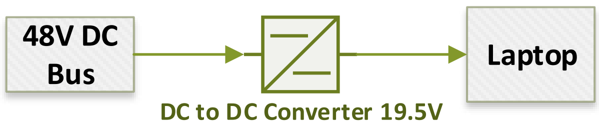

Figure 27: Laptop in DC NG

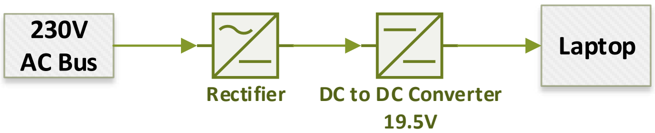

Figure 28: Laptop in AC NG

3.7.3 LED TV

The LED TV model is based on DC-Powered 21”/24” TV [12]. The TV has a working voltage of 48V and a power consumption of 30W. The LED TV is also modeled using a resistor of 76.8 ohms. Figure 29 and 30 show the implementation of LED TV in DC and AC NG respectively.

Figure 29: LED TV in DC NG

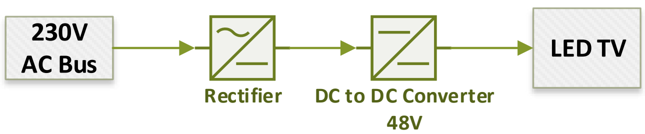

Figure 30: LED TV in AC NG

3.7.4 DC Fan

The fan model is based on 42” ceiling fan which has a working voltage of 24V and a power consumption of 14.4W [13]. A brushless DC motor is used in the fan construction. In Simulink, the fan is modeled using a permanent magnet DC machine. The parameters for the motor are set as described in the product datasheet. Since the fan is connected to the 48V bus and the working voltage is 24V, a buck converter is used to step down and regulate the voltage at 24V. Figure 32 shows the implementation of DC fan and DC refrigerator in DC NG.

3.7.5 DC Refrigerator

The refrigerator is modeled using the GEI-90C4 90 liters solar freezer [14]. It has a working voltage of 24V and a power consumption of 60W. It has a cooling performance of -18°C at 30°C ambient temperature. A brushless DC motor is used in the compressor construction. In the study, the refrigerator is modeled using a permanent magnet DC machine and the motor parameters are set as described in the product datasheet. Since the refrigerator is connected to the 48V bus and the working voltage is 24V, a buck converter is used to step down and regulate the voltage at 24V.

Figure 31: DC Fan/Refrigerator in DC NG

3.7.6 DC Air conditioner

The air conditioner model is based on HSAC-15C/C DC air conditioner [15]. It has a working voltage of 48V and a power consumption of 770W. The air conditioner has a cooling capacity of 15000 BTU/h. In compressor construction, brushless DC motor is used. In Simulink, the air conditioner is modeled using a permanent magnet DC machine. The motor parameters are tweaked according to the product specification sheet. Figure 29 shows the implementation of DC air conditioner in DC NG.

For current limiting, at the load size, current limiters are added to the motor loads as the motor draws a huge current at startup. A resistive network at the input of motor loads is used to limit the current. When the current is below the overcurrent value a switch bypasses the resistive network.

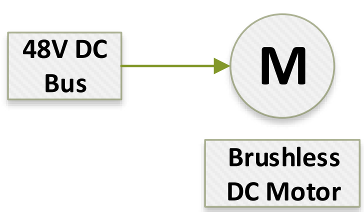

Figure 32: DC Air conditioner in DC NG

3.7.7 DC to DC converter control and overcurrent protection

Figure 31 shows the DC to DC convert control and over current protection circuit. Maximum charging current is compared with the load current and the desired value for maximum charging current is controlled using a PI controller. This generates an upper limit for the duty cycle.

For regulating charging voltage, the reference voltage is compared with the output voltage. The reference voltage is maintained using a PI controller. Then using a saturation dynamic block, the output from the PI controller is compared with the duty cycle limit, generated by comparison of the maximum charging current and load current. This protects the circuit from over currents. The output from the saturation dynamic block acts as an input to the PWM generator which generates pulses according to the required reference voltage to the MOSFET gate.

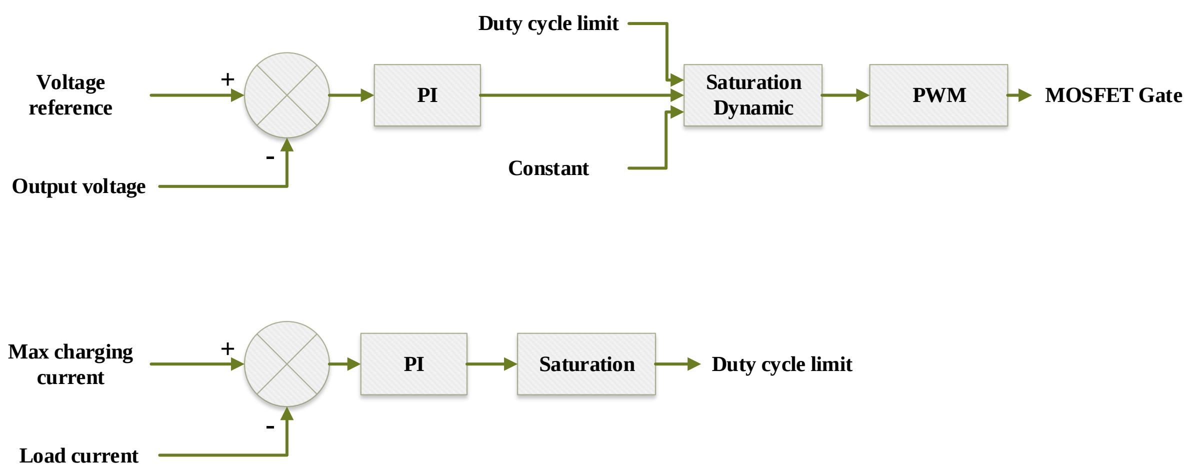

Figure 33: DC to DC converter control and overcurrent protection

3.7.8 Miscellaneous Load

The miscellaneous load is modeled using a simple resistor. The main purpose of adding this load is to balance power between the four blocks of the house.

3.8 AC Load Modeling

Four AC loads are modeled in the AC NG network, a fan, refrigerator, air conditioner and a miscellaneous load.

3.8.1 Air conditioner

For a fair comparison between the DC and AC air conditioner such an AC air conditioner is selected which has the same BTU/h (15000) as the DC air conditioner. The air conditioner model is based on DAIKIN K(E) Series (SEER 18) and has a working voltage of 230V and a power consumption of 1250W [16]. A split phase induction motor is used in compressor construction. In Simulink, the split phase asynchronous machine is used to model the air conditioner and the motor parameters are set as specified in the datasheet.

3.8.2 Fan

For a fair comparison between the DC and AC fan such an AC fan is used which has the same revolutions per minute (125) as the DC fan. Westinghouse 78545 Hercules ceiling fan with a voltage of 230V and a power consumption of 41W is used to model the fan [17]. The motor used in the fan construction is split phase induction motor and in MATLAB the fan is modeled using a split phase asynchronous machine, using motor parameters as described in the specification sheet.

3.8.3 Refrigerator

For a fair comparison between the DC and AC refrigerator such an AC refrigerator is selected which has the same cooling performance (-18°C) as the DC refrigerator. The refrigerator model is based on WHF300S2D with a working voltage of 230V and a power consumption of 142W [18]. Refrigerator compressor is made using a split phase induction motor. In Simulink, a split phase asynchronous machine is used to model the refrigerator and the motor parameters are selected as specified in the product datasheet. Figure 34 shows the implementation of the air conditioner, fan and refrigerator in AC NG.

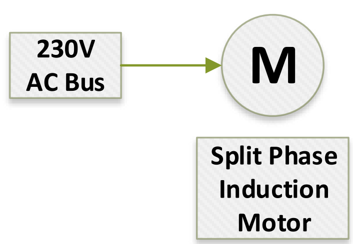

Figure 34: Air conditioner/Fan/Refrigerator in AC NG

3.8.4 Miscellaneous Load

The miscellaneous load is modeled using a simple resistor. The main purpose of adding this load is to balance power between the three phases.

Summary

This chapter gives details about the modeling of DC and AC NG. Architecture for the DC and AC NG made in Simulink is explained. Various components of the NG such as PV system, grid-tied inverter, EV and loads are explained in detail. DC and AC load modeling of six devices are included and all appliances are based on commercially available products. System protection is also explained which includes overcurrent protection and circuit breakers.

References

[1] Solaris, “American Wire Gauge Conductor Size Table,” vol. 0000. pp. 53–55.

[2] “Wire Inductance.” [Online]. Available: https://www.eeweb.com/toolbox/wire-inductance. [Accessed: 16-Oct-2017].

[3] “Part 1: Choosing the Correct Wire Size for a DC Circuit - Blue Sea Systems.” [Online]. Available: https://www.bluesea.com/resources/1437. [Accessed: 16-Oct-2017].

[4] “MPPT Algorithm - MATLAB & Simulink.” [Online]. Available: https://www.mathworks.com/discovery/mppt-algorithm.html. [Accessed: 22-Oct-2017].

[5] “MPPT charge controller techniques.” [Online]. Available: http://microcontrollerslab.com/mppt-charge-controller-techniques/. [Accessed: 14-Nov-2017].

[6] “250-kW Grid-Connected PV Array - MATLAB & Simulink.” [Online]. Available: https://www.mathworks.com/help/physmod/sps/examples/250-kw-grid-connected-pv-array.html. [Accessed: 16-Oct-2017].

[7] “Tesla Model S,” 2017. [Online]. Available: http://www.roperld.com/science/teslamodels.htm. [Accessed: 15-Oct-2017].

[8] “Fig ure 1: Overa ll battery sys stem connect ted to a three e-phase grid.” Manitoba HVDC Research Centre a division of Manitoba Hydro International Ltd., pp. 1–17, 2017.

[9] “Implement generic battery model - Simulink.” [Online]. Available: https://www.mathworks.com/help/physmod/sps/powersys/ref/battery.html. [Accessed: 16-Oct-2017].

[10] “Bulb 10 Watt LED Warm White E26 48V.” [Online]. Available: http://www.led-cfl-lighthouse.com/product/Bulb-10W-LED-48V-WW G60S. [Accessed: 16-Oct-2017].

[11] “Dell Inspiron 15R (N5110) Review | NotebookReview.com.” [Online]. Available: http://www.notebookreview.com/notebookreview/dell-inspiron-15r-n5110-review/. [Accessed: 16-Oct-2017].

[12] “DC - Powered 21"/24" TV.” [Online]. Available: http://www.cygni.com/products/48v-dc-appliances/. [Accessed: 16-Oct-2017].

[13] “DC Ceiling & Floor Fans 12 volt, 24 volt and 48 volt.” [Online]. Available: http://www.soldonsun.com/Pr/App/DC-4BladeFan.html. [Accessed: 16-Oct-2017].

[14] “90 Liters Solar Freezer.” [Online]. Available: http://www.geinnovations.net/Solar-

Freezer.html. [Accessed: 16-Oct-2017].
[15] "Solar Air Conditioner HSAC-15C/C – Harvest Air Conditioner Limited." [Online]. Available: http://www.harvest.cn/solar-air-conditioner-hsac-15cc/. [Accessed: 16-Oct-2017].
[16] E. Efficiency and A. Z. Capabilities, "Daikin." Daikin, p. 76, 2013.
[17] "Westinghouse 78545 Hercules ceiling fan, 132 cm - Decswitch.com." [Online]. Available: https://www.decswitch.com/westinghouse-78545-hercules-ceiling-fan-132-cm.html. [Accessed: 16-Oct-2017].
[18] "Horizontal Deep Freezer." [Online]. Available: https://www.indiamart.com/proddetail/horizontal-deep-freezer-3483657462.html. [Accessed: 16-Oct-2017].

CHAPTER 4

Simulation Results and Discussion

This chapter discusses the case studies designed for the loss analysis. The results of the loss analysis are also given. An economic analysis between the DC and AC devices is also discussed.

4.1 Case Studies

Three case studies were made as follows to calculate the losses in both networks. Case 1 included load usage from Monday to Friday, Case 2 was made for Saturday and Case 3 included scenarios for Sunday. The losses were calculated for a 24-hour period for each case. Since the scenarios for Monday to Friday are similar, the results include losses calculated over a three-day period (Monday, Saturday, and Sunday).

4.1.1 Case 1

Table 4: Case 1 Monday to Friday (Load usage)

Time	Living Room	Bedroom 1	Bedroom 2	Kitchen	PV	EV
12 am to 7 am	Not used	Fan, A/C	Fan, A/C	Fridge, misc. load	Not used	Not used
7 am to 9 am	2 Lights, 2 Fans, TV	Light, Fan, Laptop	Light, Fan, Laptop	Fridge, misc. load, Light, Fan	Not used	Not used
9 am to 12 pm	Not used	Light, Fan, Laptop	Not used	Fridge, misc. load, Light, Fan	Used	Not used
12 pm to 3 pm	Not used	Light, Fan, Laptop, A/C	Not used	Fridge, misc. load, Light, Fan	Used	Not used
3 pm to 5	Not used	Light, Fan,	Not used	Fridge, misc.	Not	Not used

pm		Laptop		load, Light, Fan	used	
5 pm to 9 pm	2 Lights, 2 Fans, TV, A/C	Not used	Not used	Fridge, misc. load, Light, Fan	Not used	Charging
9 pm to 12 am	Not used	Light, Fan, Laptop	Light, Fan, Laptop	Fridge, misc. load	Not used	Not used

4.1.2 Case 2

Table 5: Case 2 Saturday (Load usage, 5 pm to 12 pm house is empty)

Time	Living Room	Bedroom 1	Bedroom 2	Kitchen	PV	EV
12 am to 9 am	Not used	Fan, A/C	Fan, A/C	Fridge, misc. load	Not used	Not used
9 am to 10 am	Light, Fan, TV	Not used	Not used	Fridge, misc. load, Light, Fan	Used	Charging
10 am to 12 pm	Light, Fan, TV	Light, Fan, Laptop	Light, Fan, Laptop	Fridge, misc. load, Light, Fan	Used	Charging
12 pm to 1 pm	Light, Fan, TV	Light, Fan, Laptop, A/C	Light, Fan, Laptop, A/C	Fridge, misc. load, Light, Fan	Used	Charging
1 pm to 3 pm	Light, Fan, TV	Light, Fan, Laptop, A/C	Light, Fan, Laptop, A/C	Fridge, misc. load, Light, Fan	Used	Not used
3 pm to 5 pm	Light, Fan, TV	Light, Fan,	Light, Fan,	Fridge, misc. load, Light, Fan	Not used	Not used

		Laptop	Laptop			
5 pm to 12 pm	Not used	Not used	Not used	Not used	Not used	Not used

4.1.3 Case 3

Table 6: Case 3 Sunday (Load usage)

Time	Living Room	Bedroom 1	Bedroom 2	Kitchen	PV	EV
12 am to 9 am	Not used	Fan, A/C	Fan, A/C	Fridge, misc. load	Not used	Not used
9 am to 10 am	Light, Fan, TV	Not used	Not used	Fridge, misc. load, Light, Fan	Used	Not used
10 am to 12 pm	Light, Fan, TV	Light, Fan, Laptop	Light, Fan, Laptop	Fridge, misc. load, Light, Fan	Used	Not used
12 pm to 3 pm	Light, Fan, TV	Light, Fan, Laptop, A/C	Light, Fan, Laptop, A/C	Fridge, misc. load, Light, Fan	Used	Not used
3 pm to 5 pm	Light, Fan, TV	Light, Fan, Laptop	Light, Fan, Laptop	Fridge, misc. load, Light, Fan	Not used	Not used
5 pm to 9 pm	Light, Fan, TV	Light, Fan, Laptop	Light, Fan, Laptop	Fridge, misc. load, Light, Fan	Not used	Charging
9 pm to 12 am	Light, Fan, TV	Light, Fan, Laptop	Light, Fan, Laptop	Fridge, misc. load, Light, Fan	Not used	Not used

4.2 Steady State Loss Analysis

4.2.1 Breakdown of Energy Losses in the DC NG

In the DC NG the total loss in the system was calculated using the following equation:

$$Total\ Loss\ in\ DC\ nanogrid = Total\ Line\ Loss + Total\ Device\ Loss + Converter\ and\ Conversion\ Losses$$

Figure 35 shows the breakdown of energy loss in the DC NG for all three cases.

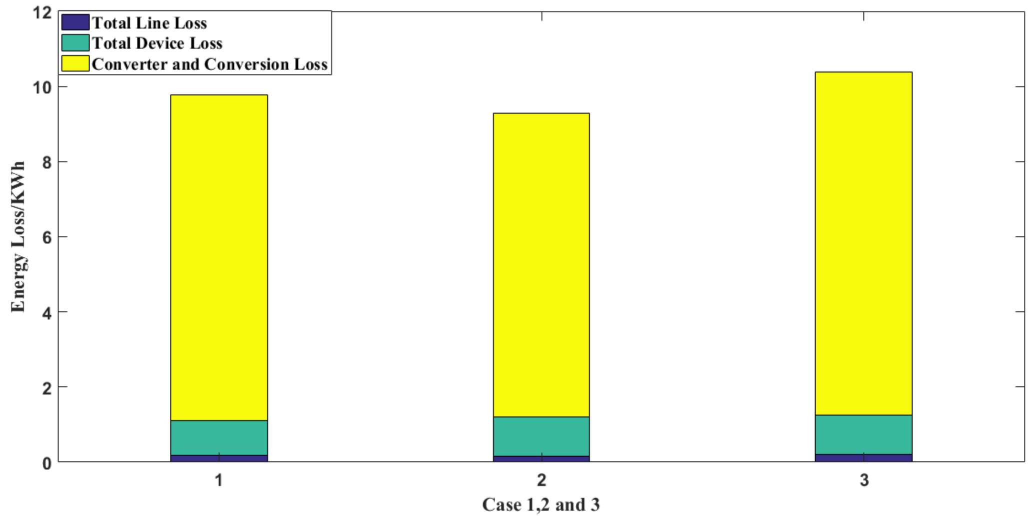

Figure 35: Breakdown of losses in the DC NG for all three cases

4.2.2 Distribution Line Losses at the 380V DC Bus vs 48V DC Bus

As mentioned earlier two cases were considered for power distribution in the DC NG. Figure 36 shows the results for distribution line losses using 380V DC Bus vs 48V DC Bus for all three cases. It is clear from the results that distribution at 380V has less energy loss as compared to distribution at 48V. This was expected as $P = V * I$ indicates that at a higher voltage energy loss decreases. But in the NG 48V was selected for power distribution the reason being safety and commercial availability of domestic appliances at 48V. Although 380V Bus provides less energy loss such a high voltage poses a great safety risk [1]. Moreover, as commercially available devices were selected for the simulation none of them were available at 380V, therefore 48V was selected for distribution within the DC NG.

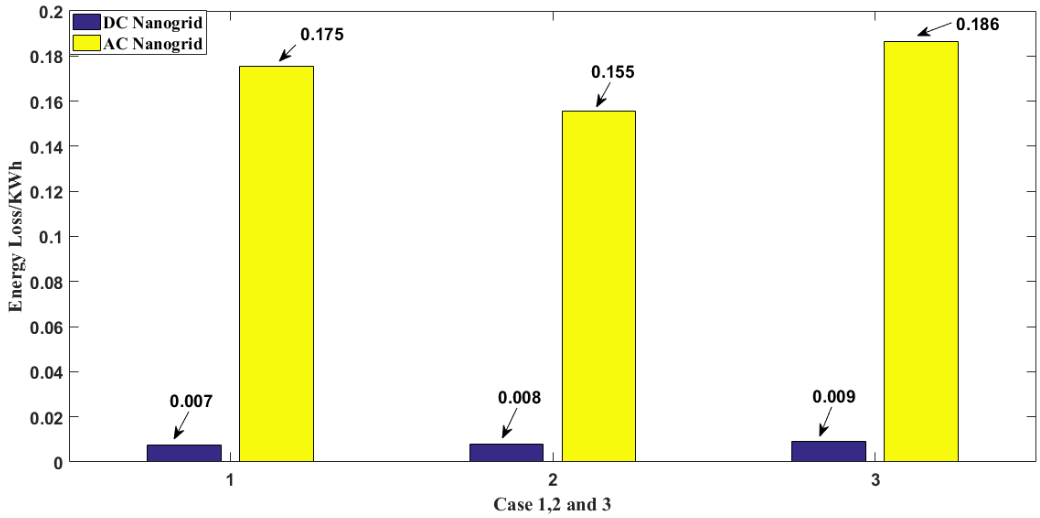

Figure 36: Distribution line losses using 380V DC Bus vs 48V DC Bus for all three cases

4.2.3 Breakdown of Energy Losses in the AC NG

Figure 37 shows the breakdown of energy losses in the AC NG for all three cases.

The energy loss for the AC NG was calculated using the following relationship:

$$\begin{aligned} &Total\ energy\ loss \\ &\quad = Total\ line\ loss + Total\ device\ loss + Converter\ and\ Conversion\ Losses \\ &\quad + Reactive\ Power\ Loss \end{aligned}$$

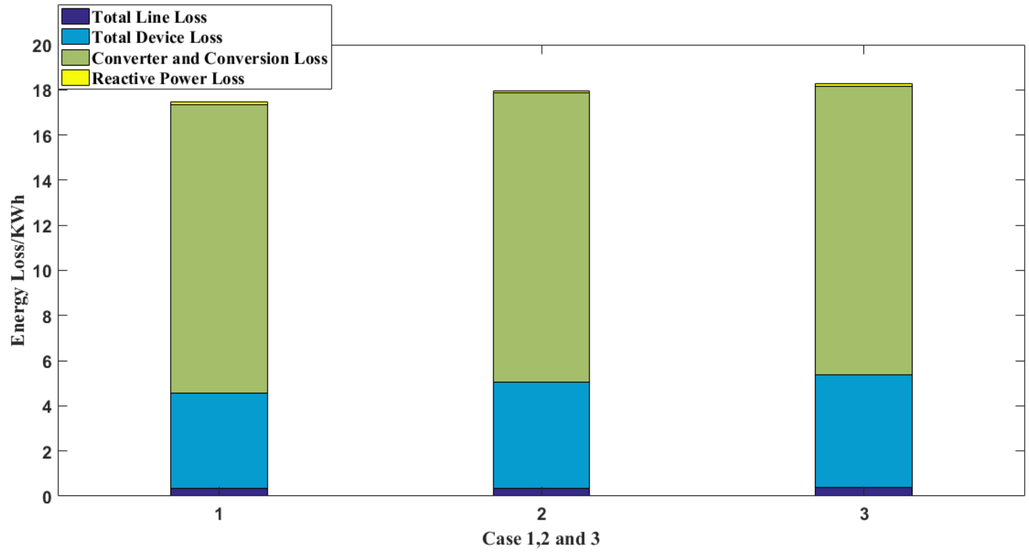

Figure 37: Breakdown of losses in the AC NG for all three cases

4.2.4 Comparison of Line Losses between the DC and AC NG

Figure 38 shows the comparison of line losses between the DC and AC NG. It is evident from the bar graph that there are fewer line losses in the DC NG as compared to the AC NG. The reason for this is more efficient DC appliances in the DC NG which require less current as compared to their AC counterparts. This reduction in current thus causes fewer line losses in the DC NG. Furthermore, AC network has an additional reactive power loss in distribution which is not present in the DC NG.

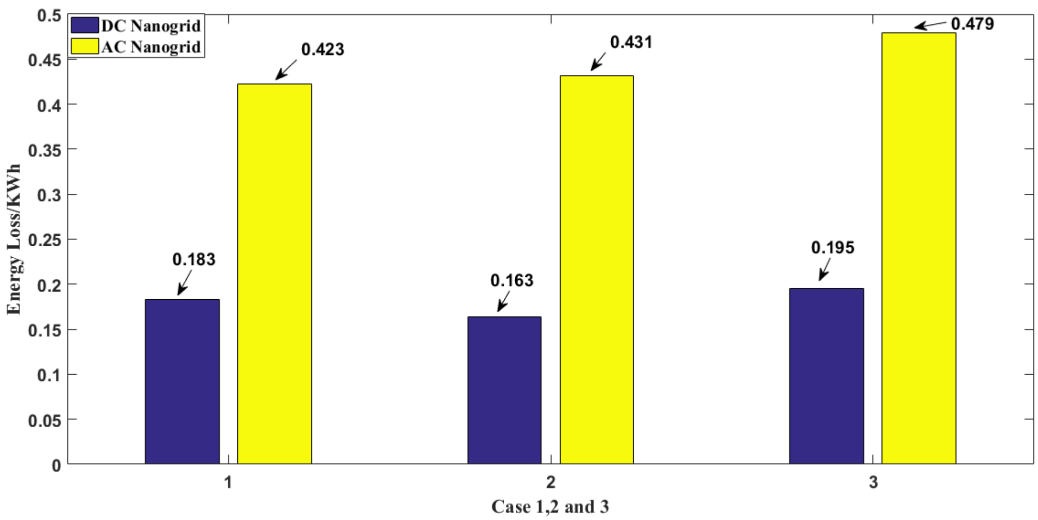

Figure 38: Total line losses in the DC NG vs AC NG for all three cases

4.2.5 Comparison of Device Losses between the DC and AC NG

Figure 39 shows a comparison between device losses in the DC and AC NGs. The results indicate that device losses in a DC NG are fewer. This is because DC appliances are more energy efficient and there are no conversion losses in the devices in the DC NG [2]. A brushless DC motor used for modeling DC motor loads in the DC NG is approximately 95% efficient [3], [4], [5] whereas the split phase induction motor used for modeling AC loads in the AC network has around 87% efficiency [6], [7]. Therefore, for loss calculation, 5% loss was considered for the brushless DC motor and 13% loss was considered for the split phase induction motor as dictated by their respective efficiencies. Moreover, AC-DC conversion in DC devices (Laptop, LED light, LED TV) present in the AC network was considered 95% efficient [8] with a 5% loss. This is an additional loss in the AC NG. Due to these respective efficiencies and no conversion losses

(AC to DC) in DC devices present in the DC NG, there are fewer devices losses in the DC network as compared to AC.

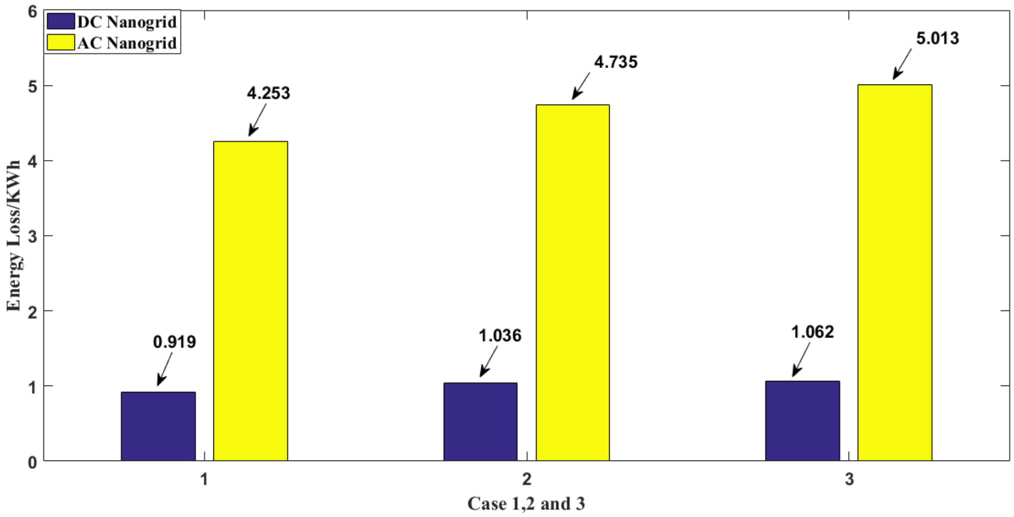

Figure 39: Total Device losses in the DC NG vs AC NG for all three cases

4.2.6 Comparison of Converter and Conversion Losses between the DC and AC NG

Figure 40 shows the comparison between total converter and conversion losses in the DC and AC NG. The converter and conversion losses in the DC NG comprised of

1. AC to DC conversion from the grid
2. DC to DC conversion from MPPT
3. DC to DC conversion for EV charging
4. DC to DC conversion between the 380V and 48V Bus.

In the AC NG, the converter and conversion losses included

1. DC to DC conversion from MPPT
2. DC to AC conversion of solar output into the 230V AC Bus,
3. AC to DC conversion for EV
4. DC to DC conversion for EV charging.

Using efficiency curves [9] the efficiency of AC to DC or DC to AC (Grid-tied inverter) conversion was considered 92% with an 8% loss whereas DC to DC conversion was considered 95% efficient with a 5% loss. It is clear from the figure that converter and conversion losses are less in the DC network the reason being the respective efficiency of AC to DC and DC to DC conversions and fewer AC to DC or DC to AC conversions in the DC NG.

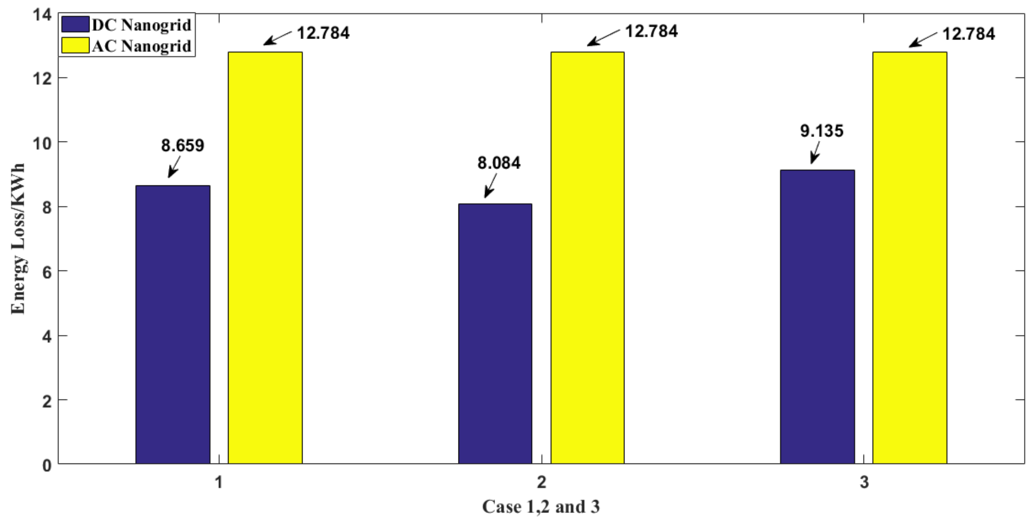

Figure 40: Total Converter and Conversion losses in the DC NG vs AC NG for all three cases

4.2.7 Comparison of Total Losses between the DC and AC NG

The total losses in both DC and AC NG are the sum of all the losses mentioned in Figure 35 and 37. Figure 41 shows the cumulative losses in a DC and AC NG. As line losses, device losses and conversion losses are less in the DC NG, the total system losses in the DC NG are fewer as compared to the AC NG as shown by the bar graph. This shows that a DC NG is better than an AC NG when compared on the basis of energy efficiency [10].

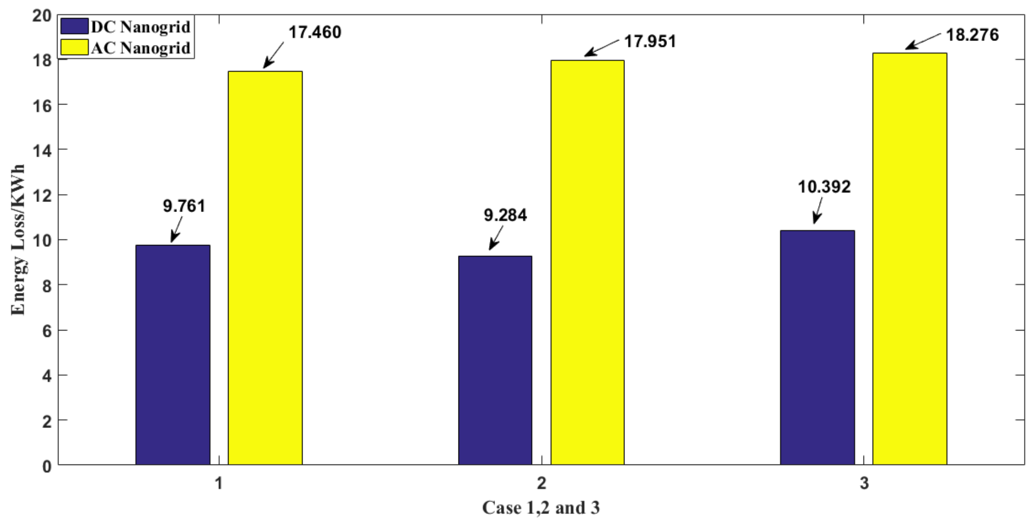

Figure 41: Total system losses in the DC NG vs AC NG for all three cases

4.2.8 Comparison of Power Drawn from the Grid between the DC and AC NG

The figure below shows the total power drawn from the grid for both DC and AC NG. It is clear the in a DC NG less power is drawn due to the high efficiency of the network.

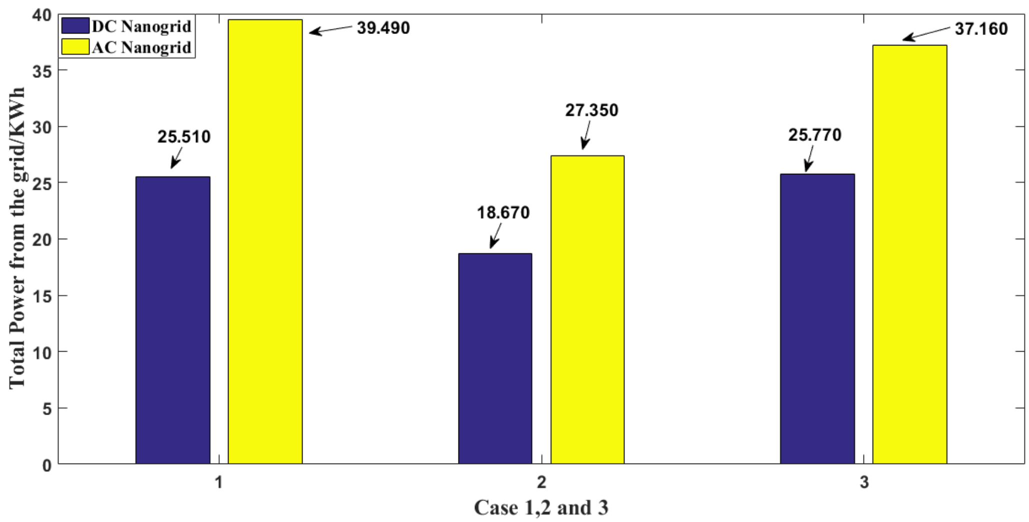

Figure 42: Total power from the grid in the DC NG vs AC NG for all three cases

Another advantage of a DC NG is less energy usage from the grid which consequently leads to fewer electric bills. Net power was calculated for both networks using the following relationship:

$$Net\ power = Total\ power\ from\ grid - Power\ from\ PV$$

Figure 43 clearly shows that net power drawn in a DC NG is less as compared to the AC NG. This is because of high system efficiency in a DC NG and availability of efficient DC devices which provide the same features at less wattage as compared to the AC devices. Therefore, energy losses are reduced in the DC NG and less power is drawn from the grid. This has immense importance for the consumers as less power from the grid means that a DC NG user will have to pay less electric bills as compared to an AC NG user.

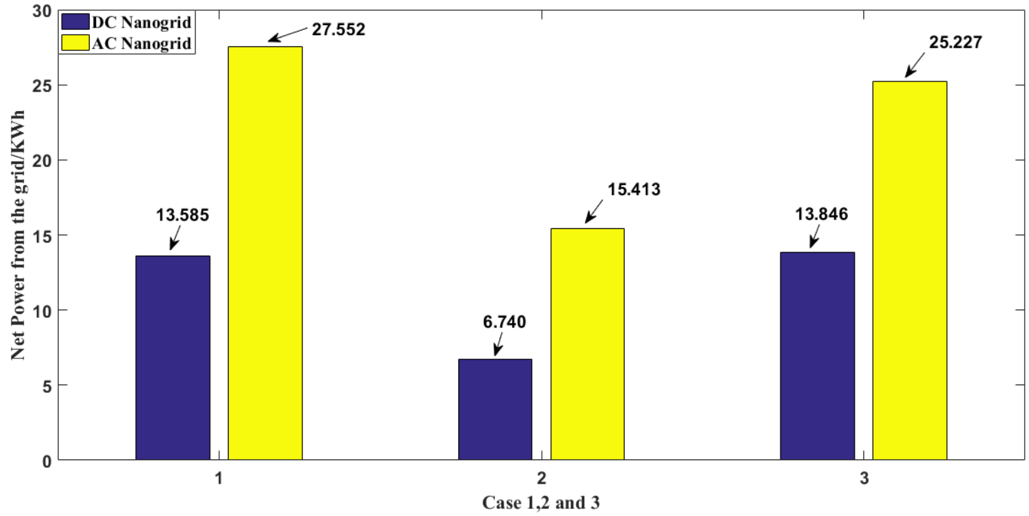

Figure 43: Net power= (Total power from grid-Power from PV) from the grid in the DC NG vs AC NG for all three cases

4.3 Economic Analysis

An economic analysis was performed between the DC and AC loads i.e. air conditioner, fan, and refrigerator. The other DC loads were excluded as those are common in both the DC and AC network. It is clear from the loss analysis that in terms of efficiency DC devices are better, this analysis was performed to determine how those energy savings affect the payback period and if it is feasible to use DC devices since their upfront cost is higher as compared to AC devices. The table below shows the cost of DC and AC devices used in both networks. For both the DC and AC air conditioners the price for 12000 BTU/h model was used as the price for15000 BTU/h model was not available.

Table 7: Cost of DC and AC Devices [11], [12], [13], [14], [15], [16]

	DC Fan	**AC Fan**	**DC Refrigerator**	**AC Refrigerator**	**DC Air conditioner**	**AC Air conditioner**
Cost (rupees)	15,593	13,907	31,608	25,000	15,8040	14,2130
Total Cost (rupees) (No. of	77,965	69,535	31,608	25,000	47,4120	42,6390

devices*cost)						

The total cost of DC devices= Rs. 58,3423

The total cost of AC devices= Rs. 52,0925

Figure 44 shows that the upfront cost of DC devices is more as compared to AC devices.

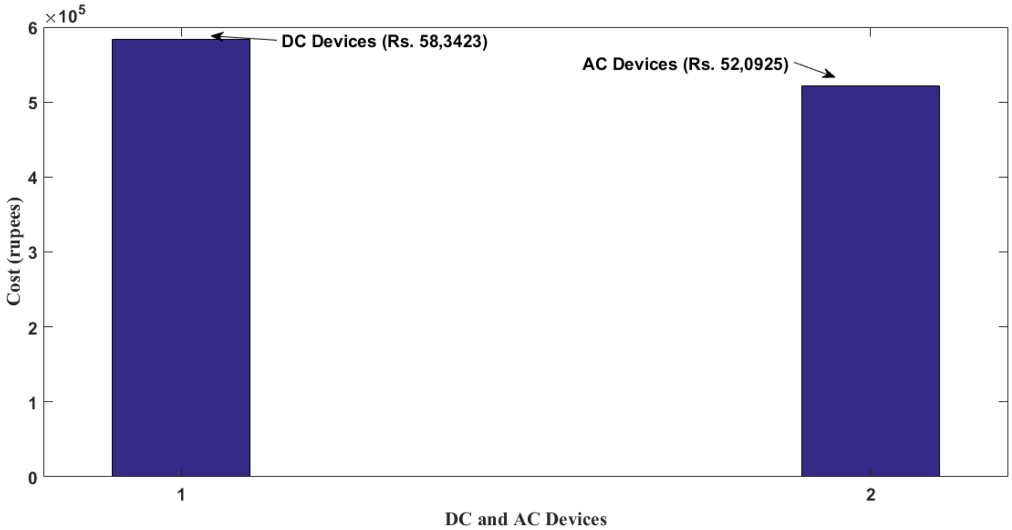

Figure 44: Cost of DC vs AC Devices

Extra cost of DC devices= 58,3423-52,0925= Rs. 62,498

Considering an average unit price of Rs. 13 [17] the total energy bills per month for the DC and AC NG can be computed as follows.

Units used in a month in the DC NG= 354.0 KWh

Units used in a month in the AC NG= 713.6 KWh

The monthly bill for a user in DC NG= 354*13= Rs. 4,602

The monthly bill for a user in AC NG= 713.6*13= Rs. 9,277

Figure 45 shows that the electric bill for DC devices is less as compared to AC devices.

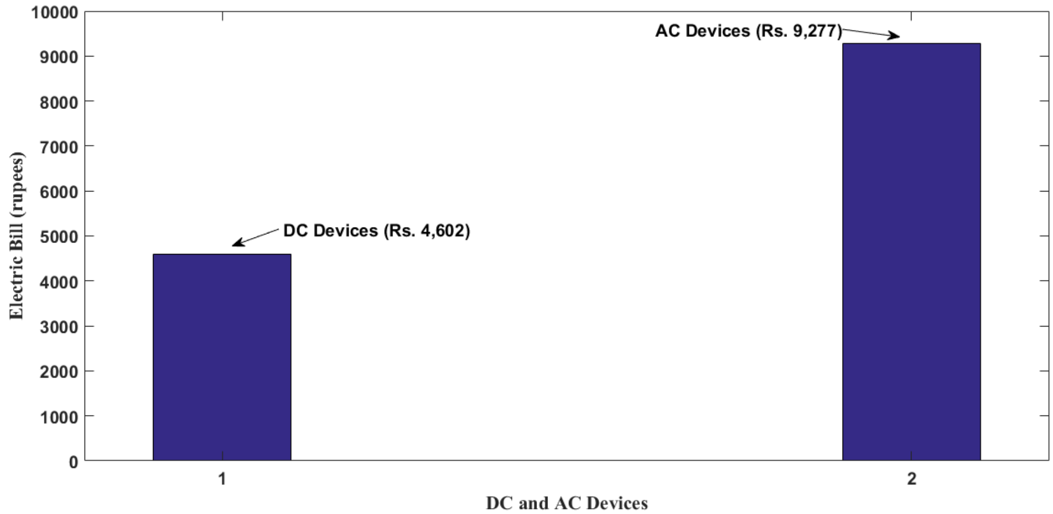

Figure 45: Monthly Bill of DC vs AC Devices

Monthly savings using a DC NG= 9,277-4,602= Rs. 4,675

Payback period for the extra cost of DC device= 62,498/4,675= 13.4 (13 and a half months)

According to this economic analysis although the upfront cost of DC devices is more than the AC devices due to the higher efficiency of DC devices, the electric bill is also reduced. The extra amount paid for the DC devices can be recovered approximately in thirteen and a half months because of the reduced electric bills.

Summary

In this chapter, detail is provided about the three case studies which are used to perform the loss analysis. The loss analysis is based on the line losses, device losses, and converter and conversion losses in both NG. The results show that in terms of efficiency a DC NG is better than an AC NG. A transient analysis is performed to check the system protection. A fault is generated at T=2 sec and the circuit breakers can successfully disconnect the loads. An economic analysis is also done on DC and AC devices. The results show that although DC devices are costly but due to their efficiency energy bill is also reduced and the extra cost of the DC device can be easily recovered.

References

[1] N. Rasmussen, “AC vs . DC Power Distribution for Data Centers,” 2011.

[2] A. Goikoetxea, J. María, C. Roberto, P. Zumeta, P. Epele, and H. Gipuzkoa, “DC versus AC in residential buildings : efficiency comparison,” pp. 3–7, 2006.

[3] M. Rao, “Energy efficient Ceiling fans using BLDC motors- A practical implementation.”

[4] “Koford Engineering.” [Online]. Available: http://www.koford.com/. [Accessed: 17-Oct-2017].

[5] “The 2016 Motor Controller — Duke Electric Vehicles,” 2016. [Online]. Available: http://www.duke-ev.org/blog/2016/11/27/the-2016-motor-controller. [Accessed: 17-Oct-2017].

[6] “Electric motors energy efficiency reference guide,” 2007.

[7] R. K. Rajput, “A Textbook of Electrical Engineering - R. K. Rajput.” [Online]. Available: https://books.google.com.pk/books?id=k22bKyWqWD0C&printsec=frontcover#v=onepage&q=Split phase induction motor with 87%25 efficiecny&f=false. [Accessed: 17-Oct-2017].

[8] “An Efficiency Primer for Switch-Mode, DC-DC Converter Power Supplies - Application Note - Maxim,” *Maxim Integrated*, 2016. [Online]. Available: https://www.maximintegrated.com/en/app-notes/index.mvp/id/4266. [Accessed: 17-Oct-2017].

[9] K. Mikhaylov, J. Tervonen, and D. Fadeev, “Development of Energy Efficiency Aware Applications Using Commercial Low Power Embedded Systems,” no. March, 2011.

[10] A. T. Elsayed, A. A. Mohamed, and O. A. Mohammed, “DC microgrids and distribution systems: An overview,” *Electr. Power Syst. Res.*, vol. 119, pp. 407–417, 2015.

[11] “DC Ceiling & Floor Fans 12 volt, 24 volt and 48 volt.” [Online]. Available: http://www.soldonsun.com/Pr/App/DC-4BladeFan.html. [Accessed: 17-Nov-2017].

[12] “Westinghouse 78545 Hercules ceiling fan, 132 cm - Decswitch.com.” [Online]. Available: https://www.decswitch.com/westinghouse-78545-hercules-ceiling-fan-132-cm.html. [Accessed: 17-Nov-2017].

[13] “Horizontal Deep Freezer at Rs 25000 /piece(s) | Domjur | Kolkata | ID: 3483657462.” [Online]. Available: https://www.indiamart.com/proddetail/horizontal-deep-freezer-3483657462.html. [Accessed: 17-Nov-2017].

[14] "Solar Deep Freezer 90 Liters Mini - Buy Freezer Deep,Freezer 90 Liters,Freezer Mini Product on Alibaba.com." [Online]. Available: https://www.alibaba.com/product-detail/solar-deep-freezer-90-liters-mini_60660101235.html?spm=a2700.7724857.main07.116.2c79dfbfnQ0pxI. [Accessed: 17-Nov-2017].

[15] "DC 48V Solar Air Conditioner with CE Certificate (HSAC-15C/C) for sale – Solar Air Conditioner manufacturer from china (95126062)." [Online]. Available: http://harvestair.sell.everychina.com/p-95126062-dc-48v-solar-air-conditioner-with-ce-certificate-hsac-15c-c.html. [Accessed: 17-Nov-2017].

[16] "Daikin 12000 BTU Heat Pump Air Conditioner 19 SEER FTX12NMVJU / RX12NMVJU | eBay." [Online]. Available: https://www.ebay.com/itm/Daikin-12000-BTU-Heat-Pump-Air-Conditioner-19-SEER-FTX12NMVJU-RX12NMVJU/231934769044?epid=1640427657&hash=item360063b794:g:9ZUAAOSwubRXK8am. [Accessed: 17-Nov-2017].

[17] "LESCO - Electricity Tariff." [Online]. Available: http://www.lesco.gov.pk/3000063. [Accessed: 17-Nov-2017].

CHAPTER 5

Conclusion and Recommendations

This chapter discusses the conclusion and recommendations of the study.

5.1 Conclusion

There is a huge debate at present between the use of AC and DC systems. This paper makes a comparison between a DC and AC NG based on system losses to determine which network is more efficient. A DC and AC NG network were modeled in Matlab with main components including a PV array, grid-tied inverter, electric vehicle and various domestic loads modeled on commercially available products. Case studies were then developed to measure the system losses in both networks. The results clearly indicate that losses in a DC NG are fewer as compared to an AC NG. The reason for this is more efficient DC devices and their increased accessibility, fewer power conversions in a DC system and availability of DC power (PV) and storage (EV) sources. Furthermore, the analysis also shows that a DC NG user draws less energy from the grid because of fewer losses and more efficient devices. This results in fewer electric bills and more economic benefit to a DC NG user. Although the cost of DC devices is more than the AC devices according to the economic analysis performed in this study the savings due to reduced electric bills in a DC NG can recover the extra cost within a period of 14 months. Thus, this study shows that a DC NG is better in terms of energy efficiency than an AC NG and also offers economic benefit to the user and therefore should be preferred in places where efficiency is a top priority.

5.2 Recommendations

- A more detailed modeling of DC and AC loads can be done in a future study.
- Work can be done on improving the system protection.
- A Hybrid NG can be designed and compared to the DC and AC NG.
- The economic analysis can be extended and done in more detail by including the cost of the whole system for both NG.

CHAPTER 6

Photovoltaic Reliability

This chapter discusses the work that was done at Arizona State University at the Photovoltaic Reliability Lab. A brief introduction, objectives, limitations, and methodology of the study are discussed.

6.1 Introduction

Due to the depletion of fossil fuels and their damaging effects on the environment focus has shifted towards renewable energy sources [1]. Within renewable energy, the use of solar PV has increased exponentially [2], [3]. Although solar modules are considered to have a field life of approximately 25 years [4] but sometimes due to various manufacturing or field hazards the module can expire before its given time. Therefore, PV reliability is very important to make sure that the PV panel works properly as claimed by its manufacturer [5]. Photovoltaic reliability lab in Arizona, US works on reliability issues of PV modules. Their work involves predicting the lifetime of solar PV modules using statistical analysis obtained using tests such as accelerated stress testing, outdoor testing, module characterization and material characterization. The testing on PV modules is of two main types non-destructive testing and performance testing. Non-destructive testing includes tests such as visual inspection, EL imaging, IR imaging, UV imaging, monitoring using data acquisition systems, diode and circuit failure testing and electrical insulation testing [6]. Performance testing includes tests such as baseline light IV, dark IV, cell IV, quantum efficiency measurements and reflectance tests [7].

Temperature coefficients play a significant role in PV sizing. Temperature coefficients can be determined for a number of PV performance parameters such as short-circuit current, maximum power current, open circuit voltage, maximum power voltage, maximum power, FF and efficiency [8]. In the PV industry, it is considered that the Pmax temperature co-efficient of a PV module does not change as the module ages. Therefore, to determine the performance ratio of a PV module the Pmax temperature co-efficient of a new module is used. This could lead to an error in the determination of performance ratio if the assumption about the Pmax temperature co-efficient is wrong. Therefore, this study was carried out to determine if the Pmax temperature coefficient of a PV module changes over time. 24 field aged modules from four different manufacturers were tested using baseline light IV, dark IV, EL imaging, IR imaging and UV imaging. The results of the baseline light IV and dark IV were used to calculate the Pmax temperature coefficient, FF, series and shunt resistances. The results showed that the series resistance of the aged modules has increased which caused the FF to decrease and the Pmax temperature coefficient to increase. Thus, according to this study, the Pmax temperature co-efficient of aged modules does change over time as compared to the supposition used by the industry. The results of this study can help the industry in determining the performance ratio of PV modules [9].

6.2 Objectives

- Selection of 20-25 field aged modules for the study
- Performing baseline light IV on the selected modules
- Performing dark IV on the selected modules
- Calculating temperature coefficients, series and shunt resistances using the data from baseline light IV and dark IV.
- Performing EL imaging
- Performing IR imaging
- Performing UV imaging

6.3 Limitations

- Baseline light IV must be performed between 9 AM to 3 PM on a sunny day.
- Placement of thermocouple for baseline light IV can affect the results.
- Measurements for series and shunt resistance can be different from baseline light IV and dark IV.
- A completely dark room is required for performing EL.
- The module can overheat during IR imaging.
- The Proper angle must be set for UV imaging otherwise a glare can occur which can distort the images.

6.4 Methodology

- Selection of 24 field aged modules from four different manufacturers.
- Performing visual inspection on the selected modules to check for visible defects.
- Performing baseline light IV and dark IV
- Using the results from baseline light IV and dark IV to determine the temperature coefficients for six performance parameters i.e. open circuit voltage, short circuit current, maximum power voltage, maximum power current, Pmax, and FF.
- Calculating series and shunt resistances using results from baseline light IV and dark IV.
- Performing EL imaging to identify cracks or defects in the modules.
- Performing IR imaging to identify hotspots in the panels.
- Performing UV imaging to determine browning and delamination.

Summary

This chapter gives details about the project that was carried out in the Photovoltaic Reliability Lab at the Arizona State University. It gives information about the importance of PV reliability. Details about the objectives, limitation, and methodology of the study are also included in the chapter.

References

[1] "Various Disadvantages of Fossil Fuels - Conserve Energy Future." [Online]. Available: https://www.conserve-energy-future.com/disadvantages_fossilfuels.php. [Accessed: 16-Nov-2017].

[2] "Solar power growth leaps by 50% worldwide thanks to US and China | Environment | The Guardian." [Online]. Available: https://www.theguardian.com/environment/2017/mar/07/solar-power-growth-worldwide-us-china-uk-europe. [Accessed: 16-Nov-2017].

[3] F. Katiraei and J. R. Aguero, "Solar PV Integration Challenges," *IEEE Power And Energy Magazine*, vol. 9, no. 3, pp. 62–71, 2011.

[4] E. D. Dunlop, D. Halton, and H. a. Ossenbrink, "20 years of life and more: where is the end of life of a PV module?," in *Conference Record of the Thirty-first IEEE Photovoltaic Specialists Conference, 2005.*, 2005, pp. 1982–1985.

[5] J. H. Wohlgemuth, D. W. Cunningham, P. Monus, J. Miller, and A. Nguyen, "Long term reliability of photovoltaic modules," in *Conference Record of the 2006 IEEE 4th World Conference on Photovoltaic Energy Conversion, WCPEC-4*, 2007, vol. 2, pp. 2050–2053.

[6] D. Veldman, I. J. Bennett, B. Brockholz, and P. C. De Jong, "Non-destructive testing of crystalline silicon photovoltaic back-contact modules," in *Conference Record of the IEEE Photovoltaic Specialists Conference*, 2011, vol. 8, no. April, pp. 003237–003240.

[7] G. S. Kinsey, "PV Module Performance Testing and Standards Geoffrey," John Wiley & Sons, 2017, pp. 362–369.

[8] D. L. King, J. A. Kratochvil, and W. E. Boyson, "TEMPERATURE COEFFICIENTS FOR PV MODULES AND ARRAYS: MEASUREMENT METHODS, DIFFICULTIES, AND RESULTS," 1997, pp. 1183–1186.

[9] F. Mahmood *et al.*, "Temperature coefficient of power (Pmax) of field aged PV modules: impact on performance ratio and degradation rate determinations," 2017, vol. 10370, pp. 1037007–1037008.

CHAPTER 7

Experimentation and Results

This chapter discusses the methodology, results, and conclusion of the work carried out at the Photovoltaic Reliability Lab.

7.1 Methodology

7.1.1 Module Selection

A total of 24 field aged monocrystalline silicon PV modules were selected for this study. The table below shows their details.

Table 8: Details of the PV modules used

Manufacturer	Module Type	Number of Modules	Time in the field (years)	Rated Power (Watts)
A	Monocrystalline Silicon	7	18	120
B	Monocrystalline Silicon	8	18	175
C	Monocrystalline Silicon	6	18	120
D	Monocrystalline Silicon	3	19	75

The figures below show the nameplate data of the modules from all four manufacturers.

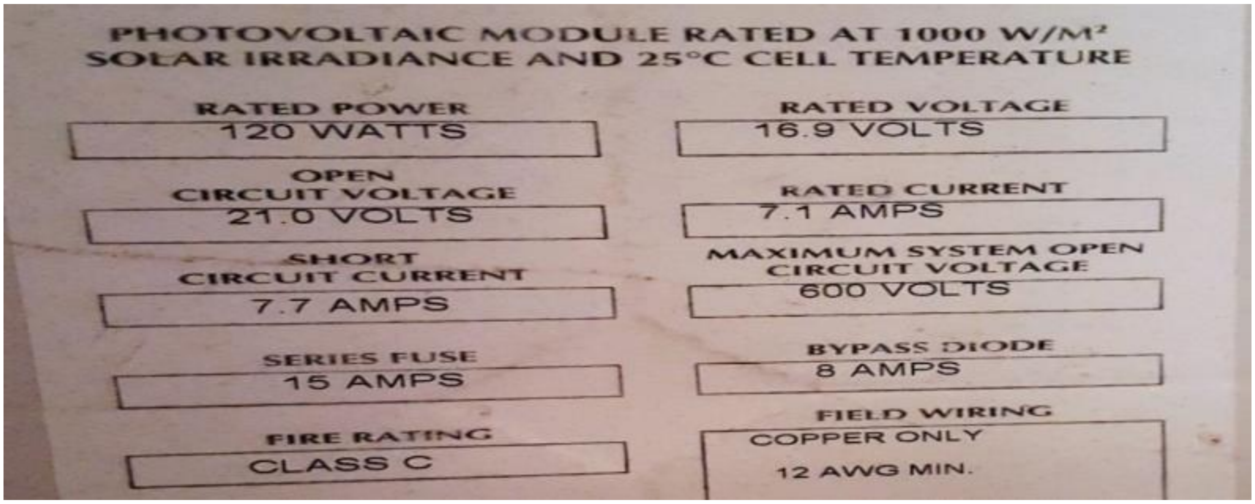

Figure 46: Nameplate data of modules from manufacturer A

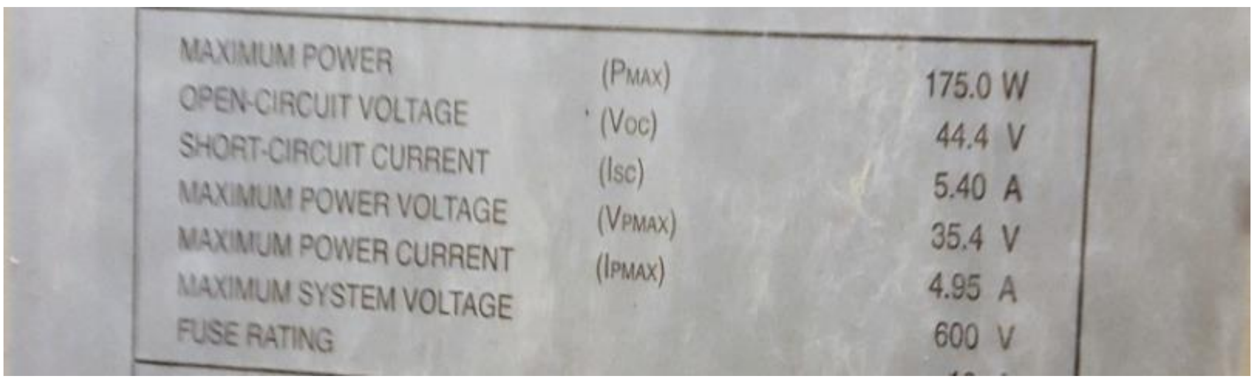

Figure 47: Nameplate data of modules from manufacturer B

Figure 48: Nameplate data of modules from manufacturer C

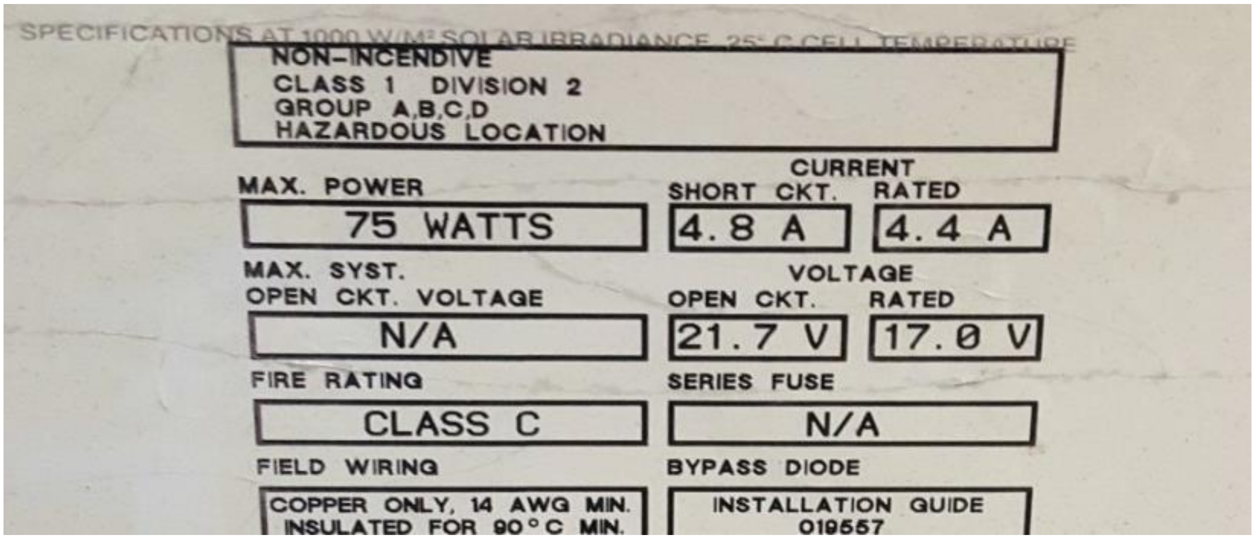

Figure 49: Nameplate data of modules from manufacturer D

Five tests were performed on all the 24 modules.

1. Baseline light IV
2. Dark IV
3. EL imaging
4. IR imaging
5. UV imaging

7.1.2 Baseline light IV

For baseline light IV the module to be tested is first kept in an environmental chamber and cooled to 15°C. Module temperature is checked using a thermocouple. Once the panel is at the desired temperature it is taken into the field covering it with a Styrofoam sheet to prevent a sudden rise in temperature. In the filed the module is placed on a two-axis mounting structure and two thermocouples are attached to the back sheet of the panel, one in the center and one towards the edge of the module. The two-axis mounting structure is adjusted to AM 1.5. The IV curves are taken on sunny days from 9 AM to 3 PM when the irradiance is close to 1000W/m^2 [1]. After placing the thermocouples, the IV tracer is attached to the module which sweeps the IV curves for the module as its temperature rises. Once the module setup is completed the Styrofoam sheet is removed and IV curves are taken as the module temperature changes from 25°C to 40°C. This process is repeated for all the other modules and the IV curves are stored. Using the data from the IV curves temperature coefficients for six PV performance parameters i.e. short-circuit current, maximum power current, short circuit voltage, maximum power voltage, Pmax, and FF are calculated. The data is also used to calculated series and shunt resistances.

7.1.3 Dark IV

For dark IV the module is placed in an environmental chamber under dark conditions at 25°C. A DC power supply is attached and fixed at the short circuit current of the module. In dark conditions, a PV panel behaves like a diode and therefore in dark IV carriers are injected into the PV panel using the DC power supply [2]. The results obtained are stored and used for calculating series and shunt resistances. The reason for calculating series and shunt resistances using both baseline light and dark IV is to cross-check the results for accuracy. The process is repeated for all other modules.

7.1.4 EL imaging

EL is carried out in a dark room using a near infra-red camera. The module is placed on a rack and attached to a DC power supply. The power supply is used to feed current into the PV panel. This process causes radiative recombination to occur and light is emitted which is detected by the near infra-red camera [3]. The process of taking EL images is done for all other modules and data is saved. EL provides a lot of information about the module. It shows defects and cracks in the module which are not visible to naked eye. It also reveals information about the uniformity of cells in the panel. The process is also very fast with and takes very less time [4].

7.1.5 IR Imaging

In IR imaging the solar module is mounted on a supporting structure outside and short-circuited. Then after five minutes, an IR camera is used to take images of the module. This process is repeated for all other modules. IR imaging displays a lot of information about the PV panel such as hotspots which are normally not visible [5]. Hotspots occur when there is a faulty cell in a string of series connected cells. The overall current of that string is limited by the faulty cell. The current from the non-faulty cells is dissipated in the faulty cell which causes a lot of heating and a hotspot occurs. This can cause cell damage, solder bond degradation or glass cracking [6].

7.1.6 UV Imaging

UV imaging is carried out in a dark room. The module is placed in a rack and several UV lamps are positioned towards the panel. The UV lamps are switched on and images of the module are taken using a camera. The process is repeated for all other modules. UV imaging reveals browning areas in a module. Browning occurs in PV modules because EVA which is used as an encapsulant in PV modules can break down when exposed to UV in the field over an extended period. Also, if the EVA used is of inferior quality this process can occur very fast. As a result of this cell, browning occurs and can also lead to cell corrosion [7].

7.2 Results and Discussion

7.2.1 Results for the Temperature Coefficient

Temperature coefficient for open circuit voltage and Pmax for all the sample set is shown in the figures 50-53 below.

The temperature coefficients for open circuit voltage are in the range from 0.3%/°C to 0.4%/°C which is the normal range for new modules. The temperature coefficient for open circuit voltage is not expected to change because it depends on the band gap of the material and as it does not change due to the aging of the module.

The temperature coefficient of Pmax observed from the results is in the range from 0.5%/°C to 0.6%/°C whereas the temperature coefficients for new modules are in the range from 0.4%/°C to 0.5%/°C. This shows that the temperature coefficient of modules increases due to aging. The reason is an increase in the series resistance which causes the FF to decrease and the temperature coefficient of Pmax to increase. Therefore, this result shows that for determining performance ratio and degradation of aged modules, the temperature coefficient of fresh modules should not be used [8].

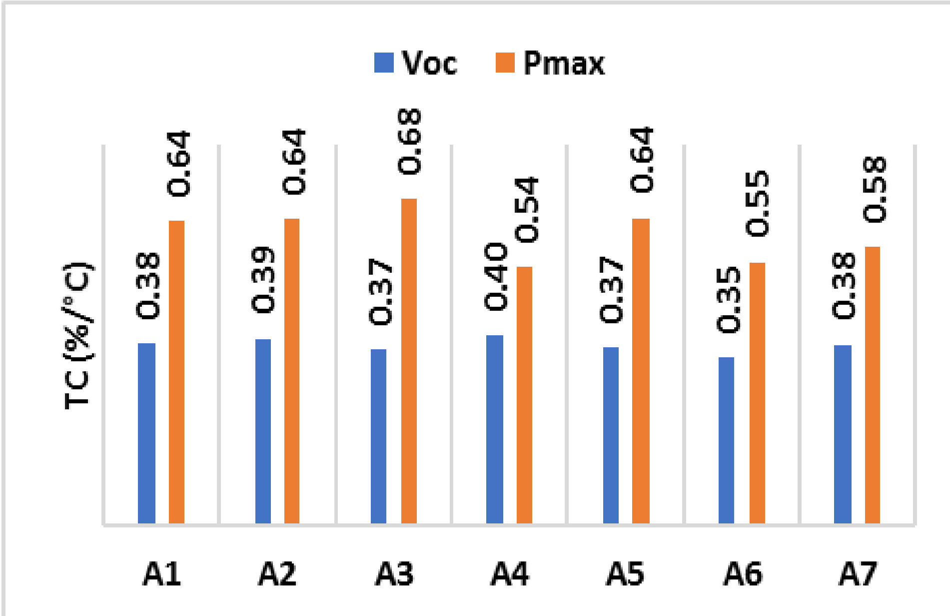

Figure 50: Temperature coefficient for Pmax and open circuit voltage for modules from manufacturer A

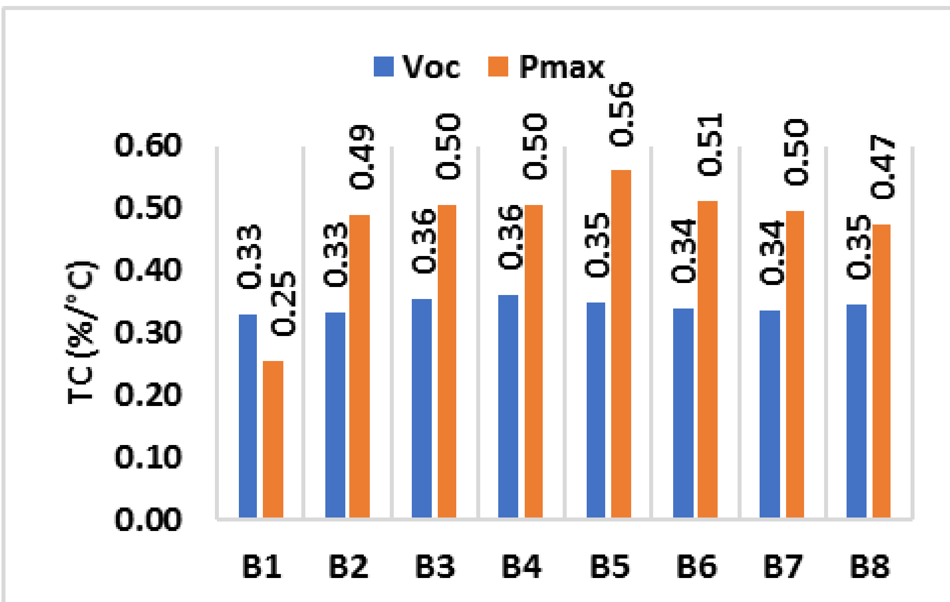

Figure 51: Temperature coefficient for Pmax and open circuit voltage for modules from manufacturer B

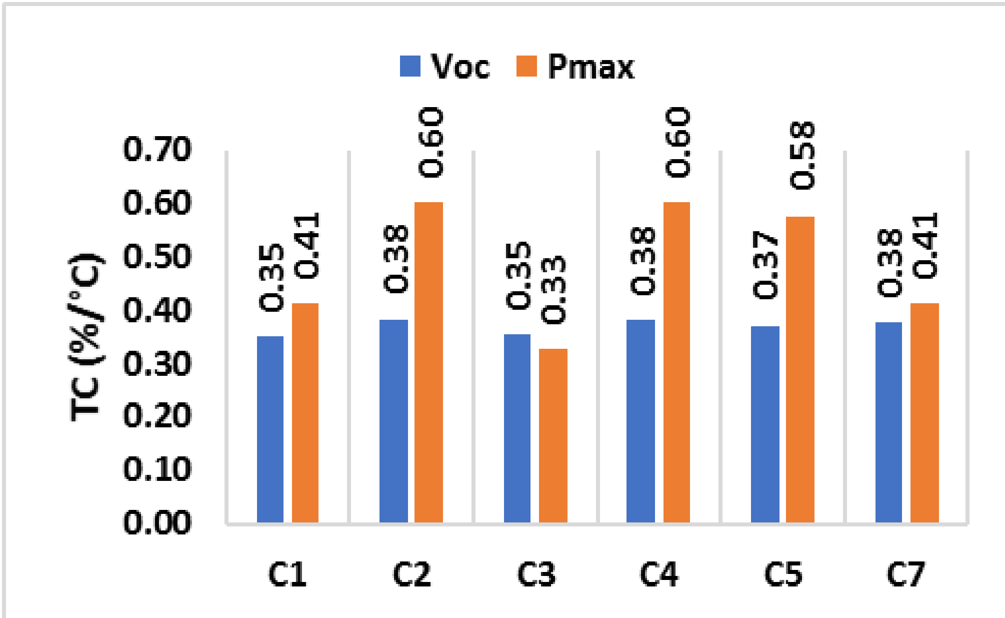

Figure 52: Temperature coefficient for Pmax and open circuit voltage for modules from manufacturer C

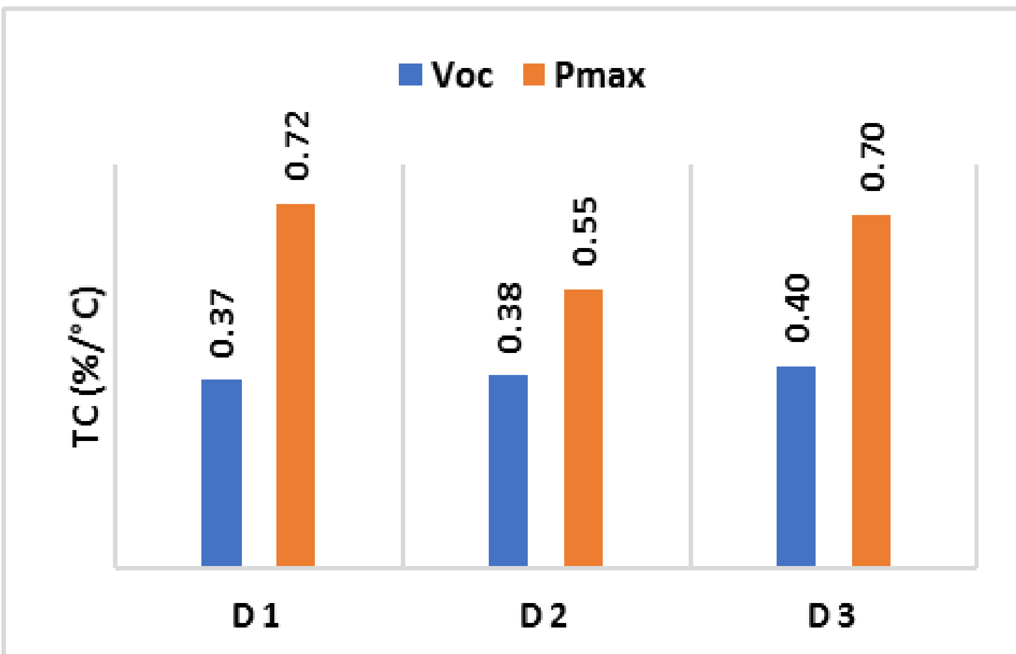

Figure 53: Temperature coefficient for Pmax and open circuit voltage for modules from manufacturer D

The figures from 54-57 show the temperature coefficient of short circuit current. The temperature coefficient of short circuit for new modules are in the range from 0.2%/°C to 0.3%/°C. The results are also in this range apart from some outliers which could be due to experimental errors such as thermocouple placement. Thus, the temperature coefficient for short circuit does not change as expected because it is dependent on the bandgap of the material which does not change due to the aging of the module [8].

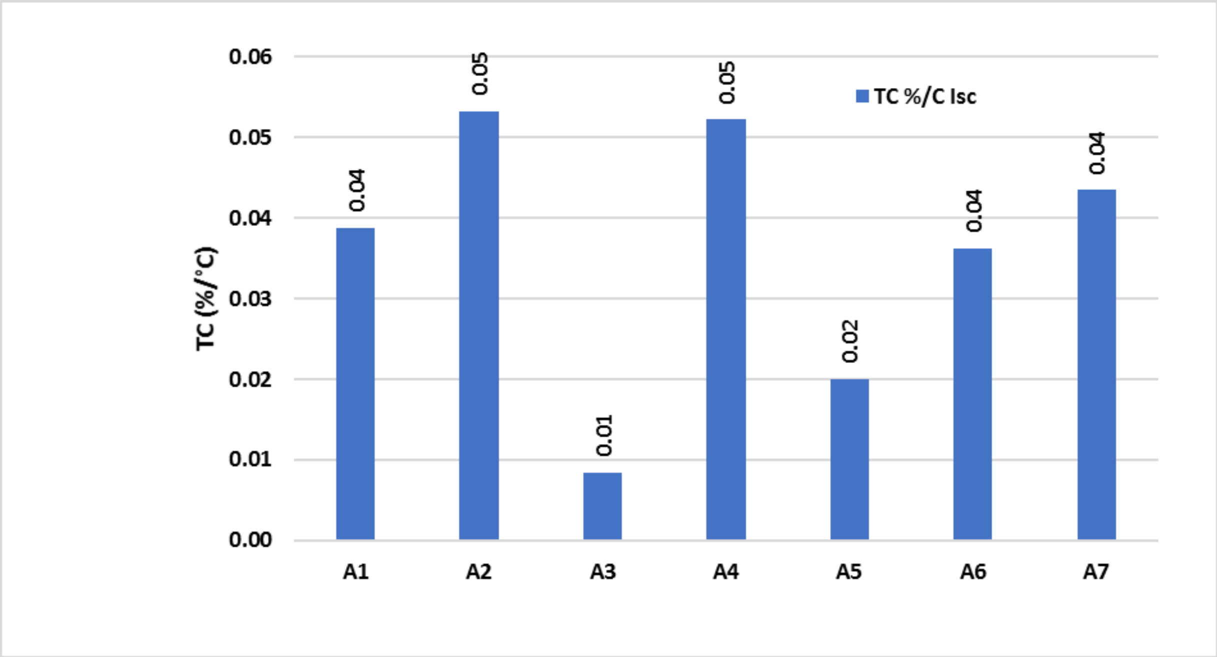

Figure 54: Temperature coefficient for short circuit current for modules from manufacturer A

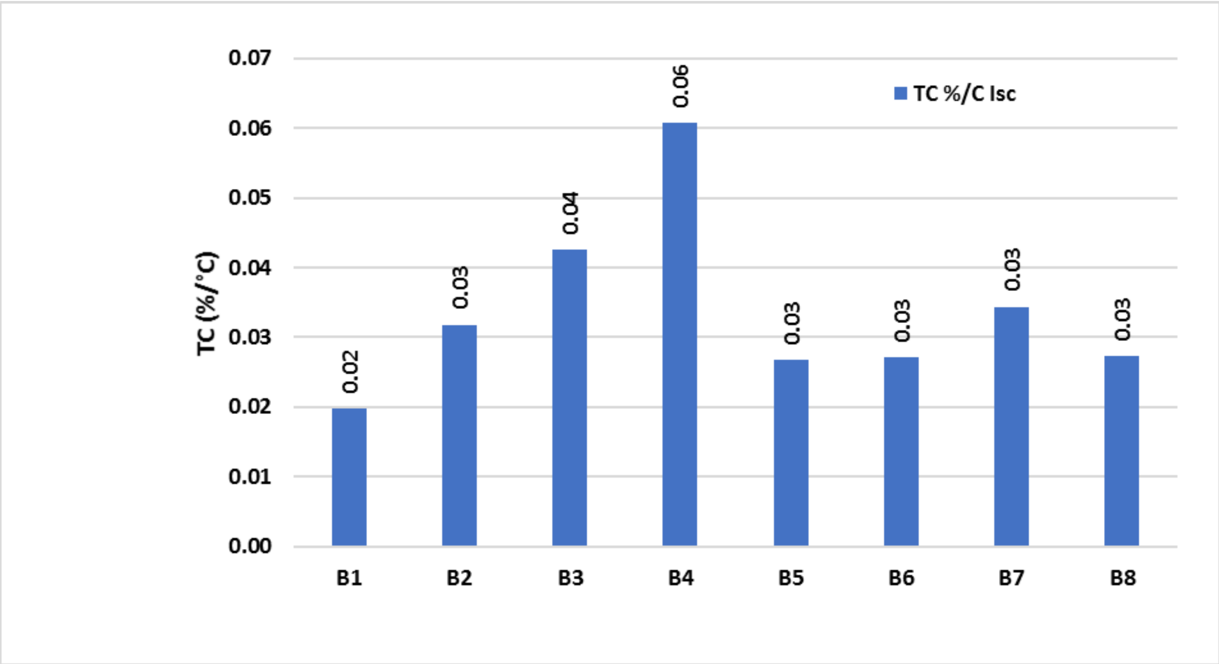

Figure 55: Temperature coefficient for short circuit current for modules from manufacturer B

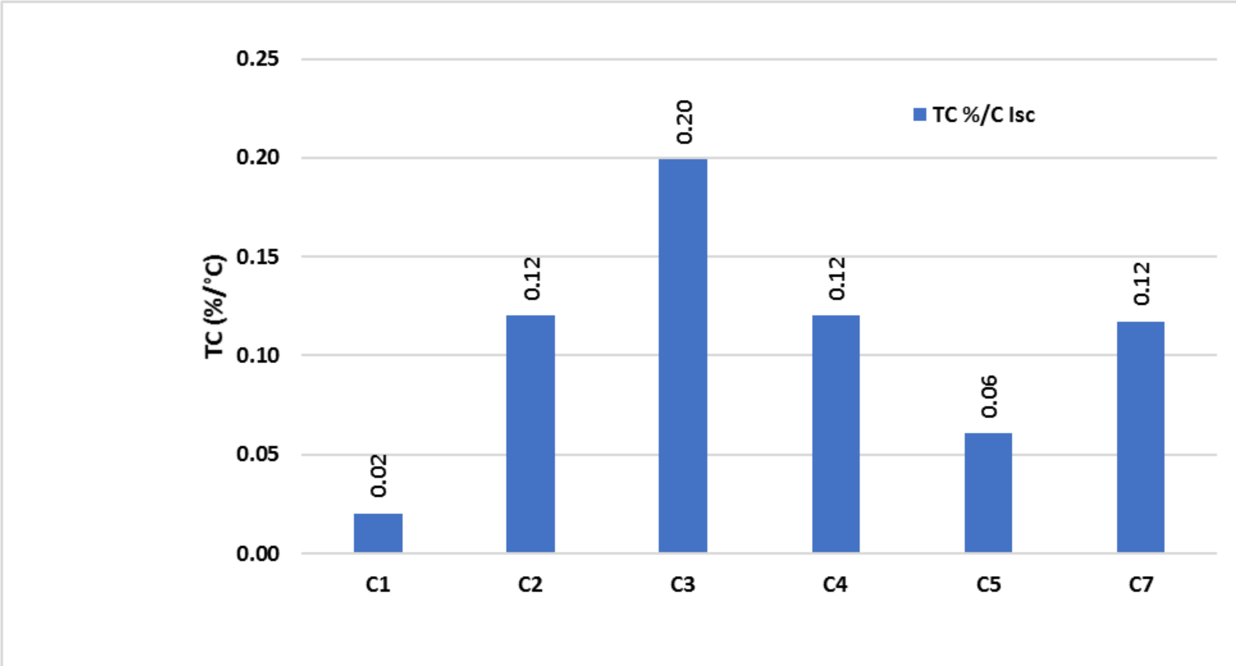

Figure 56: Temperature coefficient for short circuit current for modules from manufacturer C

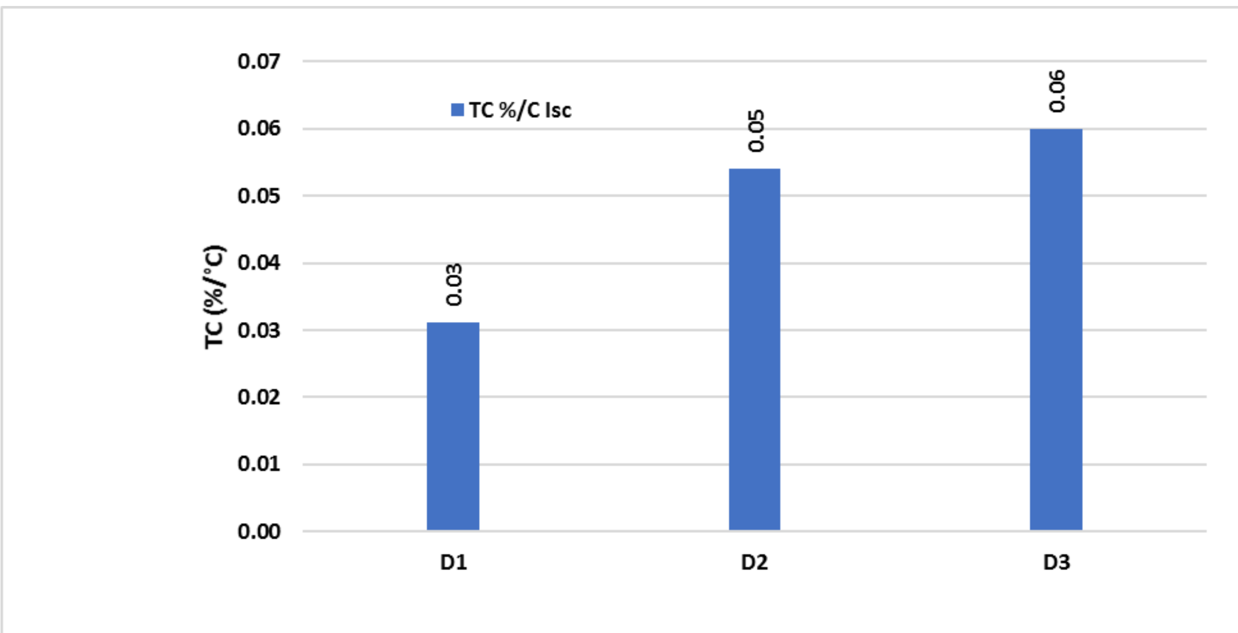

Figure 57: Temperature coefficient for short circuit current for modules from manufacturer D

7.2.2 Series and Shunt Resistances

Figure 58 and 59 show the results of the series and shunt resistances measured using baseline light and dark IV. It can be seen from the results that the series resistance from dark IV is less as compared to the values calculated from the baseline light IV. Similarly, the values for shunt resistance are higher from dark IV as compared to baseline light IV. This is because dark IV is a better method for determining series and shunt resistances. The results also show an increase in series resistance which is the cause of FF degradation and an increase in the temperature coefficient of Pmax. The increase in series resistance is mainly due to solder bond degradation [8].

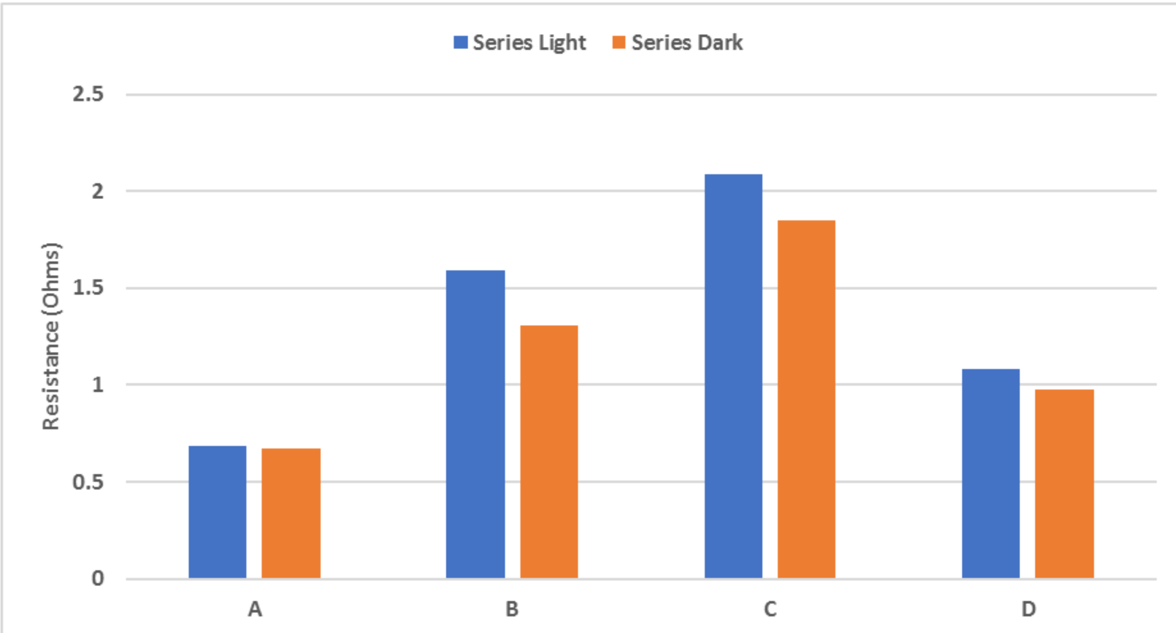

Figure 58: Series resistance from baseline light and dark IV for all modules

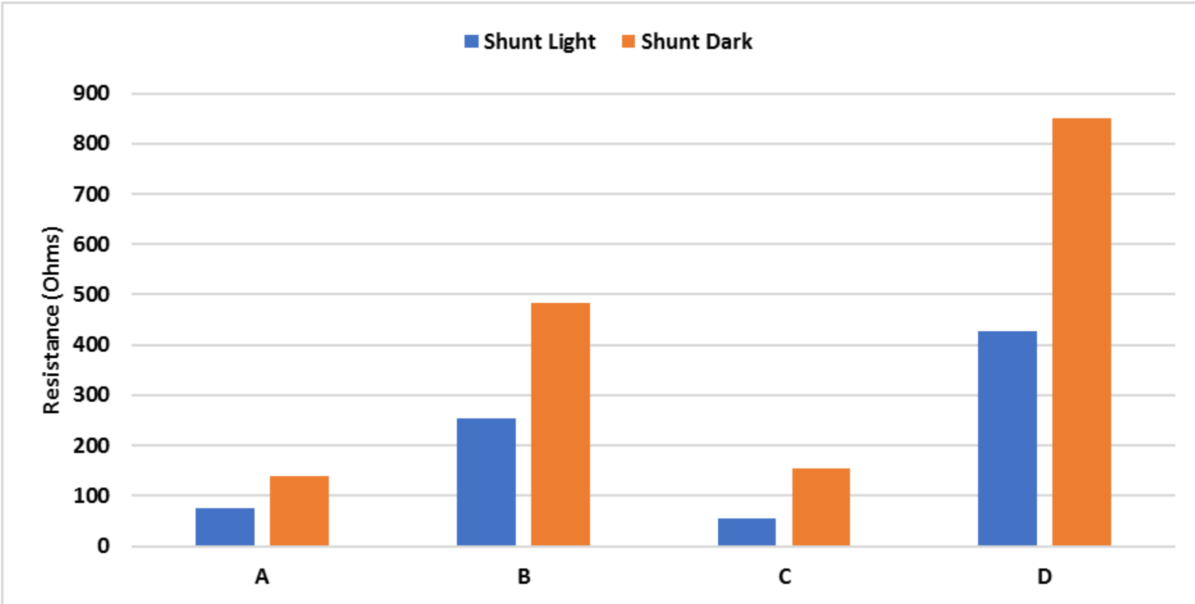

Figure 59: Shunt resistance from baseline light and dark IV for all modules

7.2.3 EL Imaging Results

The figures from 60 to 62 show the EL images. Due to a considerable number of images, one image from each manufacturer is added. The panels from manufacturer D were faulty and therefore EL could not be performed on them.

Figure 60: Module from manufacturer A

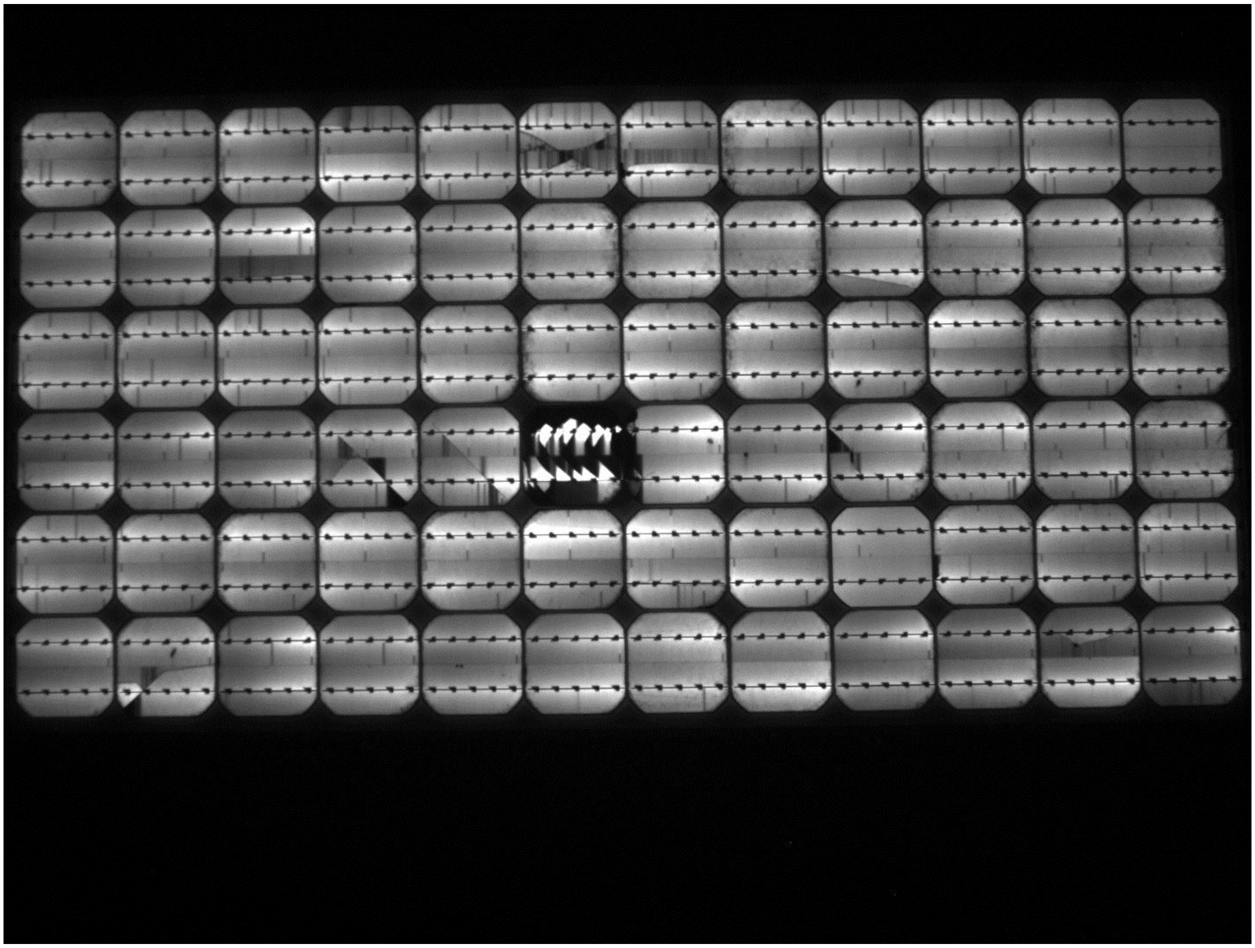

Figure 61: Module from manufacturer B

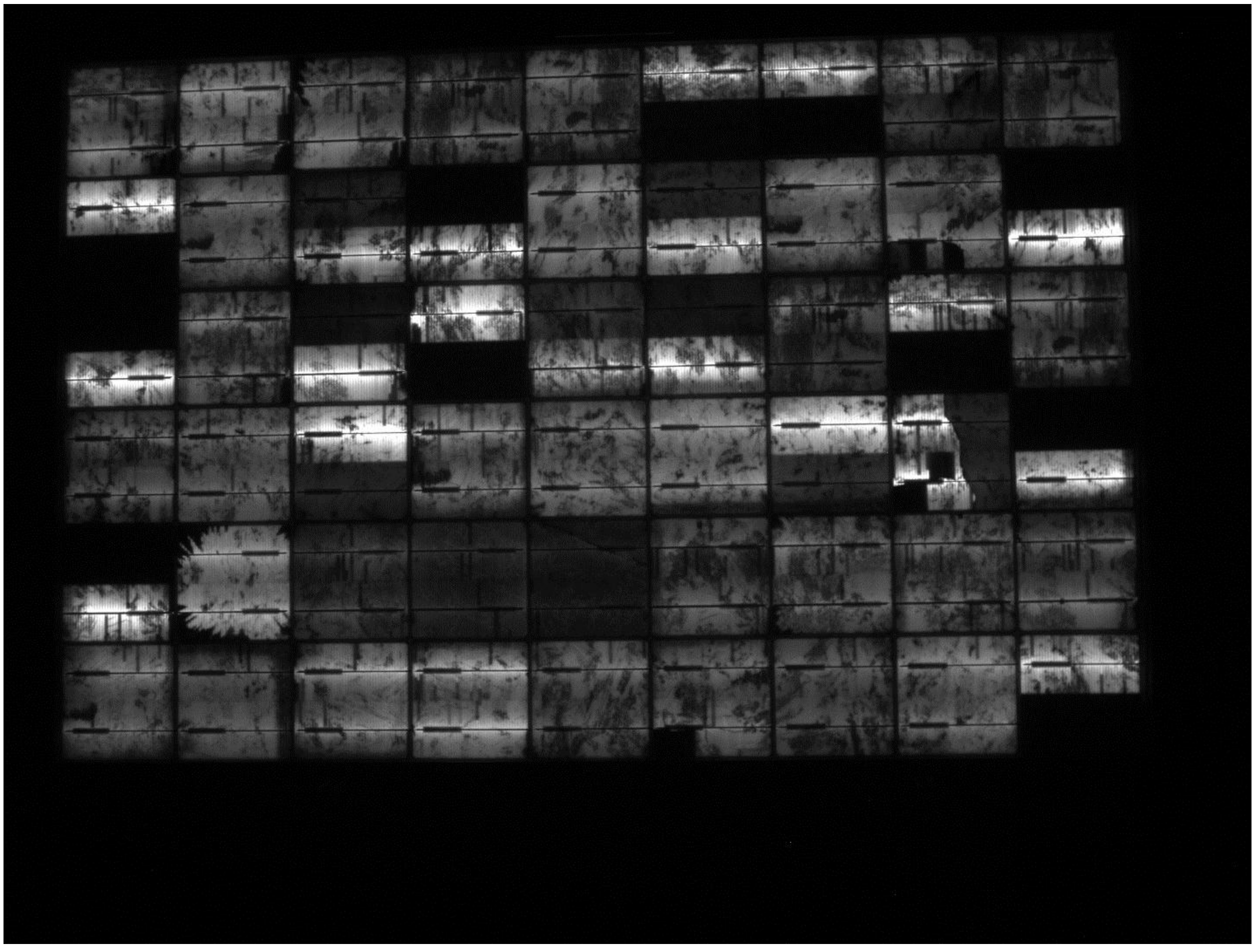

Figure 62: Module from manufacturer C

The dark areas which can be seen in the images are the cracks or defects in the module which are not normally visible. These defects could lead to a drop in the power of the module.

7.2.4 IR Imaging Results

The figures from 63 to 66 show the IR images. Due to a considerable number of images, one image from each manufacturer is added.

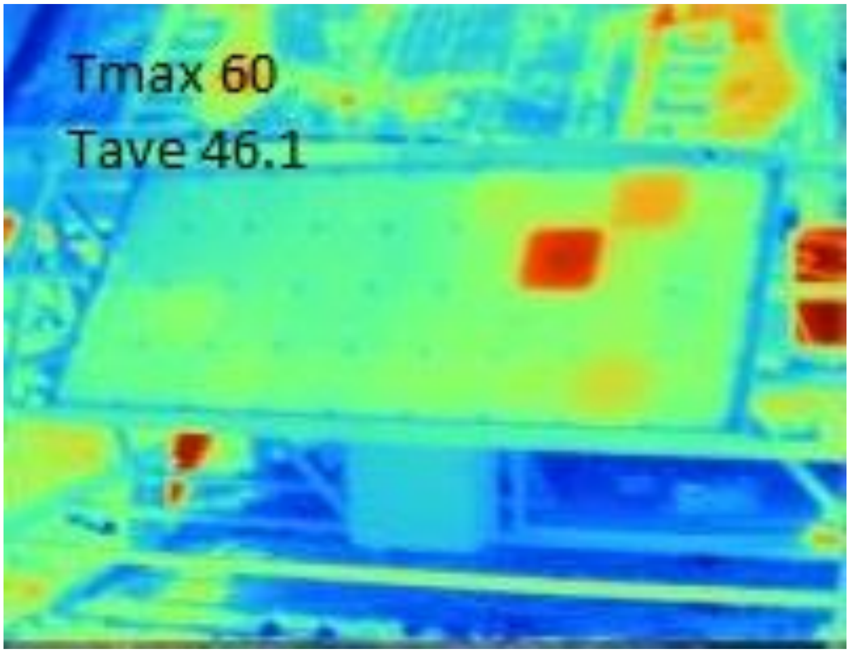

Figure 63: Module from manufacturer A

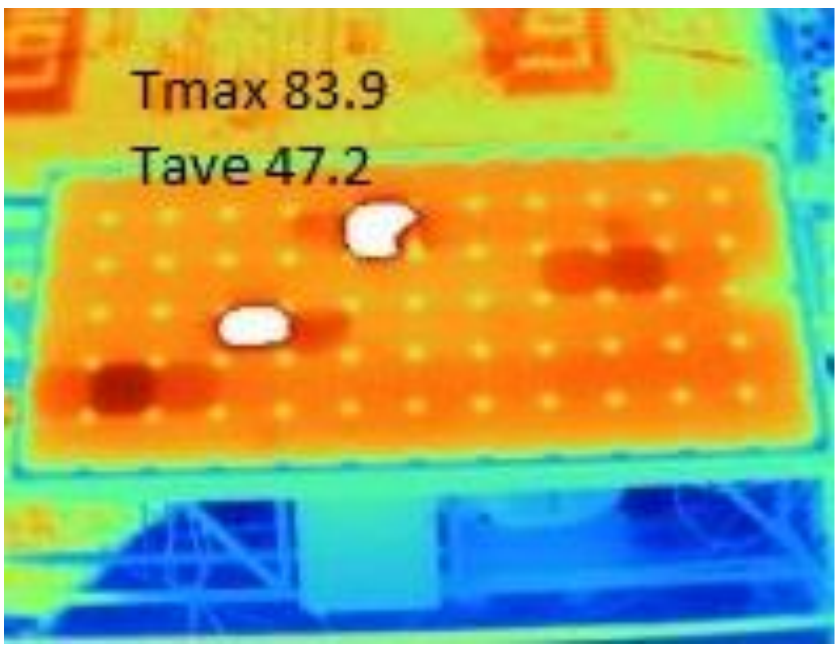

Figure 64: Module from manufacturer B

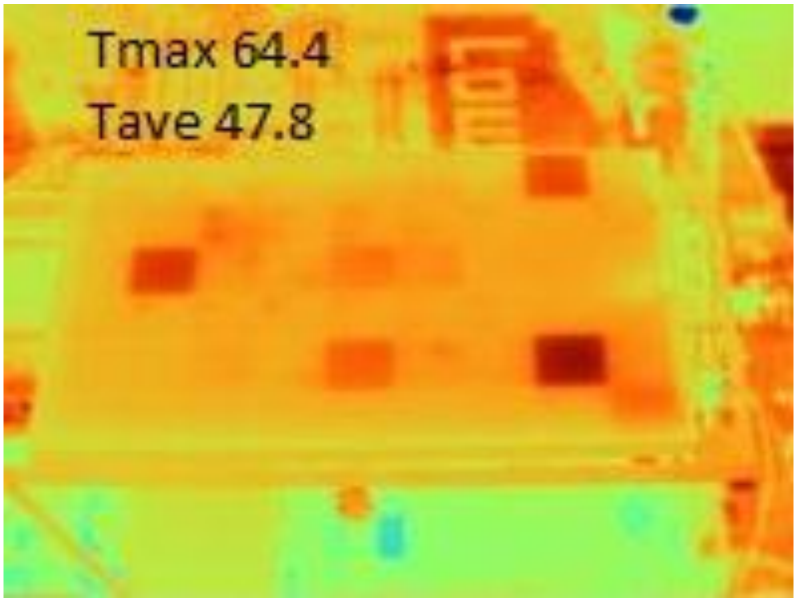

Figure 65: Module from manufacturer C

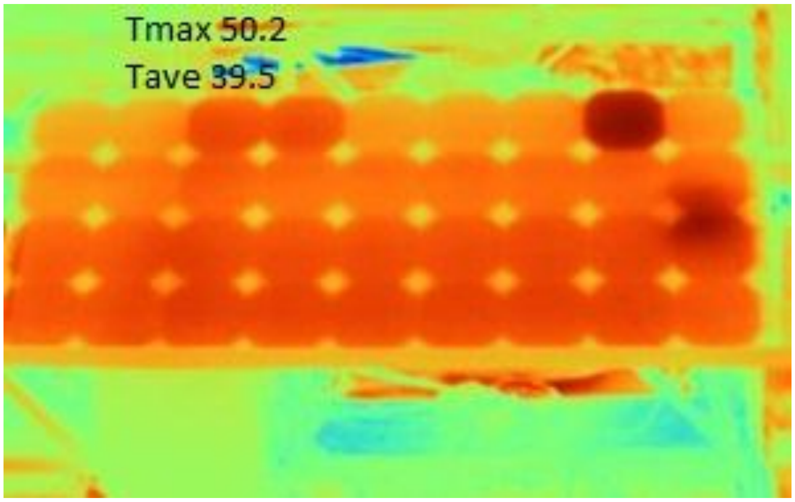

Figure 66: Module from manufacturer D

The areas in the images which appear darker could be potential hotspots. These hotspots can cause a decrease in the power and FF of the module.

7.2.5 UV Imaging Results

The figures from 67 to 69 show the UV images. Due to a considerable number of images, one image from each manufacturer is added. Modules from manufacturer B were not included in UV imaging.

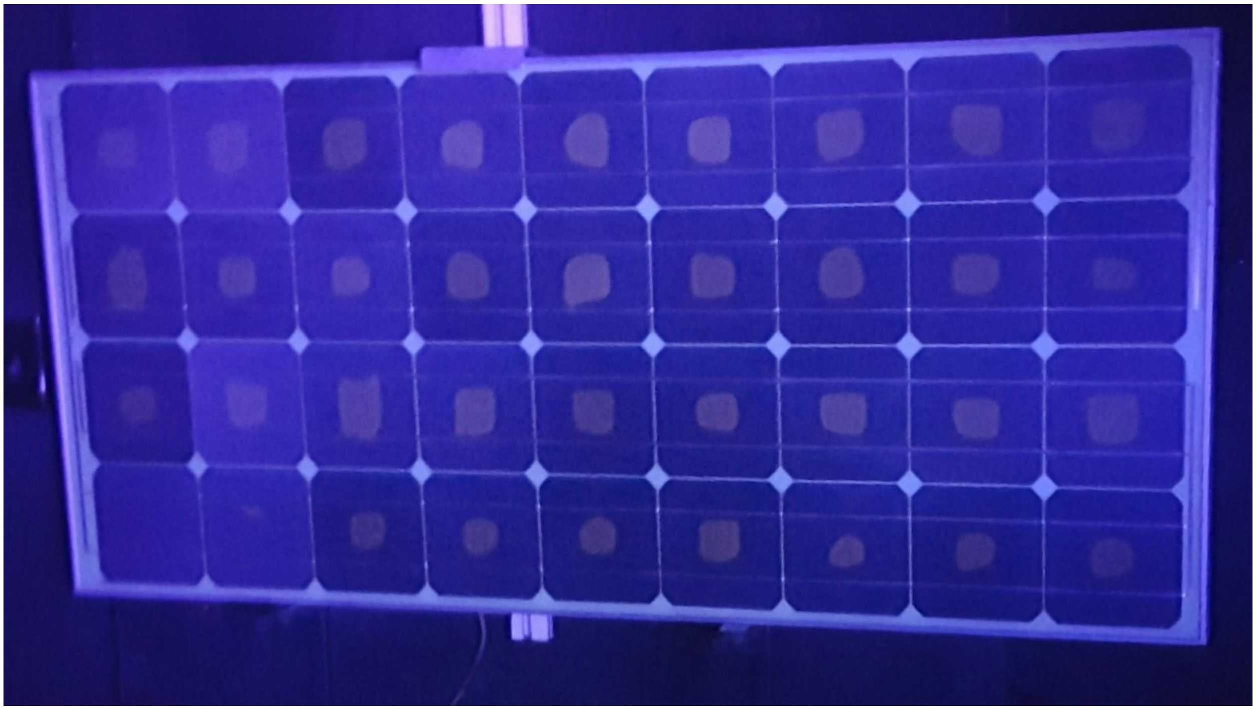

Figure 67: Module from manufacturer A

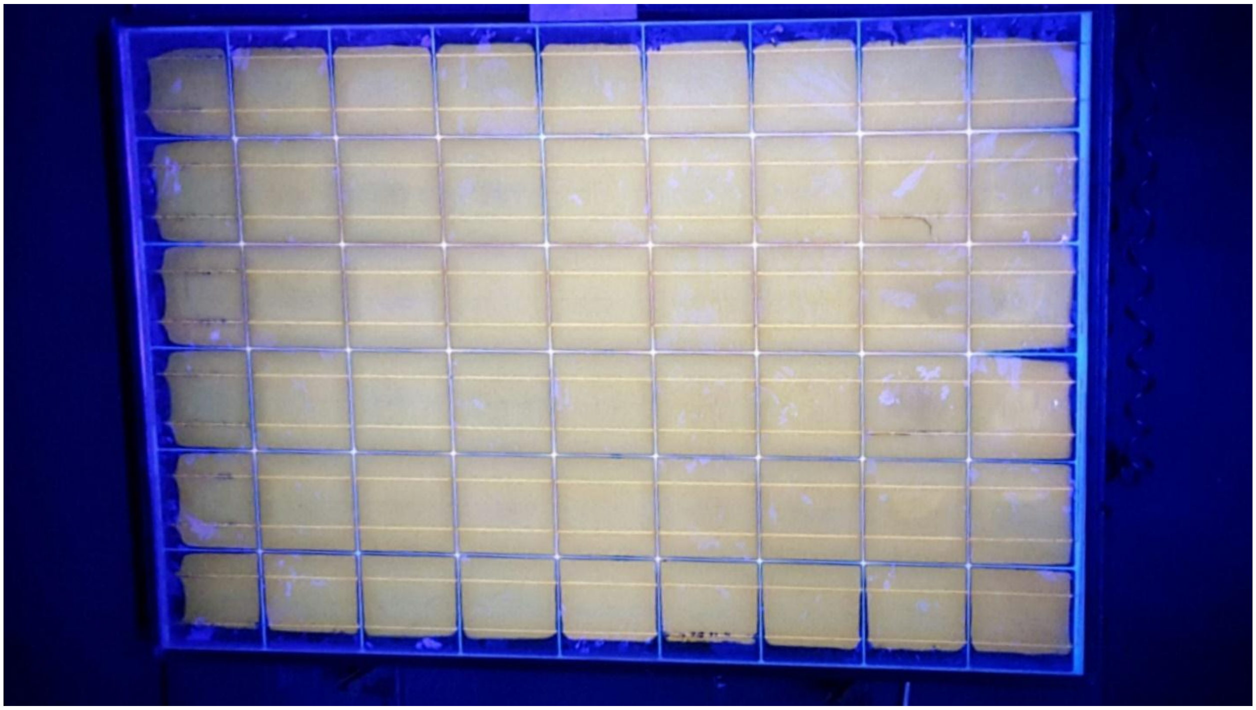

Figure 68: Module from manufacturer C

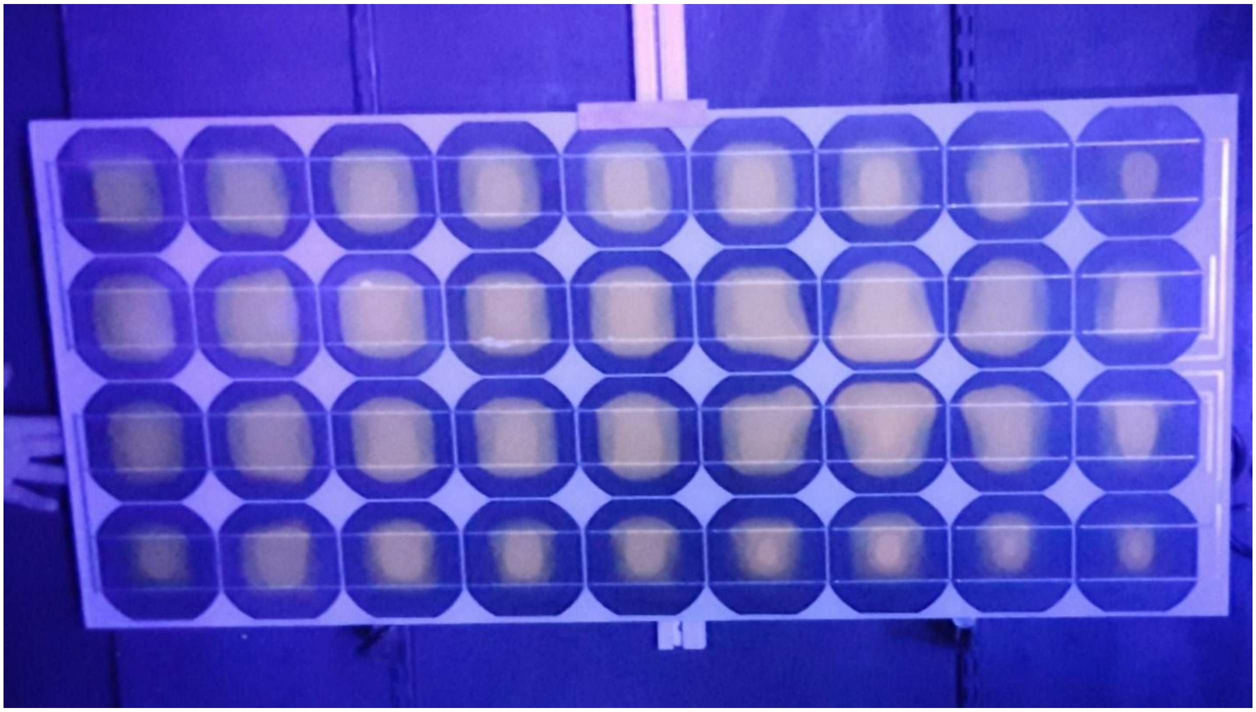

Figure 69: Module from manufacturer D

The spots in the images is browning which is not visible under normal light. Due to browning transmittance of light decreases which causes the maximum power current to decrease which leads to a drop in the power.

7.3 Conclusion

This study indicates that the temperature coefficient of Pmax of a PV module increases as the module ages. This is because the series resistance increases and causes the FF of the module to decrease. This indicates that the current industry practice of using Pmax temperature coefficient of new modules to measure performance ratio and degradation rate can give wrong results. Furthermore, EL, IR and UV imaging of the aged modules suggest that due to cracks, hotspots and browning various performance parameters of the module are affected leading to a degradation in performance. In a future study, a correlation between the images and cell defects will be done using image processing to determine the detailed effect of these defects on the performance parameters.

Summary

The chapter gives information about the methodology and results of the project carried out at Arizona State University. This study proposes that the temperature coefficient of Pmax increases as the modules ages. This is against the current industry practice in which it is considered that the Pmax temperature coefficient remains same throughout the module life. 24 field aged modules were selected for this study and five tests were performed on them baseline light IV, dark IV, EL imaging, IR imaging and UV imaging. The results of the baseline light IV were used to calculate the temperature coefficient of Pmax and series and shunt resistance. Dark IV was also used to calculate series and shunt resistance for accuracy. The results confirm that the temperature coefficient of Pmax increases as the module ages because the series resistance increase which causes the FF to decrease. The results from EL, IR and UV imaging show that due to defects, hotspots and browning the performance parameters of a module decrease causing its performance to deteriorate. In a future study, the results of EL, IR and UV imaging will also be correlated with the performance parameters using imaging processing to determine how these cell defects affect the performance of a PV module.

References

[1] E. Schneller, N. S. Shiradkar, and N. G. Dhere, "Baseline testing procedures for PV modules beyond the qualification testing," in *Proceedings of SPIE - The International Society for Optical Engineering*, 2013, vol. 8825, pp. 1–7.

[2] "Dark IV Measurements | PVEducation." [Online]. Available: http://www.pveducation.org/pvcdrom/characterisation/dark-iv-testing. [Accessed: 16-Nov-2017].

[3] T. Fuyuki, H. Kondo, T. Yamazaki, Y. Takahashi, and Y. Uraoka, "Photographic surveying of minority carrier diffusion length in polycrystalline silicon solar cells by electroluminescence," *Appl. Phys. Lett.*, vol. 86, no. 26, pp. 1–3, 2005.

[4] "Electroluminescence | PV Education." [Online]. Available: http://www.pveducation.org/pvcdrom/characterisation/electroluminescence. [Accessed: 17-Nov-2017].

[5] C. Buerhop, D. Schlegel, M. Niess, C. Vodermayer, R. Wei??mann, and C. J. Brabec, "Reliability of IR-imaging of PV-plants under operating conditions," *Sol. Energy Mater. Sol. Cells*, vol. 107, pp. 154–164, 2012.

[6] "Hot Spot Heating | PVEducation." [Online]. Available: http://www.pveducation.org/pvcdrom/modules/hot-spot-heating. [Accessed: 17-Nov-2017].

[7] "Some Common Causes of Solar PV Module Failure – First Green Consulting Pvt Ltd." [Online]. Available: http://www.firstgreen.co/2014/07/common-causes-of-solar-pv-module-failure/. [Accessed: 17-Nov-2017].

[8] F. Mahmood *et al.*, "Temperature coefficient of power (Pmax) of field aged PV modules: impact on performance ratio and degradation rate determinations," 2017, vol. 10370, pp. 1037007–1037008.